Universidade de Aveiro
2023

CARLOTA TAVARES MARCOS

Long non-coding RNA *NORAD*: a potential target for a promising human breast cancer therapy

Universidade de Aveiro
2023

CARLOTA TAVARES MARCOS

RNA longo não codificante *NORAD*: um potencial alvo para uma terapia promissora para o cancro da mama humano

Dissertação apresentada à Universidade de Aveiro para cumprimento dos requisitos necessários à obtenção do grau de Mestre em Biomedicina Molecular, realizada sob a orientação científica do Doutor Bruno Miguel Bernardes de Jesus, Professor do Departamento de Ciências Médicas da Universidade de Aveiro e da Doutora Sandrina Nóbrega Pereira, equiparada a Investigadora Auxiliar da Universidade de Aveiro.

This work was supported by Fundação para a Ciência e Tecnologia (FCT) (EXPL/BIA-CEL/0358/2021 and 2022.01199.PTDC).

“Tudo é ousado para quem nada se atreve"

- Fernando Pessoa

o júri

presidente

Prof. Doutora Ana Margarida Domingos Tavares de Sousa
professora auxiliar da Universidade de Aveiro

vogais

Doutor Bruno Miguel Correia Pereira
investigador auxiliar da Universidade do Porto - Instituto de Investigação e Inovação em Saúde

Prof. Doutor Bruno Bernardes de Jesus
professor auxiliar da Universidade de Aveiro

agradecimentos

Em primeiro lugar, agradeço ao Professor Bruno por me ter aceitado no seu grupo e por, mesmo tendo um projeto e um plano a seguir, sempre me ter dado a liberdade para “fugir” a esse plano e fazer mais. Obrigada pela disponibilidade e por todas as oportunidades que me deu ao longo deste ano. Agradeço também à Doutora Sandrina pela ajuda ao longo deste projeto e por constantemente incentivar a discussão científica, fazendo-me crescer profissionalmente. Acabo este trabalho com a certeza de que levo aprendizagens para a vida!

Um agradecimento especial ao Francisco e à Magda por todo o apoio e por todas as dicas ao longo deste percurso, vocês são, sem dúvida, grandes exemplos.

Júlia, Rafaela e Bárbara, se eu tivesse escolhido quem me acompanharia nesta aventura, não teria tido tão boas companheiras! Obrigada pelos momentos de desanuvio, por me fazerem crer que estava sempre tudo controlado e que no fim ia dar tudo certo.

Ângela, Inês, Filó e Rita, obrigada pela amizade, pelos memes e por estarem lá sempre, mesmo quando partilho os pensamentos mais insignificantes e aleatórios que podemos imaginar. Para ti Catarina, um obrigada nunca vai ser suficiente, tu és casa, um exemplo que levo para a vida!

À Mondragão agradeço a disponibilidade e amizade, mas, acima de tudo, a estupidez natural.

Obrigada à Matilde, a minha Amiga de sempre, aquela que celebra as minhas conquistas como se das dela se tratassem e que tornou a minha estadia por Aveiro bem mais fácil, mesmo quando foi embora nunca deixou de estar presente. Um obrigada também à Margarida, à Maria e à Carolina, pelo companheirismo ao longo de todos estes anos.

Obrigada, Luís, Paula, Luís Tomás e António por serem sempre casa longe de casa.

Um agradecimento muito especial à minha família por fazer sonhar e realizar os sonhos. À Avó Helena e à Avó Jesus por todo o apoio que me deram ao longo destes anos, nada disto seria possível sem a vossa ajuda. Mãe e Pai, a vocês agradeço tudo, tudo o que conquistei conquistei-o graças a vocês. Obrigada por estarem sempre aqui para mim e por me darem todas as condições para lutar sempre por mais e melhor, sem vocês não seria a pessoa que sou hoje. Maria, a tua perseverança tem sido uma inspiração ao longo deste caminho, não podia ter melhor exemplo. Obrigada pela força que me dás diariamente!

Por fim, agradeço ao Pedro por ter estado ao meu lado todos os dias durante este último ano, por todos os conselhos e dicas, e por acreditar em mim, mais do que eu alguma vez acreditei. Foste fundamental nesta conquista!

palavras-chave

Cancro da mama, cancro da mama triplo negativo, lncRNA *NORAD*, quimioterapia

resumo

O cancro da mama (CM) é uma doença heterogénea, sendo o cancro mais diagnosticado em todo o mundo. Tendo em conta as suas características moleculares, o CM pode ser classificado em diferentes subtipos. O cancro da mama triplo negativo (CMTN) é o subtipo mais agressivo, apresentando um prognóstico reservado devido às limitadas opções terapêuticas. O ARN longo não codificante ativado por danos no ADN (*NORAD*) tem sido associado à progressão de vários tipos de cancro, no entanto o seu papel no CM ainda não é conhecido. Todavia, sabe-se que, em condições normais, o *NORAD* contribui para a proteção do DNA e para a estabilidade cromossomal ao sequestrar as proteínas pumilio.

Os objetivos do presente trabalho foram avaliar se os níveis de *NORAD* estão associados à agressividade tumoral e à transformação oncogénica, determinar a localização do *NORAD* em células de CMTN e avaliar o efeito do silenciamento do *NORAD* na sensibilidade das células de CM ao tratamento com doxorrubicina, um agente quimioterapêutico.

Os resultados mostraram que os níveis de expressão de *NORAD* tendem a ser mais elevados em tecidos de pacientes com tumores mais agressivos, nomeadamente no CM luminal com elevado índice de recorrência e no CMTN com baixa resposta ao tratamento. Através de hibridização *in situ* por fluorescência, demonstrou-se que o *NORAD* se localiza no citoplasma de células de CMTN. Além disso, verificou-se que o *NORAD* participa na resposta ao dano de ADN nas células tratadas com doxorrubicina, com o seu silenciamento sensibilizando-as para o tratamento com este agente quimioterapêutico.

Estes resultados revelaram o potencial do *NORAD* como biomarcador de prognóstico e preditivo, e como alvo terapêutico no CMTN. Estas descobertas podem revolucionar o tratamento do CMTN, com o silenciamento do *NORAD* servindo como coadjuvante à quimioterapia convencional, melhorando o prognóstico dos pacientes com CMTN.

keywords Breast cancer, triple negative breast cancer, lncRNA *NORAD*, chemotherapy

abstract

Breast cancer (BC) is a heterogeneous disease, being the most diagnosed cancer worldwide. Based on its molecular characteristics, BC can be classified into different subtypes. Triple negative breast cancer (TNBC) is the most aggressive subtype with little therapeutical options, presenting a more reserved prognostic. The long non-coding RNA activated by DNA damage (*NORAD*) has been associated with the progression of several cancers, but its role in BC remains controversial. Nevertheless, it is known that *NORAD* contributes to DNA protection and chromosomal stability by sequestering pumilio proteins, in normal conditions.

The aims of the present work were to assess whether *NORAD* levels are associated with tumor aggressiveness and oncogenic transformation, to determine *NORAD* localization in TNBC cells, and to evaluate the effect of *NORAD* downregulation on the sensitivity of TNBC cells to doxorubicin, a chemotherapeutic agent.

The results showed that *NORAD* expression levels tend to be higher in tissues from patients with more aggressive BC tumors, including luminal BC with high recurrence scores and TNBC with low response to treatment. Besides this, it was demonstrated by RNA fluorescence *in situ* hybridization, that *NORAD* localizes in the cytoplasm of TNBC cells. It was also found that *NORAD* participates in DNA damage response since *NORAD* knockdown contributed for the accumulation of DNA damage in doxorubicin-treated cells, sensitizing them for the treatment with this chemotherapeutic agent.

Together, these results revealed the potential of *NORAD* as a prognostic and predictive biomarker, and as a therapeutical target in TNBC. Such findings could revolutionize TNBC treatment, with *NORAD* silencing serving as an adjunct to conventional chemotherapy, improving the prognosis of patients with TNBC.

Contents

List of figures

List of tables

List of abbreviations, symbols, and acronyms

5-FU	5-Fluorouracil
AKT	Serine/threonine protein kinase
ALYREF	Aly/REF export factor
Bax	Bcl-2 associated X
BC	Breast cancer
Bcl-2	B-cell lymphoma 2
BER	Base excision repair
BRCA1/2	Breast cancer susceptibility 1/2 gene
BUB3	Mitotic checkpoint protein BUB3
CAPN7	Calpain 7
CDC5L	Cell division cycle 5 like
CDK1	Cyclin dependent kinase 1
cDNA	Complementary DNA
ceRNA	Competing endogenous RNA
CIN	Chromosomal instability
CO2	Carbon dioxide
CRC	Colorectal cancer
CRISPR/Cas9	Clustered regularly interspaced short palindromic repeats- associated endonuclease 9
Ct	Threshold cycle
Ctrl	Control

CXCL12	C-X-X motif chemokine ligand 12
CXCR4	C-X-C motif chemokine receptor 4
DAPI	4’,6-diamidino-2-phenylindole
DD3	Differential display code 3
DDR	DNA damage response
DLBCL	Diffuse large B cell lymphoma
DMEM	Dulbecco's Modified Eagle Medium
DMSO	Dimethylsulfoxide
dNTP	Deoxynucleoside triphosphate
DSBs	Double-strand breaks
DXR	Doxorubicin
E2F3	E2F transcription factor 3
EDTA	Ethylenediaminetetraacetic acid
EGLN2	Egl-9 family hypoxia inducible factor 2
eIF2	Eukaryotic initiation factor 2
EPIC1	Epigenetically-induced lncRNA 1
ER	Estrogen receptor
ESCC	Esophageal squamous-cell carcinoma
FACS	Fluorescence-activated cell sorting
FBS	Fetal bovine serum
FENDRR	Fetal-lethal non-coding developmental regulatory RNA

FFPE	Formalin-fixed paraffin-embedded
FIGO	International Federation of Obstetrics and Gynecology
FISH	Fluorescence in situ hybridization
FOXO6	Forkhead box O6
FUBP1	Far upstream element binding protein 1
GAS5	Growth arrest-specific 5
GNAS-AS1	Guanine nucleotide binding protein antisense RNA 1
H2AX	H2A.X variant histone
HCC	Hepatocellular carcinoma
HER2	Human epidermal growth factor receptor 2
HOTAIR	HOX antisense intergenic RNA
HR	Homologous recombination
IDR	Intrinsically disordered regions
IHC	Immunohistochemistry
kb	Kilobase
KD	Knockdown
Ki67	Marker of proliferation Ki-67
LINC	Long intergenic non-coding
LNA	Locked nucleic acid
lncRNA	Long non-coding RNA
MALAT1	Metastasis associated lung adenocarcinoma transcript 1

MCM4	Minichromosome maintenance complex component 4
MCM6	Minichromosome maintenance complex component 6
miR or miRNA	Micro RNA
mRNA	Messenger RNA
mTOR	Mechanistic target of rapamycin kinase
MYC	MYC proto-oncogene
MYCN	MYCN proto-oncogene
NACT	Neoadjuvant chemotherapy
NARC1	*NORAD*-activated ribonucleoprotein complex 1
NAT	Natural antisense transcript
ncRNA	Non-coding RNA
NEAT1	Nuclear paraspeckle assembly transcript 1
NER	Nucleotide excision repair
NHEJ	Non-homologous end-joining
NORAD	Non-coding activated by DNA damage
NSCLC	Non-small cell lung cancer
ORF	Open reading frame
PARP	Poly (ADP-ribose) polymerase
PBS	Phosphate-buffered saline
PCa	Prostate cancer
PCA3	Prostate cancer associated 3

Pen/Strep	Penicillin-streptomycin
PI3K	Phosphoinositide 3-kinase
PR	Progesterone receptor
PRC1	Protein regulator of cytokinesis 1
PRE	Pumilio recognition element
PRPF19	Pre-mRNA processing factor 19
PUF	Pumilio-FEM3-binding factor
PUM1	Pumilio homolog 1
PUM2	Pumilio homolog 2
RBMX	RNA binding motif protein X-linked
RBP	RNA binding protein
RhoA	Ras homolog family member A
ROCK	Rho-associated protein kinase
RPT	Recovery post-treatment
rRNA	Ribosomal RNA
RS	Recurrence score
RT-qPCR	Real-time quantitative reverse transcriptase polymerase chain reaction
RUNX2	RUNX family transcription factor 2
SAM68	Src associated in mitosis of 68 kDa
SCR	Scramble
SIP1	Smad interacting protein 1

siRNA	Small interfering RNA
Smad2	SMAD family member 2
SOCS1	Suppressor of cytokine signaling 1
sRNA	Small RNA
SSBs	Single-strand breaks
SSC	Saline sodium citrate
STAT	Signal transducer and activator of transcription 1
TAZ	Transcriptional coactivator with PDZ-binding motif
TEAD	TEA domain transcription factors
TGF-β	Transforming growth factor-β
TME	Tumor microenvironment
TNBC	Triple negative breast cancer
TNM	Tumor-node-metastasis
TRIP13	Thyroid hormone receptor interactor 13
tRNA	Transfer RNA
UICC	Union for international cancer control
UTR	Untranslated region
XIST	X-inactive specific transcript
YAP	Yes-associated protein 1
ZEB2	Zinc finger E-box binding homeobox 2

1 Introduction

1.1 Cancer: a worldwide pandemic

1.1.1 Numbers at a glance

Despite all the scientific community efforts to better understand cancer disease and the progress made in its diagnosis and treatment, it still remains one of the leading causes of death worldwide (1). In fact, the cancer burden is still growing in both developing and developed countries, mostly due to the expansion and aging of the population, and socioeconomic development (2,3). Data from GLOBOCAN 2020 indicate that there were nearly 10 million cancer deaths, and more than 19 million persons were diagnosed with cancer only in 2020 (Figure 1A and 1B) (4,5). The deadliest cancers were the ones in the lung (18% of all cancer-related deaths), colorectal (9.4%), liver (8.3%), stomach (7.7%), and breast (6.9%) (Figure 1B) (6). Among the most diagnosed cancers, breast (11.7% of all new cases), lung (11.4%), colorectal (10%), prostate (7.3%), and stomach (5.6%) were the five-more diagnosed (Figure 1A). The forecast is that the number of cancer new cases will almost duplicate, being expected 28.4 million new cases by 2040 (4).

In Portugal, cancer incidence is lower than the incidence of the European Union average, but cancer it still is a real problem, with a tendency for the numbers to increase (7). In 2020, more than 60,000 new cases of cancer were detected, and more than 30,000 cancer-related deaths were reported. Colorectal cancer (17.4%) was the most diagnosed cancer in Portugal, followed by breast (11.6%), prostate (11.2%), lung (9%), and stomach (4.9%) (8).

Over the past decades, breast cancer (BC) burden has been rising, with female BC replacing lung cancer and becoming the most diagnosed cancer worldwide (Figure 1C) (4). However, this disease not only affects women but also men. Actually, around 11.7% of all diagnosed patients with cancer in 2020 were breast cancer cases, which is equivalent to 2.3 million new cases in one year only (4,9). BC accounts for nearly 7% of all deaths related to cancer, being in the top five of most deathly cancers (5,10). It is estimated that by 2040 the number of new cases will increase by almost 40%, reaching three million cases per year, and BC-related deaths will follow the same trend, growing up to 50% (9). In Portugal, BC is the second most diagnosed cancer (11.6% of all diagnosed cases), when both genders are considered, only being exceeded by colorectum cancer (8). When considering only the female gender, BC is the most diagnosed cancer, accounting for more than 7,000 new cases and more than 1,000 deaths in 2020 (8).

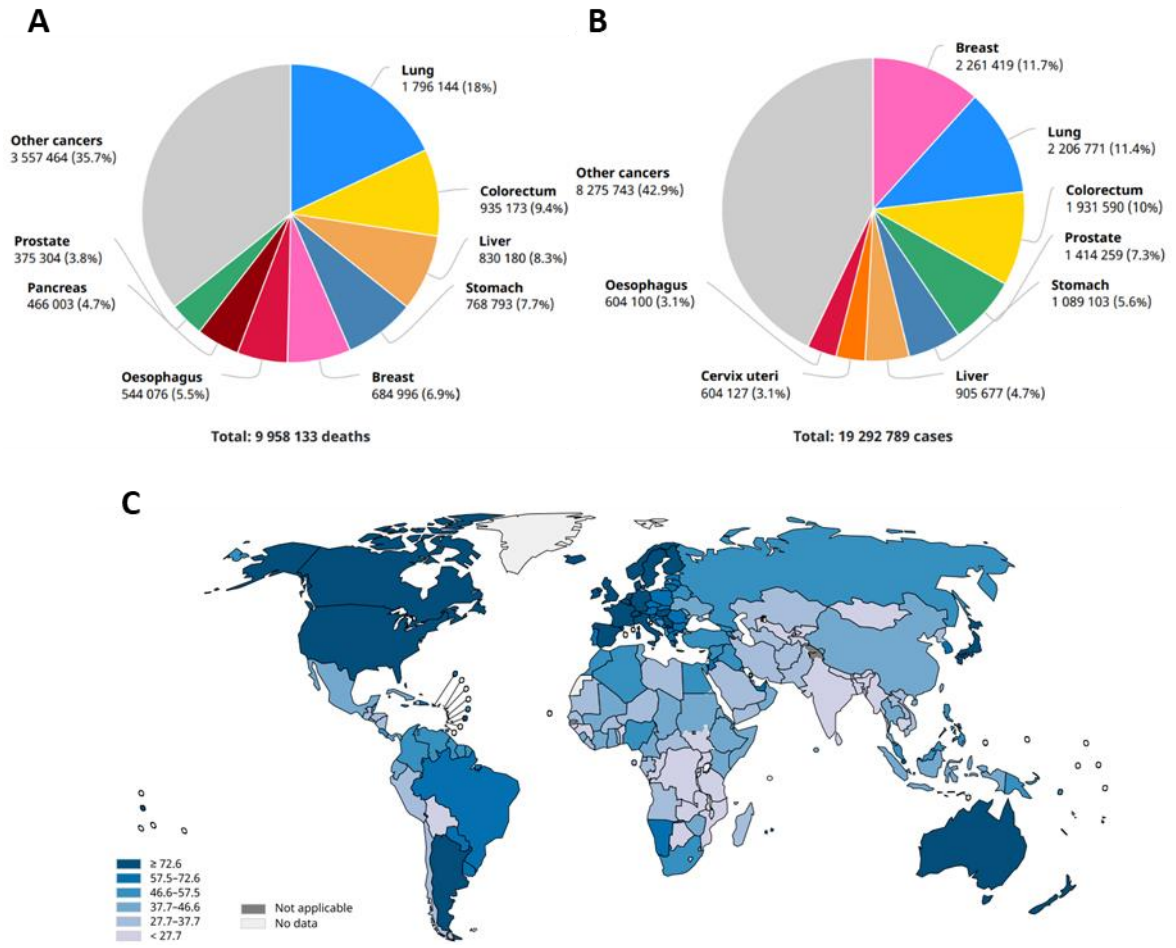

Figure 1- Cancer in numbers. Number of cancer new cases (A), number of cancer-related deaths (B), and breast cancer incidence worldwide (C). Adapted from (6) and (10).

1.1.2 From a normal cell to a cancer cell

The human body is made up of multiple different cells that grow and divide, through cell division, interacting with each other to maintain organism homeostasis (11). In normal conditions, cell machinery is capable of detecting old and damaged cells and activates programmed cell death pathways to eliminate those cells (11). Cancer is a condition where these pathways don't work properly, with damaged cells growing and multiplying abnormally, being capable to spread and evade other areas of our body (11).

Even though cancer has been under investigation worldwide for years, its development is not fully understood. Carcinogenesis is a complex process, concerning numerous changes in the genome, with hereditary mutations and exposition to certain environmental factors accelerating cancer onset, suggesting that carcinogenesis involves not only genetic factors but also environmental (12). The most popular theory is the multistage model of cancer which hypothesizes that cancer initiation and

progression is a cumulative process with the acquisition of several recessive and dominant mutations over time (13). These mutations lead to the repression of genes that inhibit cell proliferation and promote apoptosis, the tumor suppressor genes, and contrarily the activation of genes that stimulate cellular growth and division, the oncogenes (14–16). This culminates with the transformation of normal cells into cells lacking the regulatory circuits responsible for cell proliferation and homeostasis, the cancer cells (12,13).

In 2000, Hanahan and Weinberg proposed the six hallmarks of cancer: 1. self-sufficiency in growth signals, 2. insensitivity to antigrowth signals, 3. tissue invasion and metastasis, 4. limitless replicative potential, 5. sustained angiogenesis, and 6. evading apoptosis (Figure 2A) (12). These were described as biological capabilities that are acquired by most (or even all) cancer cells, during the cancer multistage process (12). Besides the cancer hallmarks, Hanahan and Weinberg described two enable characteristics responsible for the acquisition of these hallmarks by the cells: i) genomic instability (described in following sections), and ii) tumor-promoting inflammation, a process influenced by immune cells that tend to promote tumor progression by different mechanisms (17). This vision evolved and later in 2011 another two hallmarks were proposed: 7. deregulating cellular energetics, and 8. avoiding immune destruction (17). However, these eight hallmarks are not enough to explain cancer physiopathology, giving rise to the need to fill in the gaps and find the missing explanation. Over the last few years, new capabilities were suggested to be incorporated into the cancer hallmarks scheme (Figure 2B) (18,19).

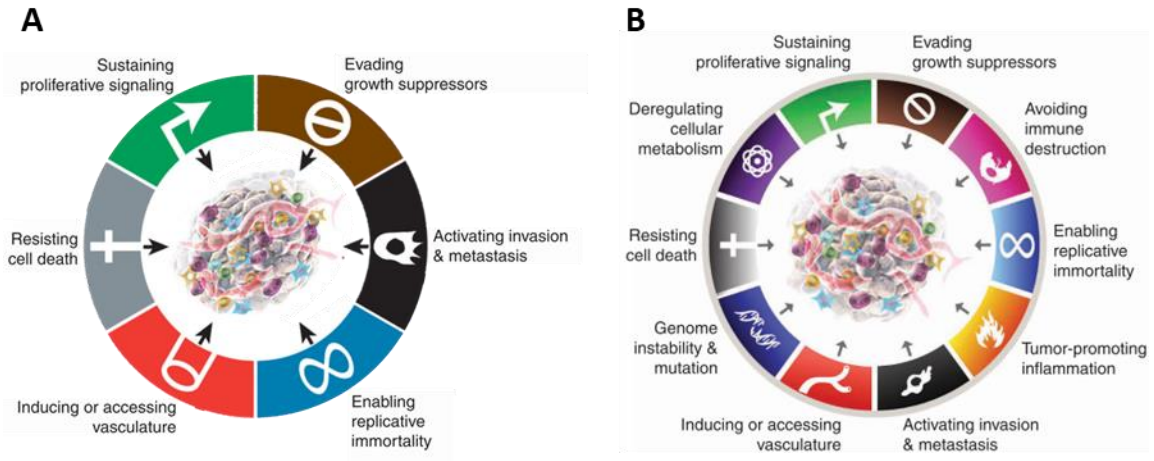

Figure 2- Cancer hallmarks evolution. Hallmarks proposed in 2000 (A) and the 2022 actualization (B). Adapted from (16) and (17).

1.1.3 Tumor microenvironment

A tumor is usually described as a group of cancer cells, but it is much more than just the cancer cells themselves. In fact, it's not even possible to understand a tumor biology by only studying an

individual group of cells (17). A tumor is a collection of different types of cells, each with its own function, including the tumor cells, immune cells (B cells, T cells, and natural killer cells, macrophages, neutrophils, and dendritic cells), and stromal cells (cancer-associated fibroblasts, endothelial cells, adipocytes, and stellate cells), that together with the factors secreted by them and the extracellular matrix form the tumor microenvironment (TME) (20,21).

Tumor cells have the ability to shape their microenvironment by secreting cytokines, chemokines, and other factors, in order to favor their growth and progression (21). Actually, within a tumor, there are several dynamic interactions between the cells that integrate the TME and the factors secreted by them, that dictate the tumor behavior (1,22). Such interactions promote the non-malignant cells to lose their features and acquire new phenotypes, leading to the development and invasion of cancer cells and to events such as angiogenesis. These cells then proliferate and can become less responsive to the treatment and even develop drug resistance, giving rise to metastasis (22–24).

This intratumor heterogeneity makes each tumor unique (25). The study of the TME components, especially the interactions between them paves the way for the understanding of tumor biology and consequently for the development of new therapeutic options, with new targets, increasing patients' life quality and survival time (20).

1.1.4 The crosstalk between DNA damage and cancer

Cells are exposed to endogenous and exogenous DNA-damaging factors that can cause DNA lesions, including mismatches, single-strand breaks (SSBs), double-strand breaks (DSBs), chemical modifications of the bases or sugars, and interstrand or intrastrand cross-links (26,27). These modifications can alter the sequence of nucleotides and result in the expression of dysfunctional proteins, leading to alterations in replication and transcription by changing the normal physiology of the cell (28,29).

The DNA damage response (DDR) is a regulatory system developed by human cells to keep genome stability and avoid unrepaired DNA through numerous DNA repair mechanisms, including cell-cycle checkpoints, apoptosis induction, and transcriptional regulation (26,27). There are different repair mechanisms for each damage type: 1. base excision repair (BER) usually to repair SSBs; 2. non-homologous end-joining (NHEJ) or 3. homologous recombination (HR) can repair DSBs; 4. nucleotide excision repair (NER) involved in the repair of bases modifications and crosslinks; and 5. mismatch repair to deal with mutations (30). However, not always this system works properly (26).

DNA damage has been implicated in the pathogenesis of many diseases, including neurological disorders, birth defects, and cancer (31). In case DDR pathways are compromised there is an

accumulation of DNA damage and mutations, leading to genomic instability and affecting cellular function (27,28).

Genomic instability is a pervasive feature of cancer, being described by Hanahan and Weinberg as an enable characteristic of cancer cells. This instability is recognized by alterations in chromosome structure and number and can trigger carcinogenesis (27,32). Several studies indicate that mutations in DNA repair related genes are associated with certain cancers. For example, BRCA1 and BRCA2 are tumor suppressor genes that encode important proteins for DSB repair (33). These genes are found mutated in some cancers, including breast, ovarian, and pancreatic cancers, leading to genetic predisposition for these diseases (34).

Nonetheless, if on one hand DNA damage can be in the genesis of cancer, on the other hand, it can be the solution to treat cancer (Figure 3) (30,35). In fact, chemo- and radiotherapeutic agents are DNA-damaging factors that lead to DNA lesions to induce cell death (27). These treatments revolutionized cancer treatment, but they have numerous negative effects on patients, can cause harm to healthy cells, and cells become resistant to them because of DDR (28,30). Thus, inhibiting specific DDR proteins can avoid cancer resistance to treatment and promote radiotherapy and chemotherapy efficacy (28). There are several DDR-inhibitor drugs that are already used in clinical practice, including topoisomerase inhibitors and poly(ADP-ribose) polymerase (PARP) inhibitors, and others in clinical trials (30,32).

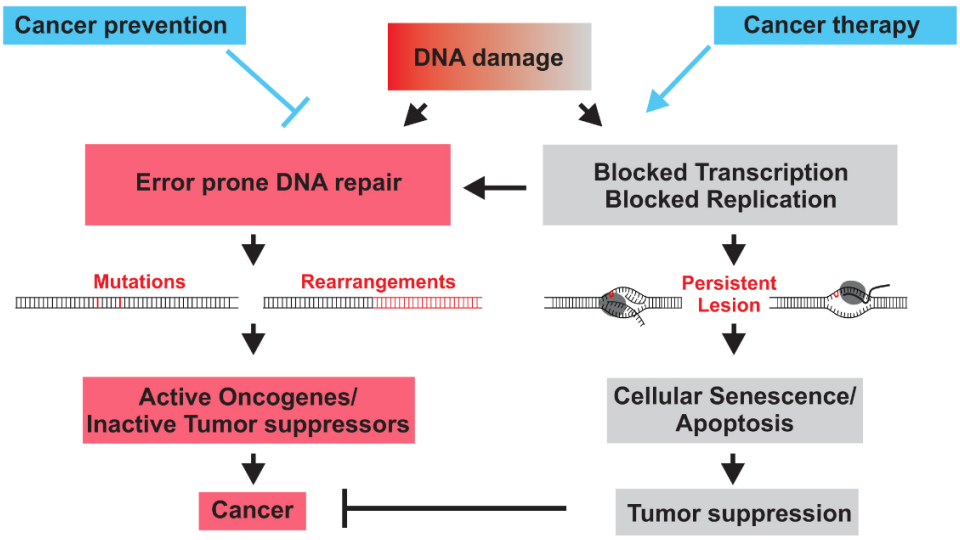

Figure 3- DNA damage response in carcinogenesis and in cancer treatment. From (36).

1.2 Breast cancer

1.2.1 Breast cancer classification

BC is a heterogeneous disease that can have different classifications according to its histological and molecular characteristics (Table 1). Based on molecular marks BC can be classified into luminal A, luminal B, human epidermal growth factor receptor 2 (HER2)-enriched, and triple negative breast cancer (TNBC) (36).

The luminal-like are the ones in which cells express estrogen receptors (ER, >1%) and/or progesterone receptors (PR, >20%) and usually are negative for HER2 (<10%) (37). Luminal A is the most common BC subtype, being responsible for almost half of all BC cases and the one with the best prognosis. This subtype presents low proliferation levels, whereas luminal B presents higher proliferative capacity, based on cell proliferation regulator (Ki67) values. Luminal B can be distinguished into HER2- and HER2+, accounting for 20-30% of BC cases (38,39).

The HER2-enriched subtype is found in 15-20% of BC patients. This class of tumors presents a high expression of HER2 and is negative for ER and PR (38).

TNBC is the least prevalent subtype of BC (10-20% of newly diagnosed cases), but the most aggressive one, with the worst prognostic. This subtype does not express any of the receptors mentioned before and presents high levels of Ki67 (38).

Table 1- Breast cancer molecular classification. Adapted from (37).

Molecular subtype	**Luminal A**	**Luminal B**		**HER2+**	**Triple negative**
		HER2-	**HER2+**		
Biomarkers	ER+, PR+, HER2-, Ki67 low	ER+, PR-, HER2-, Ki67 high	ER+, PR-/+, HER2+, Ki67 low/high	ER-, PR-, HER2+, Ki67 high	ER-, PR-, HER2-, Ki67 high
Cases frequency (%)	40-50	20-30		15-20	10-20
Histological grade	Well differentiated (grade I)	Moderately differentiated (grade II)		Little differentiated (grade III)	Little differentiated (grade III)
Prognosis	Good	Intermediate		Poor	Poor

*ER, estrogen receptor; PR, progesterone receptor; HER2, human epidermal growth factor receptor 2

1.2.2 Breast cancer treatment

Tumors are very heterogeneous at phenotypic, genetic, and epigenetic levels, promoting their escape to the standard treatments (25). As mentioned before, BC is a type of cancer that is especially heterogeneous, making its treatment a challenge in the clinical practice (40).

Over the past few years, with the understanding of BC biology and heterogeneity, progresses in finding new therapeutic options for this disease has been made, leading to the development of therapies personalized for each patient, that work more effectively (40).

BC treatment is directed to each subtype, and the most common types of treatment include surgery, radiation, chemotherapy, hormonal therapy, targeted therapy, and immunotherapy (41–43).

To treat luminal BC, the one expressing hormone receptors, endocrine therapy is used, acting by blocking the hormone effects or lowering their levels (40,41). There are several drugs with these purposes: tamoxifen, an estrogen receptor modulator that disables estrogen from binding to ER; aromatase inhibitors, that prevent the conversion of androgens to estrogens; luteinizing hormone-releasing hormone analogs, which suppress the ovary from producing hormone; and fulvestrant, a selective ER degrader (40,44). In some cases, these drugs can be used in combination (40).

For HER2-enriched subtype treatment, besides chemotherapy, a targeted therapy was developed, being used alone or together with chemotherapy (41,45). This targeted therapy directed to HER2 includes monoclonal antibodies (trastuzumab, pertuzumab), antibody-drug conjugates (ado-trastuzumab emtansine and fam-trastuzumab deruxtecan), and tyrosine kinase inhibitors (lapatinib and neratinib) (40,41,45,46).

TNBC is the one with the poorest prognosis, because of the lack of therapeutical options (47). In TNBC, cells do not express hormone receptors, neither HER2, so patients with this subtype do not benefit from hormonal therapy, nor HER2-targeted therapy, the ones mentioned before (47,48). In this way, the standard treatment for TNBC is still chemotherapy, usually anthracyclines (doxorubicin), alkylating agents (cyclophosphamide), taxanes, and antimetabolites (fluorouracil) (41,47). These drugs can be used in combination to reach better outcomes (41,45). Despite the good response to chemotherapy, patients with TNBC have higher recurrence and metastasis scores (40). Hence, it is of utmost importance to find new biomarkers that can predict the response of each patient to the treatment, and identify new therapeutic targets that can lead to more effective treatments, culminating in an increase in overall survival and 5-year survival rate (47–49).

1.3 Long non-coding RNAs

The human genome is composed of genes capable of being transduced into proteins, the coding genes, and others without protein-coding potential, the non-coding genes (50). The non-coding portion of the human genome was for many decades considered as “junk DNA” (50,51). However, with the advances in genomics technology, it was found that even this portion can produce RNA transcripts. In fact, the ENCODE project demonstrated that about 76% of the human genome is transcribed, but only less than 2% encodes proteins (52,53). Questions about the non-coding RNAs (ncRNAs) and their possible biological functions started to arise.

There are several different ncRNA classes, including transfer RNAs (tRNAs), ribosomal RNAs (rRNAs), small RNAs (sRNAs), and long non-coding RNAs (lncRNAs), with the last being the most abundant and diverse class (53). Indeed it is estimated that there are more than 16.000 lncRNA genes in the human genome, that contrary to mRNAs, do not encode proteins, but most of them are not described in the literature (54). These transcripts are characterized for having sequences with more than 200 nucleotides in length and for having little or any detectable open reading frame (ORF) (55,56). They can be classified according to their genomic location as: 1. sense lncRNA or 2. antisense lncRNA, when they overlap one or more exons of another transcript on the same or opposite strand, respectively; 3. intronic lncRNA, when derived from an intron of a second transcript; 4. intergenic lncRNA, when independent units are located in the genomic space between two genes; and 5. bidirectional lncRNA, when the expression of the lncRNA and a neighboring coding transcript on the opposite strand is initiated in close genomic proximity (57–59).

Most of all lncRNAs are transcribed by RNA polymerase II and capped at their 5’ end and then spliced and polyadenylated at their 3’ end, similar to mRNA (60,61). However, unlike mRNA, lncRNAs usually present low expression levels, tissue-specific expression patterns, being expressed in particular conditions and tissues, and poor conservation over time (53,62).

LncRNAs are a very heterogeneous RNA family that is implicated in diverse biological processes, including alternative splicing, epigenetic regulation, RNA decay, and translation, by controlling gene expression at transcriptional, translational, and post-translational levels (63–65). They are specially expressed in the nucleus and in the cytoplasm (63). In the nucleus, they regulate epigenetic and/or gene expression processes by modulating chromatin conformation and interacting with transcription factors (63,66). Whereas in the cytoplasm they have the ability to bind RNA binding proteins (RBPs) and messenger RNA (mRNA), regulating their activity and abundance, and they serve as sponges to miRNAs by acting as competitive endogenous RNA, hindering them from binding to their mRNAs targets (53,63).

1.3.1 Long non-coding RNAs in cancer

Besides having an important role in physiological functions, over the last years, lncRNAs have been described as important players in pathological conditions as well, namely in cancer (67,68). In fact, some lncRNAs were identified because of their high expression in some cancers (69). For example, metastasis-associated lung adenocarcinoma transcript 1 (MALAT1) was found due to its high expression in metastatic lung cancer cells (51).

Several studies show that lncRNAs can promote oncogenic cell proliferation and metastasis, by regulating oncogenes and tumor suppressor genes or acting themselves as these genes (53,70). Actually, lncRNAs can be up or downregulated in the TME influencing critical biological functions that are closely related to tumorigenesis and tumor progression, including proliferation, apoptosis, metastasis, genomic stability, and inflammation, by participating in or regulating several pathways that are altered in cancer (Table 2) (61,63,71).

The presence of lncRNAs in the TME makes them a current potential treatment strategy to treat cancer (21). Therefore, exploring the role of lncRNAs in cancer may lead to the understanding of mechanisms behind physiological and pathological processes, and to the discovery of new cancer biomarkers and new potential therapeutic targets, making it possible to overcome the resistance to cancer treatment (72,73). In fact, there are studies that have already shown the potential of lncRNAs as diagnostic and prognostic biomarkers in breast cancer, prostate cancer, pancreatic cancer, gastric cancer, bladder cancer, and others (71). For example, the differential display code 3 (DD3), also known as prostate cancer antigen 3 (PCA3), is a lncRNA overexpressed in prostate cancer that is already used as a clinical biomarker for this cancer (74).

Table 2- LncRNAs and their roles in several cancers.

lncRNA	Cancer type	Expression	Phenotype	References
MALAT1	Lung cancer	Up	Promotes proliferation, mobility, migration, and invasion of cancer cells	(75)
	Prostate cancer	Up	Drives PCa cell metastasis and proliferation, and invasion	(76,77)
	Thyroid cancer	Up	Inhibits inflammatory cytokines release, promotes proliferation, migration, and invasion of cells, and induces vasculature formation	(78)
	CRC	Up	Enhances cancer progression, growth, and metastasis	(79)
	DLBCL	Up	Increases proliferation, migration, and immune escape, and decreases apoptosis	(80)

Table 3 (continuation)- LncRNAs and their roles in several cancers.

HOTAIR	HCC	Up	Unfavorable prognosis, lymph node metastasis, and involved in the progression and recurrence of HCC	(81,82)
	Cervical cancer	Up	Advanced pathological stage, histology, lymph node invasion, lymphatic metastasis, and shorter overall survival	(83)
	Gastric cancer	Up	Promotes tumor escape	(84)
XIST	Esophageal cancer	Up	Oncogenic progression	(85)
	Gastric cancer	Up	Cell growth and invasion	(86)
	CRC	Up	Worse survival rates, higher lymphatic metastasis, shorter life cycles, and lower differentiation	(87)
	Pancreatic cancer	Up	Cell growth, migration, and invasion	(88)
	HCC	Up	Cell proliferation	(89)
NEAT1	HCC	Up	Tumor growth	(90)
GNAS-AS1	NSCLC	Up	Migration and invasion of non-small cell lung cancer, and decreased overall survival	(91)
LINC00926	BC	Down	Cell proliferation, invasion, and metastasis	(92)
FENDRR	HCC	Down	Potentiates tumorigenicity and cell growth in hepatocellular carcinoma	(93)
GAS5	BC	Down	Lymph node metastasis, tumor recurrence, decreased survival rates, and chemotherapy resistance	(94)
	CRC	Down	Larger tumor size and more advanced tumor-node-metastasis (TNM) staging	(95)
	Liver cancer	Down	Increases cell proliferation and cell resistance to doxorubicin	(96)

*CRC, colorectal cancer; *DLBCL, diffuse large B cell lymphoma; HCC, hepatocellular carcinoma; NSCLC, non-small cell lung cancer; BC, breast cancer

1.3.2 *NORAD*: the long non-coding RNA induced by DNA damage

The non-coding activated by DNA damage (*NORAD*), also known as *LINC00657*, is an abundant, highly conserved lncRNA with 5,3 kb, ubiquitously expressed predominantly in the cytoplasm of the cells (56,63). This lncRNA is located on chromosome 20, loci 20q11.23, and comprises one exon (56,97). It was first described by Lee et al. when exploring the role of lncRNAs as regulators of genomic stability (62,63).

Pieces of evidence show that *NORAD* is required to maintain genome stability and proper mitotic divisions in human cells by binding to pumilio proteins and negatively regulating them (54,63,65). In *NORAD* knockdown (KD) cells, they present a chromosomal instability (CIN) phenotype, characterized by a variable number of chromosomes, an increased frequency of tetraploidization, and a high rate of mitotic errors (63,98). However, when *NORAD* expression levels are restored, this phenotype is reverted (56).

1.3.3 *NORAD* and the interaction with pumilio proteins

Pumilio proteins are part of the Pumilio-FEM3-binding factor (PUF) protein family, a conserved family of RBPs that repress gene expression. There are two different pumilio proteins in humans- pumilio homolog 1 (PUM1) and pumilio homolog 2 (PUM2)- which are implicated in crucial biological processes like mitosis regulation, germline homeostasis, and neuronal activity and function (54,63). These proteins regulate mRNA expression and translation by binding to pumilio recognition element (PRE)- UGUANAUA- present in mRNA 3' untranslated regions (3' UTRs), their non-coding parts, leading to mRNA deadenylation, decapping and degradation (54,64,68).

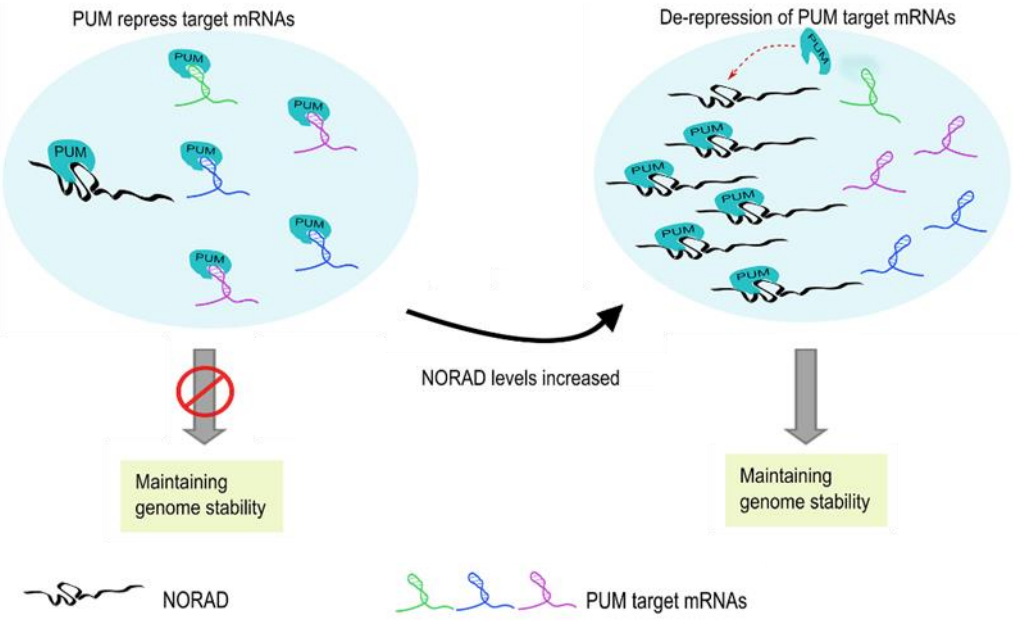

Figure 4- *NORAD* role in genomic stability maintenance by interacting with pumilio proteins. Adapted from (55).

Several studies point out that *NORAD* contains 18 PREs so, upon DNA damage, *NORAD* expression increases and pumilio proteins instead of binding to mRNA PREs bind to *NORAD* PREs, which are capable of sequestering almost all the pool of PUM1 and PUM2 in the cell (65). In this way, *NORAD* functions as a scaffold for pumilio proteins, blocking their activity and allowing pumilio targets activation, promoting adequate mitosis, DNA repair, and DNA replication regulation, and consequently genomic stability (Figure 4) (63,64). In the absence of *NORAD*, pumilio proteins lose their scaffold and are present in the cell in a hyperactivity state, repressing their mRNA targets and thus eliciting genomic instability (63,65).

1.3.4 *NORAD* in cancer

The effects described upon *NORAD* KD in cells, including chromosome segregation defects and altered cell-cycle progression, are important drivers of tumorigenesis, with *NORAD* being pointed as a player in diverse types of cancer (63,99). Besides this, this lncRNA has been described as having a pivotal role in numerous pathways, many of them related to cancer, including STAT, TGF-β, Akt/mTOR, and PI3K/AKT pathways (Table 3) (100). Consequently, the role of lncRNA *NORAD* in the physiopathology of cancer, its role as a predictive and prognostic biomarker in cancer, and as a therapeutical option started to be questioned and studied.

Zhao and his colleagues explored the role of *NORAD* in the development of renal cancer and found out that *NORAD* expression is upregulated in renal cancer cells and tissues, contrary to miR-144-3p expression. This study revealed the miR-144-3p as a target of *NORAD*, and MYCN, a member of the MYC family responsible for regulating cell cycle, cell proliferation and differentiation, and apoptosis, as a target of the miRNA. In this way, with *NORAD* overexpression, MYCN is overexpressed as well, contributing to renal cancer cell growth and differentiation. This shows the potential of *NORAD* as a new therapeutical target for preventing and treating renal cancer (101).

In another study, the role of *NORAD* in human osteosarcoma was evaluated and another *NORAD* target, miR-199a-3p, was found. As in renal cancer, *NORAD* is upregulated in osteosarcoma and its inhibition causes lower proliferation and invasion of cancer cells both *in vitro* and *in vivo*. *NORAD* binding to miR-199a-3p leads to osteosarcoma cells proliferation and invasion. Further studies may demonstrate *NORAD*'s prognostic value in human osteosarcoma (102).

There are several studies about lncRNA *NORAD* in BC, but its role in this disease remains controversial (103). Most of the studies describe that *NORAD* is upregulated in BC cells and tissues, functioning as an oncogene (97). The same studies reveal the interaction between this lncRNA and an extensive variety of genes and signaling pathways, leading to BC progression, and to a worse

overall survival rate (56,100,103). For example, besides finding an aberrant *NORAD* expression in BC tissues, Zhou et al. found that the inhibition of this lncRNA expression suppresses BC cell proliferation, migration, and invasion, and that *NORAD* regulates TGF-β signaling pathway, increasing TGF-β and downstream factors expression, like Smad2 and RUNX2, leading to BC progression (104). However, Liu et al. and Tan et al. describe *NORAD* as being downregulated in BC, and that this reduction in *NORAD* levels is associated with adverse pathological features in patients (105,106).

Table 3- LncRNA *NORAD* expression and function in cancer.

Cancer type	Expression	Target genes/ pathways	Function	References
Breast cancer	Up	miR-323a-3p, PUM1/eIF2; TGF-β/RUNX2	Poor prognosis, cell proliferation, invasion, and migration, and reduced disease-free survival	(103,104)
	Down	miR-155-5p/SOCS1; YAP/TAZ-TEAD	Cell proliferation, migration and invasion, lymph node metastasis, and poor prognosis	(105,106)
Renal cancer	Up	miR-144-3p/MYCN	Higher cell viability and migratory potential in cancer cells	(101)
Gastric cancer	Up	miR-214, Akt/mTOR; miR125a-3p, RhoA/ROCK; miR-608, FOXO6	Tumor cell proliferation and apoptosis inhibition	(99,107,108)
Bladder cancer	Up	PUM2, E2F3	Worse tumor stage, histological grade and overall survival, and lymph node metastasis	(109)
Osteosarcoma	Up	miR-199a-3p	Cell proliferation and invasion	(102)
HCC	Up	Bax, Bcl-2, miR-144-3p; miR-202-5p, TGF-β	Cell proliferation, colony formation, and apoptosis	(110,111)
Pancreatic cancer	Up	miR125a-3p, RhoA/ROCK	Epithelial-mesenchymal transition, poor prognosis	(112)

Table 3 (continuation)- LncRNA *NORAD* expression and function in cancer.

ESCC	Up	-	Reduced overall survival, increased tumor size, and higher UICC stage	(113)
CRC	Up	miR-202-5p; miR-106a	Cell proliferation, migration and invasion, and poor prognosis	(114–116)
	Down	PI3K/Akt, CAPN7	Worse prognosis, advanced tumor size, and TNM stage	(117)
Ovarian cancer	Up	miR-199a-3p	Higher proliferation, migration, and invasion of cells	(118)
Cervical cancer	Up	miR-590-3p, SIP1	Advanced FIGO stage, lymph node metastasis, and vascular invasion, and poor overall survival	(119)
Malignant melanoma	Up	miR-205/EGLN2	Cell migration and invasion	(120)
Prostate cancer	Up	miR-495-3p/TRIP13	Cell migration, proliferation, and invasion	(121)
Lung cancer	Up	CXCL12/CXCR4 and RhoA/ROCK	Cell proliferation and migration	(122)
Endometrial cancer	Down	FUBP1	Cancer cells progression	(123)
Neuroblastoma	Up	-	Poor prognosis	(124,125)
Thyroid carcinoma	Up	miR-202-5p	Cell proliferation and migration	(126)

*ESCC, esophageal squamous-cell carcinoma

1.4 Objectives

Over the past years, the role of lncRNAs in physiology and pathology has been described, with them being pointed as key players in carcinogenesis, and consequently as potential biomarkers and therapeutical targets. The lncRNA *NORAD* is not an exception and several evidence demonstrate that *NORAD* participates in some cancers development and progression. However, its participation in BC physiopathology and response to treatment is not well established, existing some uncertainty rounding this topic.

Therefore, considering *NORAD*'s contributions to genomic maintenance and in the physiopathology of several cancers and the need to find new therapeutic options for BC, the working hypothesis of this project is that *NORAD* may modulate mechanisms related to BC, consequently affecting the response to chemotherapy. Hence, the main objective is to investigate how differential expression of *NORAD* might constitute a prognostic and predictive biomarker in BC. To achieve this, three specific aims were established:

1. To assess whether *NORAD* expression levels are associated with tumor aggressiveness and oncogenic transformation by measuring its levels on tissues of patients with different subtypes of BC;

2. To assess *NORAD* localization and expression under different conditions on TNBC cell lines (MDA-MB-468 and MDA-MB-231);

3. To evaluate the effect of *NORAD* downregulation on the sensitivity of BC cells to a chemotherapeutic agent used in the clinical practice, doxorubicin, through the quantification of DNA damage levels and cellular apoptosis on a human epithelial BC cell line (MDA-MB-231).

2 Methods

2.1 Normal and breast cancer tissue samples

The BC and adjacent tissues were generously offered by Dra. Catarina Alves Vale, MD (Hospital CUF Descobertas, Lisbon, Portugal), after study approval (Project "RefªCE - JMS/is – Estudo 64") by the Ethics Committee of CUF Descobertas Hospital. Clinicopathological information was collected and slides from the selected cases were performed for further immunohistochemistry (IHC) characterization by a pathologist with experience in breast cancer pathology. Once tissue quality was assessed and the diagnosis was confirmed, representative sections of tumor and control were extracted from formalin-fixed paraffin-embedded (FFPE) samples. These samples were divided into normal without chemotherapy (control), TNBC without neoadjuvant chemotherapy (NACT), TNCB with high and low response to therapy, luminal low recurrence score (RS), and luminal high RS.

2.2 Cell culture

The human BC cell lines MDA-MB-231 and MDA-MB-468 used in this study were generously offered by Dr. Sérgio Dias (Instituto de Medicina Molecular João Lobo Antunes, Lisbon, Portugal). These cells were cultured in Dulbecco's Modified Eagle Medium (DMEM; Gibco, Paisley, UK), supplemented with 10% (v/v) fetal bovine serum (FBS; Gibco, Paisley, UK) and 1% (v/v) penicillin-streptomycin (Pen/Strep; 100U/mL:100 µg/mL; Gibco, NY, USA) in a 5% CO_2 humidified incubator at 37.ºC. During all experiments, cells were maintained in these conditions.

When cells reached a 70-80% confluence, they were detached with 0.05% trypsin-EDTA (Gibco, Paisley, UK) that was then inactivated with the culture medium mentioned above. Cells were centrifuged at 300*g* for 3 minutes and subcultured at an appropriate ratio.

To freeze cells, these were trypsinized and centrifuged at 300*g* for 3 minutes, with the supernatant being discarded after centrifugation. The cellular pellet was resuspended in 90% FBS and 10% DMSO (Sigma-Aldrich, MO, USA), being stored at -80ºC.

All cell manipulation procedures were performed in a sterile environment inside a laminar flow chamber.

2.3 RNA extraction, cDNA synthesis and RT-qPCR

To assess *NORAD, PUM1, PUM2, BUB3, MCM6, PARP1,* and *CDK1* expression levels in control and BC tissues, and in TNBC cells, real-time quantitative reverse transcriptase polymerase chain reaction (RT-qPCR) was performed.

Total RNA was extracted from the tissues through the PureLink™ FFPE Total RNA Isolation Kit (Invitrogen™, CA, USA). First, the FFPE tissues were deparaffinized using a melting buffer and proteinase K, and then the tissues lysate was separated from paraffin by centrifugation, for 1 minute at 15.000*g*. Binding buffer and 100% (v/v) ethanol were added to tissues lysate and passed through a spin cartridge in a collection tube, being centrifugated for 1 minute at 800*g*, twice. The flow through was discarded and the cartridge was washed three times with wash buffer with ethanol, and centrifugated for 1 minute at 15.000*g*. In the end, the RNA was eluted in RNase-free water. From TNBC cells, total RNA was isolated using GRS Total RNA Kit (GRiSP, Porto, Portugal) as described in the manufacturer's protocol. Briefly, the cellular pellet was incubated for 5 minutes with buffer R1 and β-mercaptoethanol (Carl Roth, Karlsruhe, Germany) and filtered through a column by centrifugation, 1 minute at 1.000*g*. Then 70% (v/v) ethanol was added to the filtrate and passed through a spin column by centrifugation for 2 minutes at 16.000*g*, twice. The spin column was washed with wash buffer 2 and centrifuged at 16.000*g* for 30 seconds, with DNase I reaction buffer and DNase I solution being added after and incubated for 15 minutes. Later the spin column was washed again with wash buffer 1 and 2, and after some centrifugations, the RNA was eluted with RNase-free water. The quality and quantity of RNA were assessed using NanoDrop spectrophotometer (DeNovix, Wilmington, USA), measuring the absorbance at 230 nm, 260 nm, and 280 nm, particularly based on the $A_{260/280}$ and $A_{260/230}$ ratios.

Then, cDNA synthesis was performed with 500ng-1µg of RNA using oligo$(dT)_{12-18}$, random hexamer mix, and dNTP mix from NZY First-Strand cDNA Synthesis Flexible Pack (NZYTech, Lisboa, Portugal). After adding reaction buffer, NZY ribonuclease inhibitor, and NZY reverse transcriptase the reaction occurred in a T100 PCR thermal cycler (BioRad, CA, USA). The program on thermocycler consists of 10 minutes at 25ºC, 50 minutes at 50ºC and to finish five minutes at 85ºC.

Finally, the *NORAD*, *PUM1*, and *PUM2* mRNA levels were measured in both tissues and cells, whereas *BUB3*, *MCM6*, *PARP1*, and *CDK1* mRNA levels were only measured in cells, through RT-qPCR. Each real-time PCR reaction was performed in duplicate using SYBR Green PCR Master Mix (Applied Biosystems, CA, USA) in a final volume of 15µL containing 5µL of cDNA in the 7500 Real-Time PCR System (Applied Biosystems, CA, USA). The program consists of a two-step holding stage, with the first being performed at 50ºC for two minutes, and the second at 95ºC for 10 minutes, followed by 40 cycles of 15 seconds of denaturation at 95ºC and a 1-minute combined annealing and extension step at 60ºC. The relative expression levels of these genes were defined using the $2^{-\Delta\Delta Ct}$ method and 18s rRNA was used as an internal reference.

Table 4- Sequences of the primers used in this study

Primers	Sequences
***NORAD* 4**	Forward: 5'- TGATAGGATACATCTTGGACATGGA-3'
	Reverse: 5'- AACCTAATGAACAAGTCCTGACATACA-3'
PUM1	Forward: 5'- CCGGGCGATTCCTGTCTAA-3'
	Reverse: 5'- CCTTTGTCGTTTTCATCACTGTCT-3'
PUM2	Forward: 5'- GGGAGCTTCTCACCATTCA-3'
	Reverse: 5'- CCATGAAAACCCTGTCCAGATC-3'
BUB3	Forward: 5'- GGTTCTAACGAGTTCAAGCTG-3'
	Reverse: 5'- GGCACATCGTAGAGACGCAC-3'
MCM6	Forward: 5'- GAGGAACTGATTCGTCCTGAG-3'
	Reverse: 5'- CAAGGCCCGACACAGGTAAG-3'
PARP1	Forward: 5'- ATCCACCTCATCGCCTTTTC-3'
	Reverse: 5'- GCAGAGTATGCCAAGTCCAACAG-3'
CDK1	Forward: 5'- TTTTCAGAGCTTTGGGCACT-3'
	Reverse: 5'- CCATTTTGCCAGAAATTCGT-3'
18s rRNA	Forward: 5´ - GGATGTAAAGGATGGAAAATACA - 3'
	Reverse: 5' - TCCAGGTCTTCACGGAGCTTGTT - 3'

2.4 *NORAD*, PUM1 and PUM2 knockdown

MDA-MB-231 and MDA-MB-468 cells were seeded in culture plates, with *NORAD* knockdown being achieved by using 1 siRNA and 1 antisense LNA GapmeR with the following sequence: 5'-CTAGACGTAAATTAGG- 3'. For PUM1 and PUM2 knockdown, 2 siRNAs were used, one for each. A scramble siRNA, directed to non-specific sequences, was used as the negative control. All the siRNAs and the LNA™ GapmeR were used at a final concentration of 25 nM. Knockdown was achieved by transfecting twice with a 24 hours interval, using Lipofectamine™ RNAiMAX (Invitrogen™, CA, USA).

Table 5- Sequences of the siRNAs used in this study.

Target mRNA	Sequence (5'-3')	Reference
NORAD	CUGUGUAUAUAGCGGACAA	Lincode SMARTpool Human LOC647979 038095-00-0010 (Dharmacon)
	CAUCUAAGCUUUACGAAUG	
	AGUGCACAAUGUAGGUUAA	

Table 5 (continuation)- Sequences of the siRNAs used in this study.

	CGACCCAAGCCUCGACGAA	
PUM1	GGUCAGAGUUUCCAUGUGA	ON-TARGETplus SMARTpool L-014179-00-0005 (Dharmacon)
	GGAGGAGGCGGCUAUAAUA	
	GGAGAUAAGCUAGGAGAUU	
	CGGAAGAUCGUCAUGCAUA	
PUM2	CUGAAGUAGUUGAGCGCUU	ON-TARGETplus SMARTpool L-014031-02-0005 (Dharmacon)
	GCAGAGUAAUUCAGCGCAU	
	GACAAAUGGUAGUGGUCGA	
	AGACAUAACAGUAACACGA	

2.5 RNA Fluorescence *In Situ* Hybridization (FISH)

To assess *NORAD* localization and expression in TNBC cells, MDA-MB-231 and MDA-MB-468 cells were seeded on 24-well plates coated with 0.1% gelatin, $4x10^4$ cells/well and $5x10^4$ cells/well, respectively. Four treatment conditions were performed: untreated, treated with scramble siRNA, silenced for *NORAD*, and silenced for PUM2. Coverslips were washed with PBS, permeabilized, and fixed according to the Stellaris® RNA FISH Protocol for Adherent Cells. After fixation, cells were washed with wash buffer (80% SSC 2X, 10% formamide, and 10% nuclease-free water) and hybridization was performed using hybridization buffer (90% Stellaris RNA FISH Hybridization Buffer and 10% deionized formamide) containing *NORAD* probe and other containing MALAT1 probe. Both are Stellaris® FISH probes labeled with Quasar® 570 dye. *MALAT1* was used as the positive control. Coverslips were mounted onto the slides using Vectashield Mounting Medium containing 4',6-diamidino-2-phenylindole (DAPI; Vector Laboratories, CA, USA), and kept at 4ºC until microscope visualization. Images were acquired using an inverted confocal laser scanning microscope, Zeiss LSM 880 with Airyscan (Carl Zeiss, Göttingen, Germany).

To try to optimize the protocol the cells were permeabilized with 0,5% (v/v) Triton X-100 (Sigma-Aldrich, MO, USA) for 10 minutes, instead of using 70% (v/v) ethanol. Besides this, instead of using 1µL of the probe in 100µL of hybridization buffer, 2µL were added.

2.6 *NORAD*, PUM1, and PUM2 knockdown and treatment with doxorubicin

MDA-MB-231 cells were seeded in 24-well plates at a density of $4x10^4$ cells/well and transfected for *NORAD*, PUM1, and PUM2 knockdown, as previously explained. 24h after the second transfection, the medium was replaced, and doxorubicin was added to each well to a final desired

concentration (0.1, 0.6 and 5.0μM). On the following day, the medium with doxorubicin was replaced by fresh medium, and the intended analysis was performed.

2.7 Single-cell gel electrophoresis assay- Comet assay

To evaluate if *NORAD* knockdown increases DNA damage in TNBC cells treated with doxorubicin, DNA damage levels were measured by the comet assay. First, MDA-MB-231 cells were divided into different wells of 24-well plates, silenced for *NORAD*, PUM1 and PUM2, and treated with doxorubicin, as mentioned before. After the treatments, cells were harvested and washed with PBS. Finally, cells were resuspended at a final concentration of $1x10^5$ cells/mL in PBS. The Alkaline CometAssay® was performed using CometAssay® Reagent Kit for Single Cell Gel Electrophoresis Assay (Catalog # 4250-050-K) following the manufacturer's instructions. Slides were visualized under the optical microscope Zeiss Axio lmager Z1 (Carl Zeiss, Göttingen, Germany). Images were analyzed with CometScore software (TriTek Corporation, v2.0.0.38).

2.8 Cell apoptosis analysis

To assess cell apoptosis after silencing *NORAD* and doxorubicin treatment, the annexin V levels were analyzed by flow citometry using an Annexin V Apoptosis Detection Conjugate (Thermo Fisher Scientific, A35110). Cells were trypsinized, centrifuged at 300*g* for 5 minutes, washed with PBS, and resuspended in 1x binding buffer solution at a final concentration of $1x10^6$ cells/mL. Then 2.5μL of Annexin V-APC conjugate was added to each 100μL of cell suspension and incubated for 15 minutes at RT in the dark. After incubation, 400μL of 1x binding buffer solution was added, cells were transferred to FACS tubes and analyzed in an Accuri C6 Flow Cytometer (BD Biosciences, USA). The data analysis was conducted using the FlowJo software (v10; BD Biosciences, USA).

2.9 Statistical analysis

Statistical analysis was performed using GraphPad Prism software (v9.0.0.121, GraphPad Software, San Diego, CA, USA). First, the normality of the data was evaluated through the Shapiro-Wilk test. Since non-normality was achieved by the data, all multiple comparisons were performed using the non-parametric Kruskal-Wallis test for multiple comparisons. Statistically significant results were considered if $p<0.05$.

3 Results

3.1 *NORAD, PUM1* and *PUM2* expression profiles in human breast cancer tissues

Since there are contradictory studies about *NORAD* expression levels in human BC, its levels, along with *pumilio* transcripts levels, were assessed in human BC tissues (104,105). To evaluate the expression profiles of the lncRNA *NORAD* and *pumilio* transcripts (*PUM1* and *PUM2*) by RT-qPCR, breast cancer tissues and healthy tissues from the adjacent tumor area (control) were used. Tumor samples were divided based on cancer subtype and some clinical features. Thus, the following categories were defined: RS, NACT, and response to treatment, into luminal high and low RS, TNBC without NACT, and TNBC with high and low response to treatment.

There is no significant alteration in *NORAD* expression levels among the tissue's samples (Figure 5). However, it was observed that tumor tissues had a tendency to have higher *NORAD* expression levels, particularly tissues from patients with TNBC treated without NACT, where *NORAD* levels increase 125%, and with more aggressive tumors including luminal BC with high RS and TNBC with low response to treatment, with an increase of more than 200% and 140%, respectively.

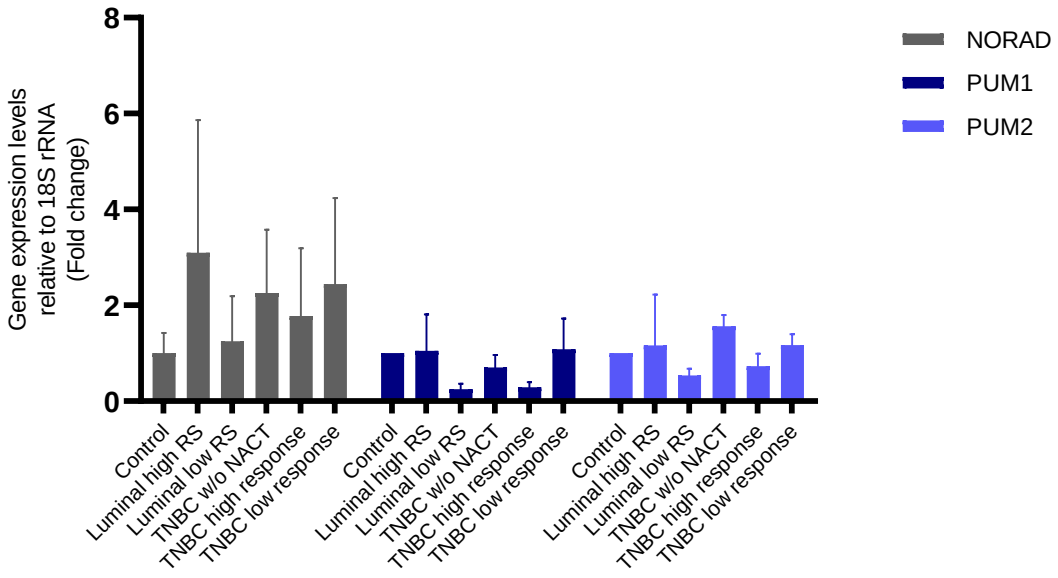

Figure 5- *NORAD, PUM1,* and *PUM2* expression levels in BC tissues. *NORAD*, PUM1, and PUM2 levels were measured by RT-qPCR in normal breast tissue (control, n=3) and BC tissues (luminal high RS, n=3; luminal low RS, n=4; TNBC w/o NACT, n=3; TNBC high response, n=2; TNBC low response, n=2). In all graphs, bars represent the mean values, and the error bars corresponds to the standard deviation. For statistical analysis was used Kruskal-Wallis with a control condition for multiple comparisons. No-symbol p>0.05.

Like *NORAD* levels, there are no significant differences in *PUM1* and *PUM2* levels between the different tissues. Yet, the expression levels of both *pumilio* transcripts follow an identical profile, with their expression levels in BC tissues not varying from the control tissue, except in tissues from patients with luminal low RS and TNBC with high response to treatment. In these tissues, *pumilio* levels tend to be lower than in the others, particularly *PUM1* transcripts that have a more pronounced decrease, 75% in luminal low recurrence score and 70% in TNBC high response.

These results suggested that more aggressive BC tumors and tumors that don't benefit from NACT have higher expression levels of *NORAD* when compared to healthy tissues, while tissues from luminal BC with a low recurrence score and TNBC with high response to treatment have low levels of *PUM1* and *PUM2* transcripts.

3.2 *NORAD, PUM1* and *PUM2* expression levels upon knockdown in triple negative breast cancer cell line

To address the objectives of this work, *NORAD*, PUM1 and PUM2 were silenced in TNBC cells lines. Therefore, MDA-MB-231 cell line was transfected with a LNA GapmeR directed to *NORAD* and with siRNAs directed to *NORAD*, PUM1, and PUM2, individually. The knockdown effectiveness was analyzed by RT-qPCR (Figure 6A, B and C). All transcripts' expression levels

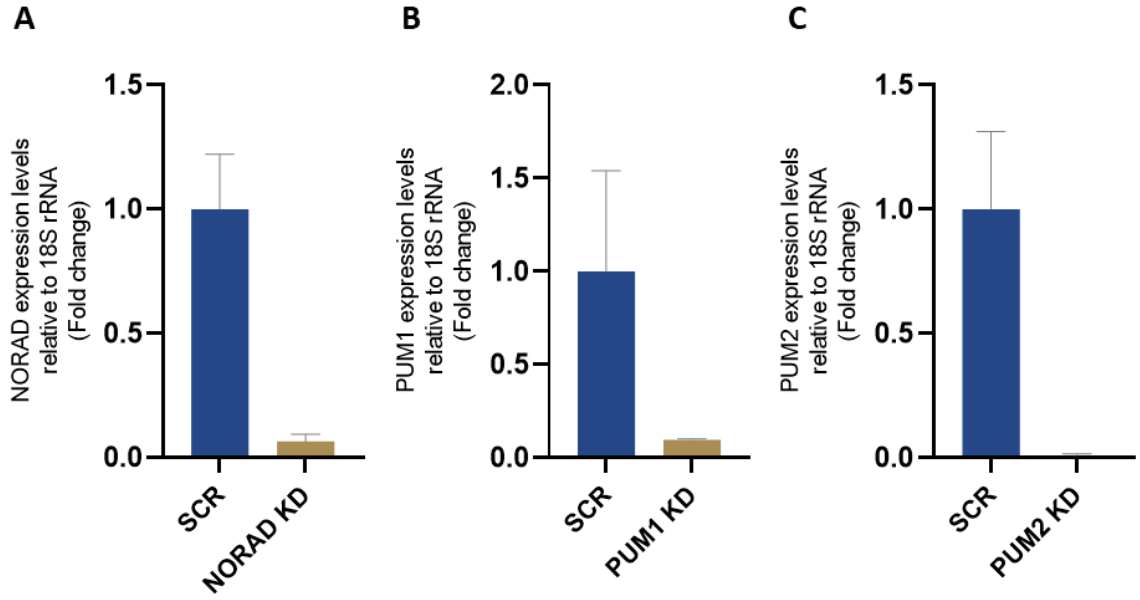

Figure 6- *NORAD, PUM1,* and *PUM2* expression levels in TNBC cells. *NORAD* (A), PUM1 (B), and PUM2 (C) levels were measured by RT-qPCR in MDA-MB-231 cells (n=2). In all graphs, bars represent the mean values, and the error bars corresponds to the standard deviation. For statistical analysis was used Kruskal-Wallis with a control condition for multiple comparisons. No-symbol p>0.05.

decreased near zero, proving that the transfection occurred and *NORAD*, PUM1, and PUM2 were silenced in those cells.

3.3 FISH protocol optimization

The lncRNA *NORAD* has been described as a cytoplasmatic lncRNA, however, some studies show its expression in the nucleus as well (56,127). Thus, FISH assay was performed to clarify this point.

The human epithelial BC MDA-MB-231 and MDA-MB-468 cell lines are widely used to study TNBC (128). Despite both are TNBC derived cell lines, they are different in some physiological aspects. MDA-MB-231 cells present a Ki67 and claudin-low profile, whereas MDA-MB-468 cells have a high expression of Ki67 and respond better to chemotherapy (129). Throughout this project, the preferable cell line chosen was MDA-MB-231. However, MDA-MB-468 presents higher *NORAD* expression levels and a bigger cytoplasm compared to MDA-MB-231, facilitating *NORAD* visualization when performing FISH (128,130). In this way, for optimizing this technique protocol

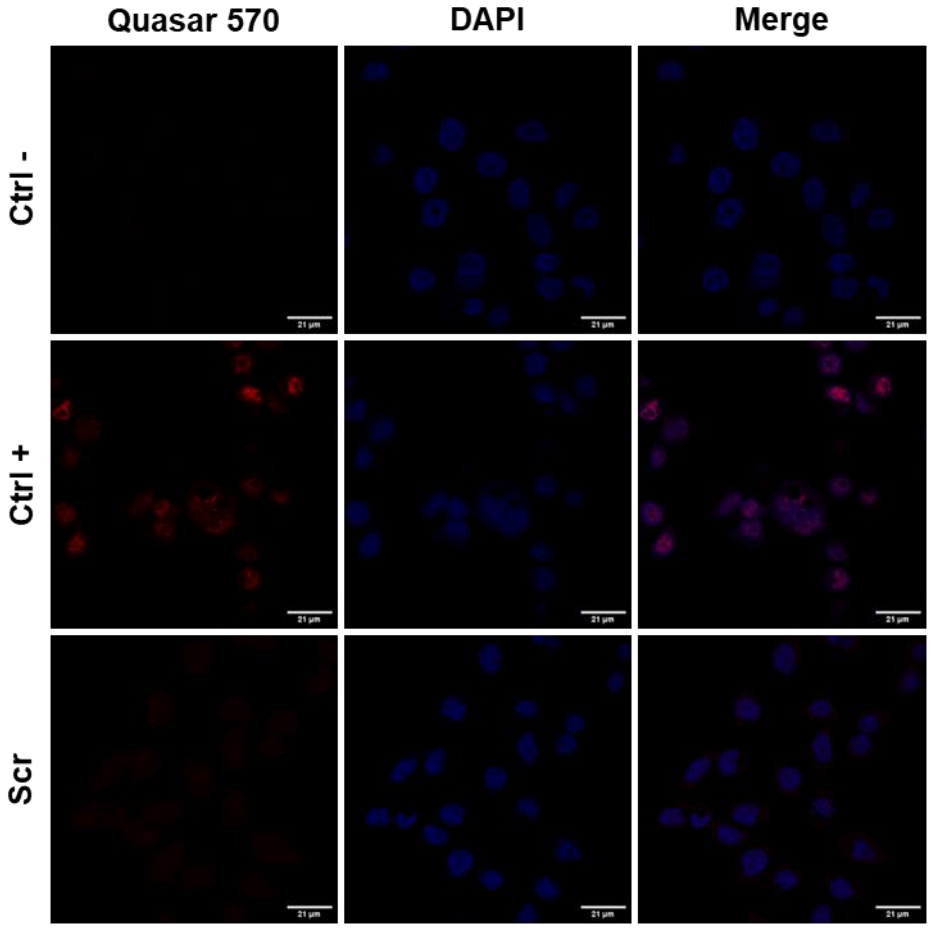

Figure 7- RNA FISH protocol to detect *NORAD* in MDA-MB-468 cells. Confocal images of RNA FISH in MDA-MB-468 cells using a MALAT1 probe in positive control and a *NORAD* probe in scramble, both labeled with Quasar 570. Quasar 570 signal in red, DAPI counterstain in blue.

all the procedures were done utilizing MDA-MB-468.

First, the protocol was performed following manufacturer's instructions. Cells were permeabilized with ethanol 70% (1h) and incubated with hybridization buffer (4h). Upon visualization of the samples under confocal microscope, it was only possible to observe staining in the positive control (Figure 7). The scramble condition and the negative control did not show any *NORAD* staining. So, it was not possible to detect any *NORAD* expression in these conditions.

Therefore, to try to detect *NORAD* expression some changes in the protocol were applied. The permeabilization time was increased to 4 days instead of 1 hour, probe concentration was duplicated, and hybridization time was set to 16 hours. No changes were detected in the confocal images when compared to the images from the first protocol (Figure 8). Nevertheless, positive control presented a more intense staining.

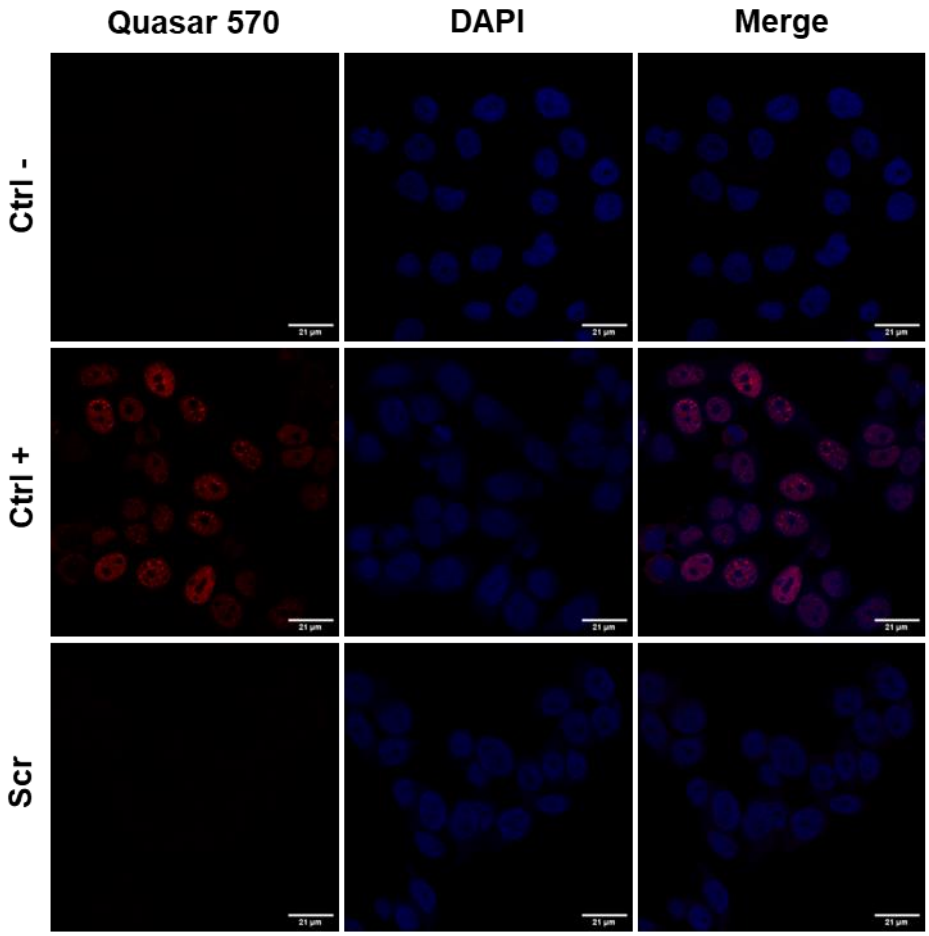

Figure 8- RNA FISH protocol to detect *NORAD* in MDA-MB-468 cells, after increasing permeabilization time. Confocal images of RNA FISH in MDA-MB-468 cells using a MALAT1 probe in positive control and a *NORAD* probe in scramble, both labeled with Quasar 570. Quasar 570 signal in red, DAPI counterstain in blue.

To optimize the protocol, the cells permeabilization method was altered. In this way, all the alterations mentioned before were kept, but cells were permeabilized using 0,5% Triton X-100 for 10 minutes, instead of using ethanol 70%. With this new approach, it was possible to detect *NORAD* in the cytoplasm of MDA-MB-468 cells (Figure 9).

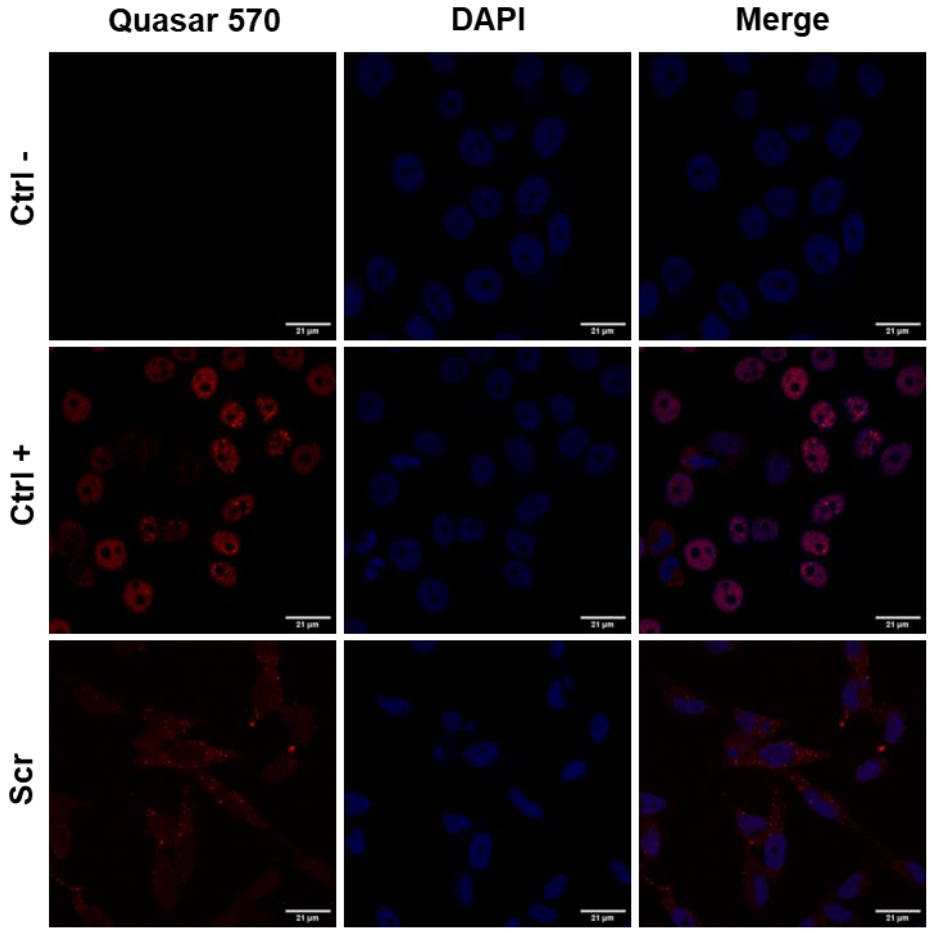

Figure 9- *NORAD* localization and expression in MDA-MB-468 cells, after changing permeabilization method. Confocal images of RNA FISH in MDA-MB-468 cells using a MALAT1 probe in positive control and a *NORAD* probe in scramble, both labeled with Quasar 570. Quasar 570 signal in red, DAPI counterstain in blue.

After optimizing the protocol in the MDA-MB-468 cell line, *NORAD* localization in the MDA-MB-231 cells was questioned. Although it was possible to detect *NORAD* in the scramble condition, the staining intensity was low (Figure 10). In this way, the work plan was followed using MDA-MB-468 cell line when performing FISH to evaluate *NORAD* localization and expression upon pumilio proteins knockdown.

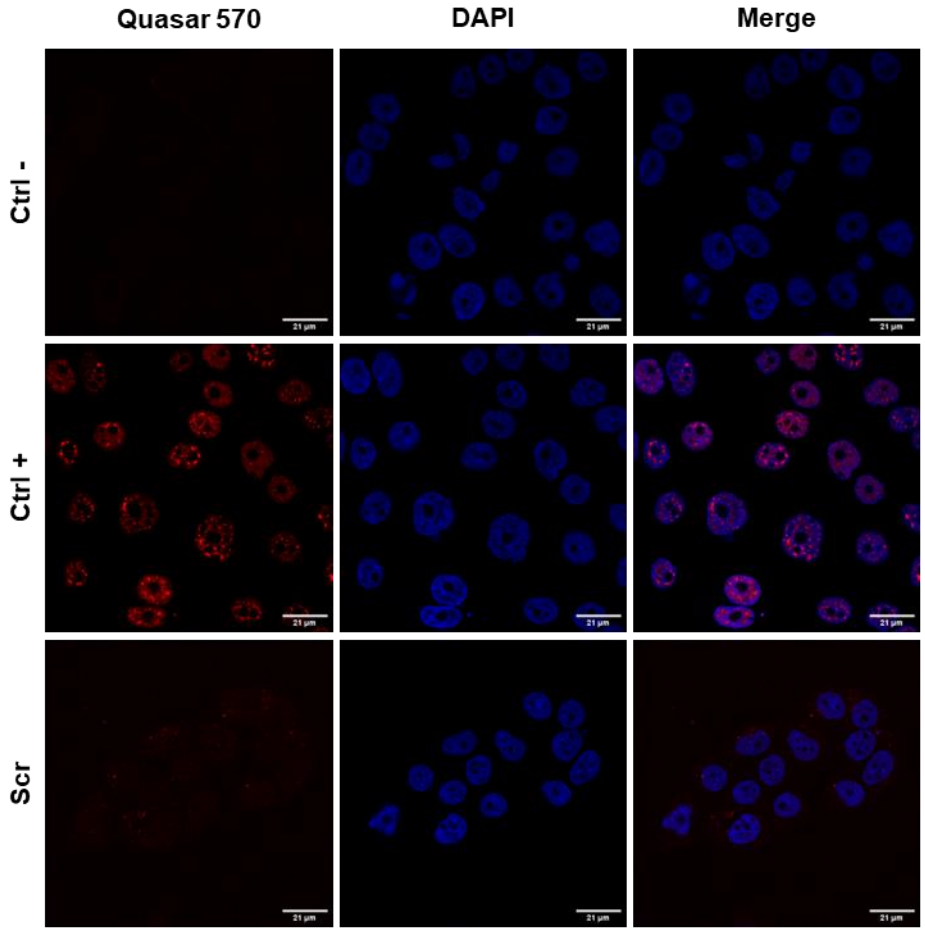

Figure 10- RNA FISH protocol to detect *NORAD* in MDA-MB-231 cells, after protocol optimization. Confocal images of RNA FISH in MDA-MB-231 cells using a MALAT1 probe in positive control and a *NORAD* probe in scramble, both labeled with Quasar 570. Quasar 570 signal in red, DAPI counterstain in blue.

3.4 *NORAD* localizes in the cytoplasm and its expression is altered by pumilio levels

After protocol optimization, FISH assay was performed to confirm *NORAD* localization in the cell and to evaluate its expression when pumilio proteins levels were downregulated. For that reason, besides the conditions already studied during protocol optimization, another four conditions were added to the study: i) cells silenced for *NORAD*; ii) cells silenced for PUM1; iii) cells silenced for PUM2; and iv) cells silenced for both pumilio proteins.

As observed in figure 11, the only condition where *NORAD* was detectable was in the cells were PUM1 was knockdown, showing *NORAD* located in the cytoplasm of the cells.

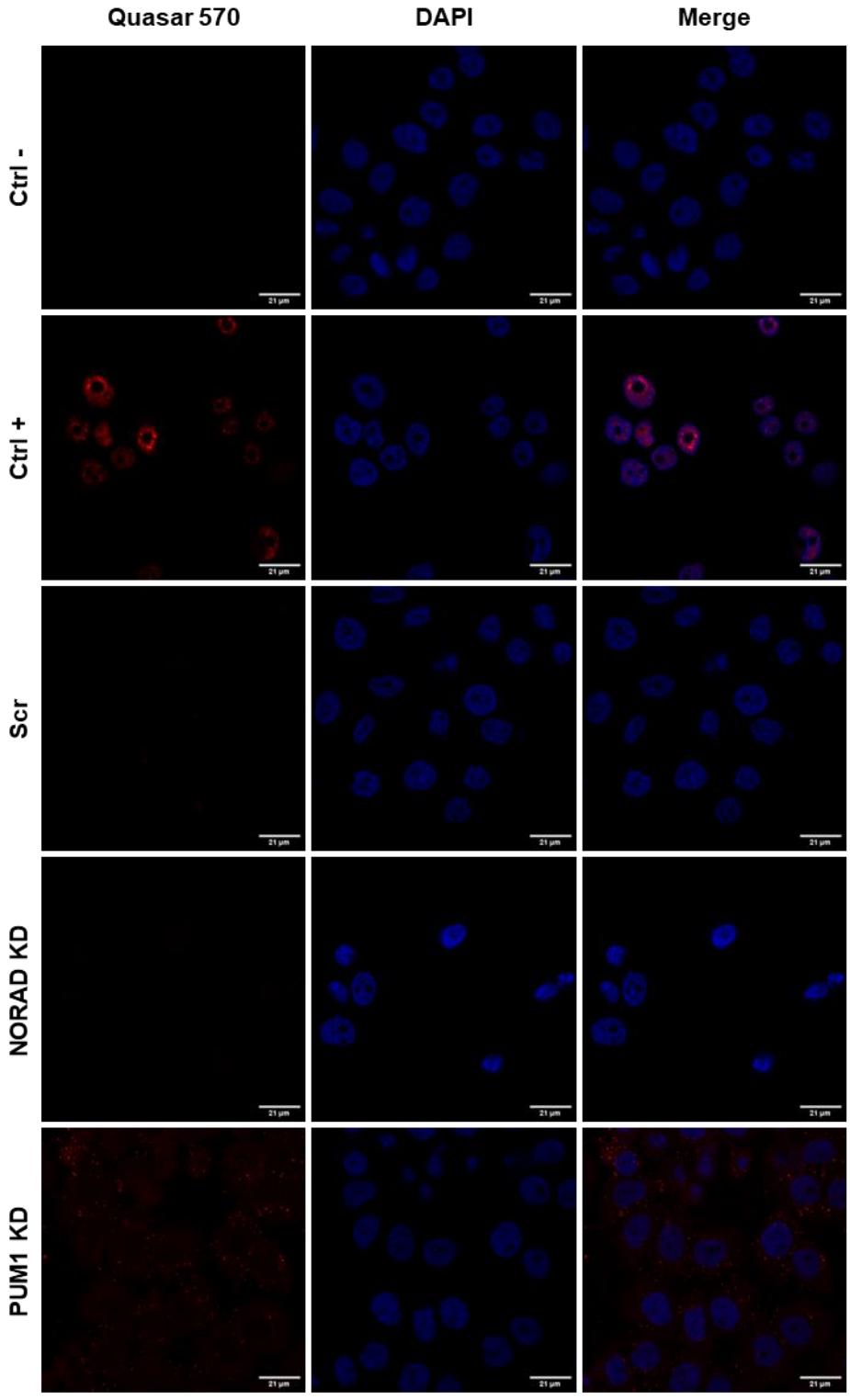

Figure 11- ***NORAD*** **localization and expression in MDA-MB-468 cells, after pumilio proteins knockdown.** Confocal images of RNA FISH in MDA-MB-468 cells using a MALAT1 probe in positive control and a *NORAD* probe in scramble, both labeled with Quasar 570. Quasar 570 signal in red, DAPI counterstain in blue.

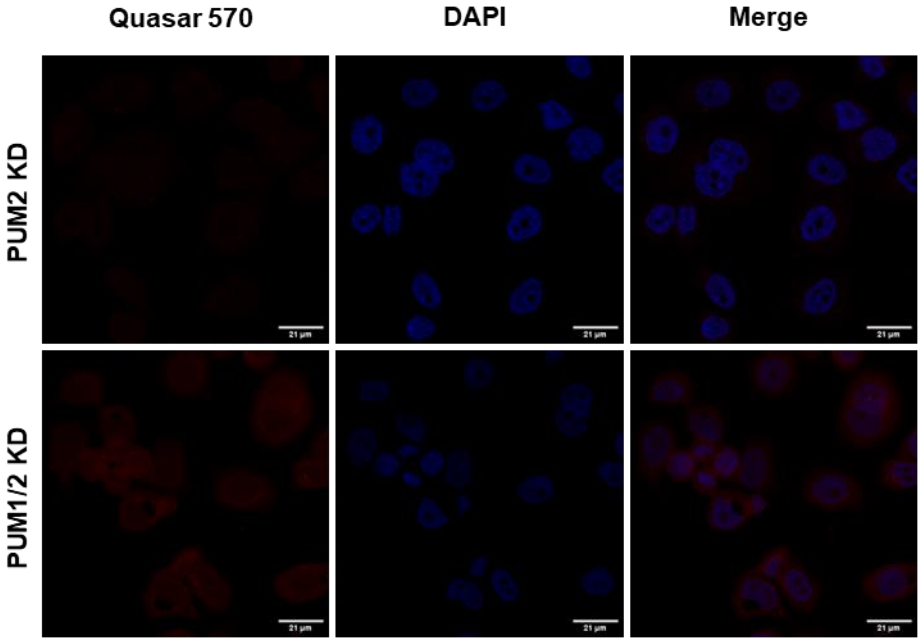

Figure 11 (continuation)- *NORAD* localization and expression in MDA-MB-468 cells, after pumilio proteins knockdown. Confocal images of RNA FISH in MDA-MB-468 cells using a MALAT1 probe in positive control and a *NORAD* probe in scramble, both labeled with Quasar 570. Quasar 570 signal in red, DAPI counterstain in blue.

Due to these contradictory results, *NORAD* expression levels were measured through RT-qPCR in the conditions studied in FISH. PUM1 knockdown appeared to lead to an increase in *NORAD* expression levels (Figure 12). On the other hand, PUM2 knockdown led to a decrease in *NORAD* levels, whereas the silencing of both pumilio proteins led to a recovery of *NORAD* levels to basal levels.

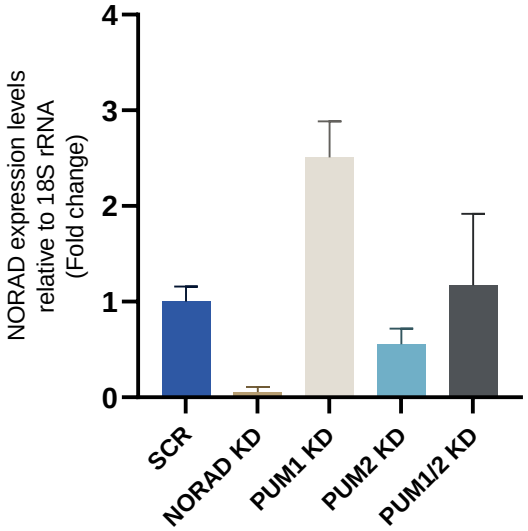

Figure 12- *NORAD* expression levels upon pumilio knockdown in TNBC cells. *NORAD* levels were measured by RT-qPCR in MDA-MB-468 cells (n=2). In all graphs, bars represent the mean values, and the error bars corresponds to the standard deviation. For statistical analysis was used Kruskal-Wallis with a control condition for multiple comparisons. No-symbol p>0.05.

Taking this into consideration, it is possible to say that *NORAD* localizes in the cytoplasm of the cells and pumilio proteins knockdown may alter *NORAD* expression in TNBC cells.

3.5 *NORAD* has a low impact at the transcriptional level of proteins involved in DNA damage pathways

The proteomic analysis carried out by Alves-Vale *et al.* demonstrated that upon *NORAD* silencing there is a decreased in the levels of proteins involved in DDR, including MCM protein 6 (MCM6), mitotic checkpoint protein BUB3, PARP1, and cyclin-dependent kinase 1 (CDK1) (130). Thus, to

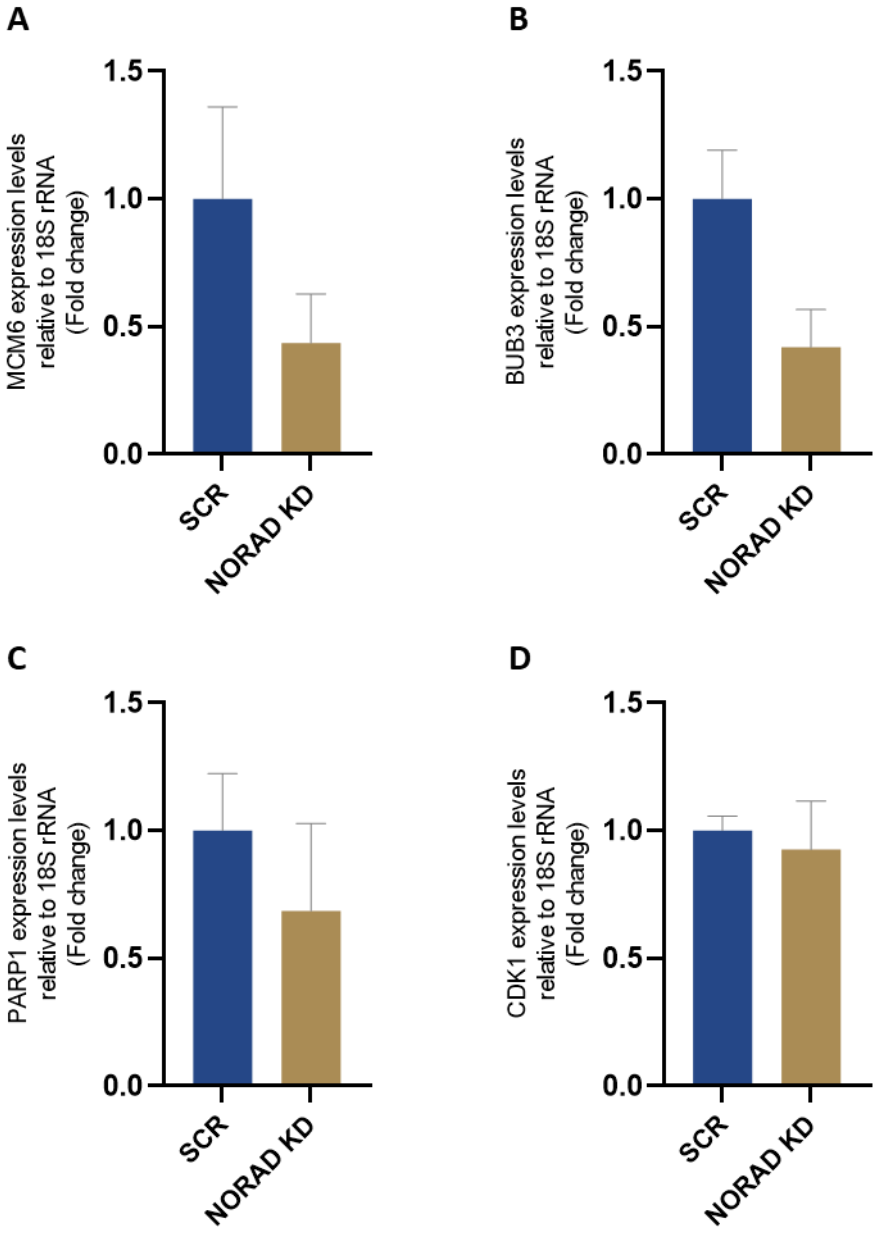

Figure 13- MCM6, BUB3, PARP1, and CDK1 expression levels in TNBC cells. MCM6, BUB3, PARP1, and CDK1 transcripts levels were measured by RT-qPCR in MDA-MB-231 cells (n=2). In all graphs, bars represent the mean values, and the error bars corresponds to the standard deviation. For statistical analysis was used Kruskal-Wallis with a control condition for multiple comparisons. No-symbol $p>0.05$.

see whether *NORAD* was regulating the expression of these proteins their mRNA levels were analyzed by RT-qPCR.

The results showed that there was just a tendency for the transcripts levels to decrease in *NORAD* silenced cells (Figure 13). In *CDK1* transcripts this tendency was even less evident, with their levels being barely altered in *NORAD* knockdown condition in comparison to scramble.

This suggests that *NORAD* may regulate the levels of these proteins by other pathways rather than at the transcriptional level only.

3.6 DNA damage levels increase in triple negative breast cancer cells upon *NORAD* knockdown and treatment with doxorubicin

Chemotherapeutic agents' final purpose is to damage cells' DNA, leading to genomic instability that results in cell death (27). However, this may not be so linear. In fact, cells can acquire resistance to the chemotherapy, with the treatment not being effective and with cancer continuing to progress (28). Therefore, it is of extreme importance to look for new strategies that can help chemotherapy to be more effective.

Based on *NORAD* levels in human BC tissues and on the proteomic analysis presented by Alves-Vale *et al*., it was hypothesized that this lncRNA can have a role in the response to chemotherapy through its involvement in the DDR (130). Thus, DNA damage levels were measured by comet assay in MDA-MB-231 cells silenced for *NORAD* and treated with doxorubicin. This is a technique that combines DNA gel electrophoresis with fluorescence microscopy to evaluate DNA strands migration from cells combined with agarose (131). If there are DNA breaks, the negatively charged DNA is relaxed and the cleaved fragments are able to migrate when subjected to an electrical field (131). DNA damage can be measured by the presence of DNA in the comet tail, which indicates DNA break extension (131).

First, the cells were treated with different concentrations of doxorubicin to choose which concentrations to use in the following steps. All concentrations used (0.1µM, 0.6 µM, and 5 µM) significantly increased in the DNA present on the tail compared to untreated cells (Figure 14A and B). However, a dose-dependent effect was expected, meaning that higher concentrations of doxorubicin were associated with greater amounts of DNA in the tail. This was not observed for the concentration of 5µM. In this way, the highest concentration was excluded for subsequent analysis.

TNBC cells were silenced for *NORAD* or simultaneously for *NORAD*, PUM1, and PUM2, followed by treatment with different concentrations of the chemotherapeutic agent. Besides this, there was a

group of cells that had a 24h period of recovery post-treatment (RPT) and only after this period the levels of DNA damage were measured.

In figures 15A and 15B, it was possible to see that there are no significant differences between the conditions treated with 0.1µM of doxorubicin. In fact, the condition only treated with 0.1µM of doxorubicin presents lower levels of DNA damage than the condition silenced for *NORAD* (p=0.0031) and similar levels to the untreated condition (p>0.9999). Besides this, the treatment with 0.6µM of doxorubicin led to an accumulation of DNA damage in the cells compared to the untreated condition (p=0.0089). This accumulation it's even higher in the cells silenced for *NORAD* (p<0.0001), which without the treatment didn't present any alteration when compared to untreated cells (p=0.1144). However, DNA damage levels in cells that recovered from the treatment are as low as the ones in untreated cells (p>0.9999).

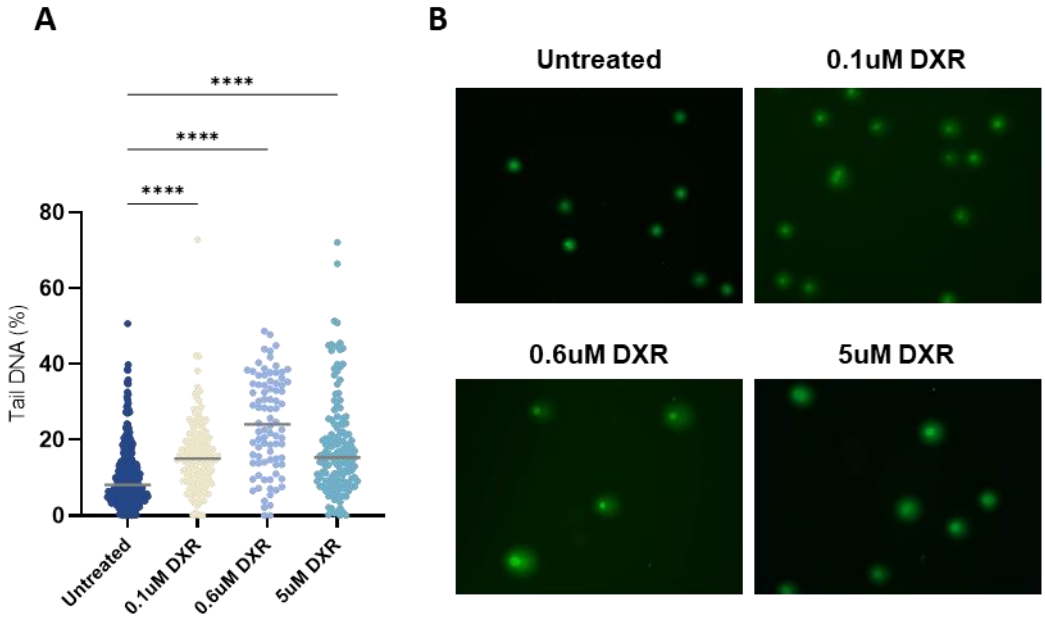

Figure 14- DNA damage evaluation after doxorubicin treatment by comet assay. Comet assay data quantification by CometScore software- graphs representing the parameter tail DNA of the cells (n=2) (A). Comet images of MDA-MB-231 untreated cells and cells treated with 0.1µM, 0.6µM and 5µM of doxorubicin (B). In all graphs, horizontal bars represent the mean values. For statistical analysis was used Kruskal-Wallis with a control condition for multiple comparisons. No-symbol p>0.05, * p<0.05, ** p<0.01, ***p<0.001 and **** p<0.0001.

On the other hand, cells silenced for *NORAD*, PUM1, and PUM2 presented higher levels of DNA damage compared to untreated cells (p<0.0001) (Figure 15A and C). The cells with the triple knockdown and treated with 0.1µM of doxorubicin have higher DNA damage levels in comparison with cells only treated with 0.1µM of doxorubicin (p=0.0067). Yet, they present a significant decrease in those levels when compared with cells with triple knockdown (p<0.0001). Although cells with triple knockdown and treated with 0.6µM of doxorubicin had a higher accumulation of DNA

damage in comparison with cells only treated with doxorubicin (p=0.0031), they did not present a significant difference when compared to cells with triple knockdown (p>0.9999).

Taken together, it is possible that *NORAD* is implicated in the DDR and that its silencing can potentiate chemotherapy efficacy by sensitizing cells to the treatment, contrarily to PUM1 and PUM2 silencing.

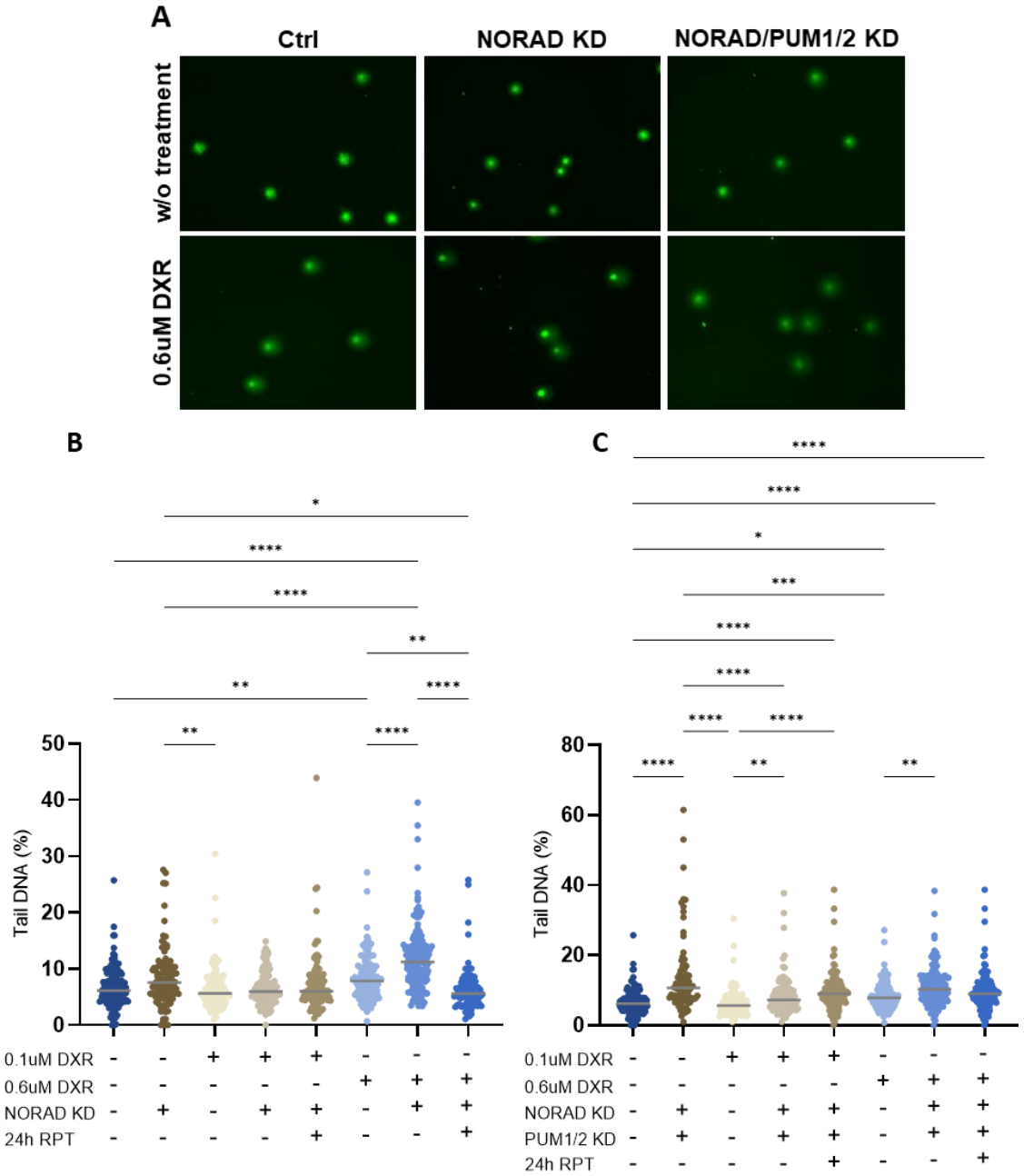

Figure 15- DNA damage evaluation after treatment with doxorubicin in *NORAD* silenced cells by comet assay. Comet images of MDA-MB-231 untreated cells, cells treated with 0.6µM doxorubicin, and silenced cells treated with doxorubicin, stained with SYBR green, and observed under fluorescent microscope (A). Comet assay data quantification by CometScore software- graphs representing the parameter tail DNA of the cells (B) and cell silenced for *NORAD*/PUM1/2 (C) (n=2). In all graphs, horizontal bars represent the mean values. For statistical analysis was used Kruskal-Wallis with a control condition for multiple comparisons. No-symbol p>0.05, * p<0.05, ** p<0.01, ***p<0.001 and **** p<0.0001.

3.7 *NORAD* knockdown sensitizes triple negative breast cancer cells to doxorubicin treatment

In order to test if the accumulation of DNA damage levels in cells silenced for *NORAD* and treated with doxorubicin seen previously in comet assay is translated in a sensibilization of BC cells to chemotherapy, cell apoptosis analysis was performed.

After the analysis, it is evident that cells treated with doxorubicin presented higher levels of annexin V when silenced for *NORAD* compared to the scramble group without treatment, although there is not a significant difference, or even to cells only treated with doxorubicin (p=0.0184), and to cells silenced for *NORAD* but without treatment (p=0.0048) (Figure 16A and B).

This means that treating *NORAD*-silenced MDA-MB-231 cells with doxorubicin, generates more death than just the chemotherapy by itself, which means that *NORAD* knockdown sensitizes BC cells to chemotherapeutic treatment with doxorubicin.

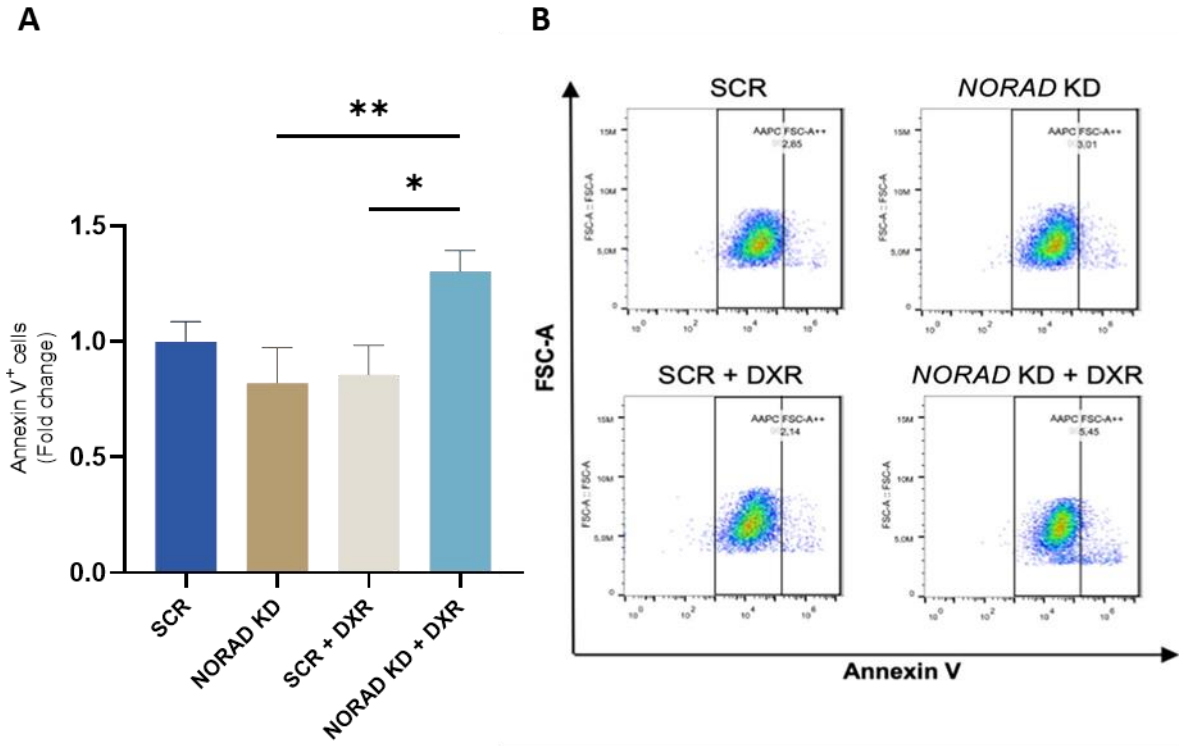

Figure 16- Annexin V⁺ levels in MDA-MB-231 cells treated with doxorubicin and silenced for *NORAD*. Quantification of Annexin V⁺ levels (A) (n=3). … In all graphs, bars represent the mean values, and the error bars corresponds to the standard deviation. For statistical analysis was used Kruskal-Wallis with a control condition for multiple comparisons. No-symbol p>0.05, * p<0.05, ** p<0.01, ***p<0.001 and **** p<0.0001.

4 Discussion

Cancer is one of the leading causes of death worldwide, causing millions of deaths every year (5). This is a complex disease that besides all the investigation to unveil its etiology it's still lacking an effective treatment, becoming increasingly urgent to find new therapeutic approaches or to improve the ones that already exist (1).

Breast cancer is the most diagnosed cancer around the world, accounting for more than two million cases and almost 700,000 deaths, just in 2020 (9). This type of cancer is known by its heterogeneity, being classified into different subtypes, according to distinct molecular characteristics (36). Triple negative breast cancer is the most aggressive subtype and the one with the worst prognosis, due to the limited therapeutical options (38). Although this is the least prevalent subtype of BC it's the one with the worst five-year overall and disease-free survival in comparison with the other subtypes (132).

In the last decades, the majority of cancer-related research was around protein-coding genes and their role in cancer development and progression (53). The majority of the human genome does not encode proteins, but it can be transcribed into RNA, known as non-coding RNA (53). Long non-coding RNA is a class of ncRNA that is implicated in several biological processes by interacting with proteins, DNA, and RNA (133). This class has been associated with carcinogenesis, being pointed out as a regulator of cancer cells behavior by being involved in the cancer hallmarks (67). For example, the lncRNA EPIC1 promotes cell-cycle progression through the interaction with MYC, leading to sustained proliferative signaling (134). Such findings can pave the way for the development of cancer therapies. Thus, lncRNAs have gained some notoriety in cancer research and brought new hope to cancer diagnosis, prognosis, and treatment.

NORAD is a lncRNA that has been associated with several types of cancers, including renal, gastric, bladder, breast, and pancreatic cancers, demonstrating its potential role in assessing patient prognosis, anticipating treatment outcomes, and functioning as a therapeutic target (55). Therefore, the focus through the present work was to understand if *NORAD* acts as an oncogene or tumor suppressor and to study *NORAD* potential as a predictive and prognosis biomarker, or as a new therapeutic target in BC.

In all cancers mentioned above, the lncRNA *NORAD* has been described as upregulated (55). The results from this work partially corroborate the results from already published studies. First, in this work, the expression levels of *NORAD* were measured in human BC tissues and adjacent healthy tissues, however, contrarily to previous studies that only compared normal tissues vs. cancer tissues, here BC tissues were divided according to subtype and other characteristics, including recurrence

score, treatment with neoadjuvant chemotherapy, and response to treatment. This shows a different *NORAD* expression profile than the ones already described, with *NORAD* expression levels tending to be increased in the most aggressive tumors, namely in luminal BC with high RS and TNBC with low response to treatment, and in tumors treated without neoadjuvant chemotherapy. Besides this, *NORAD* expression in luminal BC with low RS and TNBC with high response to treatment are similar or just slightly higher than the control group, respectively. This supports the idea that *NORAD* levels are increased in distinct BC subtypes that are more aggressive, and not in BC in general.

On the contrary, some studies describe *NORAD* as being downregulated in different types of cancer, namely in BC (105,106). Such differences can be explained by experimental settings done by the authors, that compared control tissues with BC tissues, without taking into consideration any further characteristic of the tumor physiology. Besides this, clinical samples are always very heterogeneous, showing that each patient is different and that such differences may be crucial during diagnosis, prognostic, and treatment, revealing once again the importance of personalized medicine in the clinical practice (135).

The lncRNA *NORAD* interacts with a wide variety of partners, from mRNAs and miRNAs to proteins (100). The most well-known interactor of *NORAD* is pumilio proteins, which are described as repressors of mRNAs involved in DNA repair, replication, mitosis, and cancer pathways (e.g., PARP1, MCM4, PRC1, STAT3) (63,136). However, interactions between *NORAD* and other proteins are also described, namely SAM68 and RBMX. In fact, the interaction between *NORAD* and pumilio is facilitated by *NORAD* interaction with SAM68 which leads to a more avidly binding to pumilio than other PRE-containing target RNAs (137). Regarding RBMX, this is a RNA binding protein that is implicated in DDR, by assembling a ribonucleoprotein complex- *NORAD*-activated ribonucleoprotein complex 1 (NARC1)- that is formed by topoisomerase 1, Aly/REF export factor (ALYREF), and the pre-mRNA processing factor 19 (PRPF19)-cell division cycle 5 like (CDC5L) complex (64). There is some discussion about whether *NORAD* is required or not for the assembly of NARC1, and whether its role in maintaining genome stability is exclusively mediated by pumilio proteins or by other proteins, like RBMX (64). In the present study, only the pumilio proteins interaction with *NORAD* was explored.

In line with previous studies, it is possible to observe that *NORAD* is expressed in the cytoplasm of the cells, presenting a punctate profile. This profile can be explained by the fact that *NORAD* sequesters pumilio proteins in a biomolecular condensate (51). These condensates are a product of phase separation which is a major mechanism of subcellular compartmentalization and can be used by RNA to regulate its interactors, including RBPs (65,138). In this way, RBPs are recruited by

RNA, and the association between intrinsically disordered regions (IDRs) is decreased, leading to the formation of ribonucleoprotein granules (65). Elguindy et al. have demonstrated that *NORAD* can out-compete thousands of other transcripts to regulate pumilio proteins activity by inducing pumilio phase separation, therefore inhibiting pumilio mRNA targets, and ensuring genome stability. They also showed that when *NORAD* is absent pumilio proteins disperse and the punctate profile disappears (65).

Contrary to what was expected, was not possible to make any conclusions about the role of PUM1 and PUM2 in *NORAD* expression levels through RNA FISH. This is a technique that allows the visualization and localization of RNA in fixed cells through the hybridization with labeled probes, however, it has some limitations (139). The problems can start right from the beginning when designing the probes. This can be a challenging task because probes must be designed with the right length and sequence, and when this doesn't happen the outcome is a poor hybridization efficiency and sensitivity, with little or even any signal being detected (139). After this, the sample preparation is a crucial step in the protocol. For example, without the proper permeabilization the probe is not able to penetrate the cell and bind to its target, as it was possible to see in the optimization procedure when the method of permeabilization was changed and it was possible to see *NORAD* expression in the cells (139). Besides this, the aim of this study was to evaluate the expression of a lncRNA molecule, that is known for being more unstable than protein-coding mRNA, so if not under the right conditions can be easily degraded, this could explain why *NORAD* expression was not always detected during this work (140). It is also important to note that lncRNAs have complex secondary structures or, like *NORAD*, they can form RNA-protein complexes, making it difficult for the probes to hybridize to their targets (141). Interestingly, the only condition where is possible to detect *NORAD* expression is the one where PUM1, a protein known to interact with this lncRNA, is downregulated, leaving open the possibility that this interaction could be blocking probe hybridization to its target.

Pumilio proteins are RBPs that regulate gene expression through posttranscriptional mechanisms, with both PUM1 and PUM2 being associated with several types of cancer and interacting with *NORAD* (136,142,143). Although they are very similar and some studies have described them as functionally redundant, other studies demonstrated that they act differently in terms of mRNA recognition and regulation (143). For example, it was demonstrated that PUM1 promotes differentiation in embryonic stem cells by repressing pluripotency transcription factors, with its depletion leading to reduced differentiation, but PUM2 silencing had no effect (143). In cancer, PUM1 has been associated with the proliferative capacity of cancer cells, whereas PUM2 is associated with cell viability, migration, and invasion, however, its role it's controversial (136).

Pumilio proteins are described as upregulated in BC tissues, contrarily to what was seen in the results of this work, this may be explained because in this work pumilio transcripts expression levels were measured, while in the other studies scientists were looking at protein levels, and the correlations between RNA and protein is notoriously low (103,144,145). The consequences of this upregulation in BC are tumorigenesis and cancer development, in the case of PUM1, and decreased overall survival and relapse-free survival, in the PUM2 case (103,144). Therefore, it is relevant to try to understand if in BC, particularly in TNBC, both PUM1 and PUM2 or just one of them has an impact on *NORAD* expression levels.

Although both pumilio proteins interact with *NORAD*, it is described that *NORAD* affinity for PUM2 is higher than for PUM1 (146). It is also described that when PUM1 or PUM2 are downregulated the other pumilio protein can compensate this difference (147). The truth is that in this work it was possible to observe that *NORAD* expression levels don't suffer notable alterations when pumilio proteins are silenced in TNBC cells, except in PUM1 knockdown cells, that present higher levels of *NORAD*. This can suggest that when PUM1 is silenced, PUM2 compensates its absence and consequently, because of PUM2's high affinity with *NORAD*, the levels of this lncRNA tend to increase. Besides this, it is possible to say that pumilio proteins have different roles in regulating *NORAD* expression levels.

Previous studies have demonstrated that *NORAD* contributes to genomic stability maintenance by being implicated in DDR (130). Actually, Alves-Vale *et al*. showed that upon *NORAD* knockdown the proteomic profile of TNBC cells changes, with proteins involved in DDR and in cell cycle regulation being repressed, including, for example: MCM6, a DNA replication regulator that has been associated with cancer progression; BUB3, a mitotic checkpoint protein frequently overexpressed in some cancers; PARP1, responsible for detecting DNA strand breaks and facilitating their repair by recruiting DNA repair machinery to damage sites; and CDK1, a regulator of cell cycle progression through the G2/M phase transition and activation of homologous recombination (130,148–151). However, when measuring the mRNA levels of the proteins mentioned above there isn't any alteration between the conditions scramble and *NORAD* knockdown, meaning that these proteins are regulated by *NORAD* not only at a transcriptional level. Although the majority of lncRNAs that are already characterized are involved in transcriptional regulation, some of them are described as being involved in post-transcriptional events, including in alternative splicing and functioning as competing endogenous RNAs (ceRNAs) or RNA sponges (133). For example, the natural antisense transcript of zinc finger E-box binding homeobox 2 (ZEB2-NAT) is a lncRNA that regulates alternative splicing by binding to ZEB2 mRNA, preventing its splicing (133). This shows

that the myriad of *NORAD* interacting partners can lead it to regulate not only those interactors but also their downstream molecules in a post-transcriptional manner.

All the proteins mentioned above are necessary to maintain DNA integrity, however, in cancer, the expression of such proteins could mean cancer cells progression, indicating that under *NORAD* knockdown, when they are repressed, there could be an accumulation of DNA damage in TNBC cells with those being sensitized to chemotherapy treatment.

Here, it is evident that when treating TNBC cells with different concentrations of doxorubicin there is an increase in DNA damage levels, with this increase not being as high as was thought it would be in the highest concentration (5µM). This could be because there is a saturation of DNA damage levels, or because such high concentration could result in cell death, not being possible to measure higher levels of damage. Also, DNA damage levels are higher when cells were silenced for *NORAD*, especially in cells treated with 0.6µM of doxorubicin, with 0.1µM not being sufficient to cause a significant difference in DNA damage levels. This result supports the one published by Alves-Vale *et al*. that shows an accumulation of γH2AX, the phosphorylated form of the histone H2AX and a biomarker of DSBs, in *NORAD* knockdown cells (130). However, when DNA damage levels are measured 24h after recovery from doxorubicin treatment, they show lower levels comparing to cells only treated with doxorubicin. This suggests the effect of *NORAD* knockdown in the DNA damage levels of cells treated with doxorubicin is transient, with these levels decreasing after 24 hours upon the treatment with doxorubicin. Regarding *NORAD*/PUM1/2 knockdown the scenario was identical, unless that even in the absence of doxorubicin there is an increase in DNA damage levels linked to the knockdown. Although there is an increase in DNA damage levels in cells with triple knockdown and treated with 0.6µM of doxorubicin, it was expected that this increase was more pronounced, considering the effect of the triple knockdown by itself. Since that in the absence of pumilio proteins, their targets stop being inhibited and can act in DNA repair, replication, and mitosis, this result could mean that there are PUM1 and PUM2 mRNA targets that condition the accumulation of DNA damage in cells treated with doxorubicin. Taken together, these results suggest that *NORAD* is implicated in DDR and that *NORAD* knockdown leads to DNA damage and may sensitize TNBC cells to treatment with doxorubicin.

The standard treatment of TNBC is still chemotherapy, but this usually presents low rates of success, due to adverse effects and resistance to chemotherapeutic agents (47). Therefore, there is a need to overcome these problems, with the combination of conventional chemotherapeutic agents with novel molecular-targeted agents being a promising strategy (46,49). Some targeted agents that have been under study are molecules involved in DNA repair, because of its dual role in cancer, with low levels

of DNA repair sensitizing cells to chemotherapy, and high levels promoting cancer progression (46). Also, considering the expression of lncRNAs in some cancers and their role in regulating protein activity, therapies targeting them can be more refined and less toxic than therapies whose target it's the protein itself (133).

Several studies already associated the lncRNA *NORAD* with chemoresistance to chemotherapeutic agents (152). For example, *NORAD* overexpression leads to doxorubicin resistance in neuroblastoma and to 5-fluorouracil (5-FU) resistance in colorectal cancer (153,154). Also, *NORAD* acts as a ceRNA in bladder cancer, mediating gemcitabine chemoresistance (155). Supporting those studies, the results from the present work suggest that *NORAD* expression levels might be responsible for resistance to chemotherapy in TNBC. When *NORAD* was silenced in TNBC cells, it was possible to see an increase of Annexin V^+ cells after the treatment with doxorubicin. This means that there was more cell death in that group and that such death is promoted by the low levels of *NORAD*, because the levels of Annexin V^+ cells are significantly higher than the levels in the group only treated with doxorubicin. Since *NORAD* expression levels are higher in TNBC cells and patients with a low response to treatment, these results indicate that *NORAD* acts as an oncogene in TNBC, promoting cell resistance to treatment. On the other side, *NORAD* knockdown increases TNBC cell death upon treatment with doxorubicin, overcoming cell resistance to chemotherapy which may help in tumor clearance.

5 Conclusions and future perspectives

In the current work, it was possible to demonstrate that the lncRNA *NORAD* has a tendency to be overexpressed in more aggressive types of cancer, including the ones with low response to treatment and with high recurrence score, with *NORAD* knockdown proving to be efficacy in sensitizing BC cells to the treatment with doxorubicin. This demonstrates *NORAD*'s potential as a prognostic and predictive biomarker, and as a possible targetable molecule to use in combination with chemotherapy.

It was also reported that *NORAD* localizes in the cytoplasm of TNBC cells where interacts with pumilio proteins, regulating them and their mRNA targets. However, the expression of pumilio proteins also has an impact on *NORAD* expression levels. Besides this, it is now known that *NORAD* can regulate proteins not only at the transcriptional level but also at the post-transcriptional level.

In the future, it would be interesting to evaluate *NORAD* expression levels in BC tissues of a larger number of patients to actually associate it as a biomarker of BC.

In *in vitro* experiments, the assays done in this work should be replicated in other BC cell lines, including luminal BC cell lines, like MCF-7, and other chemotherapeutic agents should be tested, since they present different mechanisms of action. Also, another genome-editing method, such as CRISPR/Cas9, should be employed to test if, upon a stable *NORAD* knockdown, BC cells continue to be sensitized to chemotherapy. Besides this, it would be of utmost importance to optimize the RNA FISH protocol to apply it to the tissues of patients with BC to evaluate *NORAD* expression levels in specific tissue structures.

Lastly, it would also be important to try to recapitulate these findings in 3D structures, where BC cells interact with other cells that are present in the tumor microenvironment.

References

1. Wang J-J, Lei K-F, Han F. Tumor microenvironment: recent advances in various cancer treatments. Eur Rev Med Pharmacol Sci. 2018 Jun;22(12):3855–64.

2. Roy P, Saikia B. Cancer and cure: A critical analysis. Indian J Cancer. 2016;53(3):441.

3. Cao W, Chen H-D, Yu Y-W, Li N, Chen W-Q. Changing profiles of cancer burden worldwide and in China: a secondary analysis of the global cancer statistics 2020. Chin Med J (Engl). 2021 Apr 5;134(7):783–91.

4. Sung H, Ferlay J, Siegel RL, Laversanne M, Soerjomataram I, Jemal A, et al. Global Cancer Statistics 2020: GLOBOCAN Estimates of Incidence and Mortality Worldwide for 36 Cancers in 185 Countries. CA Cancer J Clin. 2021 May 4;71(3):209–49.

5. Deo SVS, Sharma J, Kumar S. GLOBOCAN 2020 Report on Global Cancer Burden: Challenges and Opportunities for Surgical Oncologists. Ann Surg Oncol. 2022 Oct 15;29(11):6497–500.

6. The Global Cancer Observatory. All Cancers - GCO [Internet]. Vol. 419, IARC. 2020 [cited 2023 Sep 21]. p. 2. Available from: https://gco.iarc.fr/today

7. Commission E. State of Health in the EU Portugal Country Health Profile. OECD, European Observatory. 2021.

8. IARC. Portugal Source: Globocan Incidence, Mortality and Prevalence by cancer site [Internet]. IARC. 2021 [cited 2023 Sep 20]. p. 2. Available from: https://www.iarc.who.int/

9. Arnold M, Morgan E, Rumgay H, Mafra A, Singh D, Laversanne M, et al. Current and future burden of breast cancer: Global statistics for 2020 and 2040. The Breast. 2022 Dec 1;66:15–23.

10. GLOBOCAN. Age standardized (World) incidence rates, breast, all ages. [Internet]. Vol. 876, International Agency for Research on Cancer. 2020 [cited 2023 Sep 21]. p. 1–2. Available from: https://gco.iarc.fr/today

11. The American Cancer Society medical and editorial content team. What is Cancer? | Cancer Basics | American Cancer Society [Internet]. Ultima revisión 14/02/2022. 2020 [cited 2023 Jan 6]. Available from: https://www.cancer.org/treatment/understanding-your-diagnosis/what-is-cancer.html

12. Hanahan D, Weinberg RA. The Hallmarks of Cancer. Cell. 2000 Jan 7;100(1):57–70.

13. Plutynski A. Cancer and the goals of integration. Stud Hist Philos Sci Part C Stud Hist Philos Biol Biomed Sci. 2013 Dec;44(4):466–76.

14. Osborne C, Wilson P, Tripathy D. Oncogenes and Tumor Suppressor Genes in Breast Cancer: Potential Diagnostic and Therapeutic Applications. Oncologist. 2004 Jul 1;9(4):361–77.

15. Lee EYHP, Muller WJ. Oncogenes and Tumor Suppressor Genes. Cold Spring Harb Perspect Biol. 2010 Oct 1;2(10):a003236–a003236.

16. Chow AY. Cell Cycle Control, Oncogenes, Tumor Suppressors | Learn Science at Scitable [Internet]. Vol. 3, Nature Education. 2010 [cited 2023 May 23]. p. 7. Available from: https://www.nature.com/scitable/topicpage/cell-cycle-control-by-oncogenes-and-tumor-14191459/

17. Hanahan D, Weinberg RA. Hallmarks of Cancer: The Next Generation. Cell. 2011 Mar;144(5):646–74.

18. Hanahan D. Hallmarks of Cancer: New Dimensions. Cancer Discov. 2022 Jan 1;12(1):31–46.

19. Senga SS, Grose RP. Hallmarks of cancer—the new testament. Open Biol. 2021 Jan 20;11(1):0–2.

20. Anderson NM, Simon MC. The tumor microenvironment. Curr Biol. 2020 Aug;30(16):R921–5.

21. Wu Z, Ju Q. Non-Coding RNAs Implicated in the Tumor Microenvironment of Colorectal Cancer: Roles, Mechanisms and Clinical Study. Front Oncol. 2022 Apr 28;12(April):1–12.

22. Baghban R, Roshangar L, Jahanban-Esfahlan R, Seidi K, Ebrahimi-Kalan A, Jaymand M, et al. Tumor microenvironment complexity and therapeutic implications at a glance. Cell Commun Signal. 2020 Dec 7;18(1):59.

23. Wang Q, Shao X, Zhang Y, Zhu M, Wang FXC, Mu J, et al. Role of tumor microenvironment in cancer progression and therapeutic strategy. Cancer Med. 2023 May 21;12(10):11149–65.

24. Bussard KM, Mutkus L, Stumpf K, Gomez-Manzano C, Marini FC. Tumor-associated stromal cells as key contributors to the tumor microenvironment. Breast Cancer Res. 2016 Aug 11;18(1):84.

25. Goyette M-A, Lipsyc-Sharf M, Polyak K. Clinical and translational relevance of intratumor heterogeneity. Trends in Cancer. 2023 Sep;9(9):726–37.

26. Samavarchi Tehrani S, Mahmoodzadeh Hosseini H, Yousefi T, Abolghasemi M, Qujeq D, Maniati M, et al. The crosstalk between trace elements with DNA damage response, repair, and oxidative stress in cancer. J Cell Biochem. 2019 Feb;120(2):1080–105.

27. Li LY, Guan Y Di, Chen XS, Yang JM, Cheng Y. DNA Repair Pathways in Cancer Therapy and Resistance. Front Pharmacol. 2021 Feb 8;11:629266.

28. Alhmoud JF, Woolley JF, Al Moustafa A-E, Malki MI. DNA Damage/Repair Management in Cancers. Cancers (Basel). 2020 Apr 23;12(4):1050.

29. Giglia-Mari G, Zotter A, Vermeulen W. DNA Damage Response. Cold Spring Harb Perspect Biol. 2011 Jan 1;3(1):a000745–a000745.

30. Moon J, Kitty I, Renata K, Qin S, Zhao F, Kim W. DNA Damage and Its Role in Cancer Therapeutics. Int J Mol Sci. 2023 Mar 1;24(5):4741.

31. Martin LJ. DNA Damage and Repair. J Neuropathol Exp Neurol. 2008 May;67(5):377–87.

32. Lord CJ, Ashworth A. The DNA damage response and cancer therapy. Nature. 2012 Jan 18;481(7381):287–94.

33. Hopkins JL, Lan L, Zou L. DNA repair defects in cancer and therapeutic opportunities. Genes Dev. 2022 Mar 1;36(5–6):278–93.

34. Robson M, Im S-A, Senkus E, Xu B, Domchek SM, Masuda N, et al. Olaparib for Metastatic Breast Cancer in Patients with a Germline BRCA Mutation. N Engl J Med. 2017 Aug 10;377(6):523–33.

35. Torgovnick A, Schumacher B. DNA repair mechanisms in cancer development and therapy. Front Genet. 2015 Apr 23;6(APR).

36. Harbeck N, Gnant M. Breast cancer. Lancet. 2017 Mar;389(10074):1134–50.

37. Weigelt B, Geyer FC, Reis-Filho JS. Histological types of breast cancer: How special are they? Mol Oncol. 2010 Jun 18;4(3):192–208.

38. Nascimento RG do, Otoni KM. Histological and molecular classification of breast cancer: what do we know? Mastology. 2020;30:1–8.

39. Dias K, Dvorkin-Gheva A, Hallett RM, Wu Y, Hassell J, Pond GR, et al. Claudin-Low Breast Cancer; Clinical & Pathological Characteristics. Chu P-Y, editor. PLoS One. 2017 Jan 3;12(1):e0168669.

40. Tong CWS, Wu M, Cho WCS, To KKW. Recent Advances in the Treatment of Breast Cancer. Front Oncol. 2018 Jun 14;8(JUN):227.

41. Waks AG, Winer EP. Breast Cancer Treatment. JAMA. 2019 Jan 22;321(3):288.

42. Burstein HJ, Lacchetti C, Anderson H, Buchholz TA, Davidson NE, Gelmon KA, et al. Adjuvant Endocrine Therapy for Women With Hormone Receptor–Positive Breast Cancer: ASCO Clinical Practice Guideline Focused Update. J Clin Oncol. 2019 Feb 10;37(5):423–38.

43. Breast Cancer Treatment Options - National Breast Cancer Foundation [Internet]. 2020 [cited 2023 Sep 6]. Available from: https://www.nationalbreastcancer.org/breast-cancer-treatment/

44. Reinert T, Barrios CH. Optimal management of hormone receptor positive metastatic breast cancer in 2016. Ther Adv Med Oncol. 2015 Oct 20;7(6):304–20.

45. Sledge GW, Mamounas EP, Hortobagyi GN, Burstein HJ, Goodwin PJ, Wolff AC. Past, Present, and Future Challenges in Breast Cancer Treatment. J Clin Oncol. 2014 Jul 1;32(19):1979–86.

46. Schlam I, Swain SM. HER2-positive breast cancer and tyrosine kinase inhibitors: the time is now. npj Breast Cancer. 2021 May 20;7(1):56.

47. Won K-A, Spruck C. Triple-negative breast cancer therapy: Current and future perspectives (Review). Int J Oncol. 2020 Dec 1;57(6):1245–61.

48. Wahba HA, El-Hadaad HA. Current approaches in treatment of triple-negative breast

cancer. Cancer Biol Med. 2015 Jun 1;12(2):106–16.

49. Jerusalem G, Collignon J, Schroeder H, Lousberg L. Triple-negative breast cancer: treatment challenges and solutions. Breast Cancer Targets Ther. 2016 May 20;8:93.

50. Kopp F, Mendell JT. Functional Classification and Experimental Dissection of Long Noncoding RNAs. Cell. 2018 Jan;172(3):393–407.

51. Somasundaram K, Gupta B, Jain N, Jana S. LncRNAs divide and rule: The master regulators of phase separation. Front Genet. 2022 Aug 10;13(August):1–12.

52. Schaukowitch K, Kim T-K. Emerging epigenetic mechanisms of long non-coding RNAs. Neuroscience. 2014 Apr;264:25–38.

53. Sun M, Kraus WL. From Discovery to Function: The Expanding Roles of Long NonCoding RNAs in Physiology and Disease. Endocr Rev. 2015 Feb 1;36(1):25–64.

54. Tichon A, Gil N, Lubelsky Y, Havkin Solomon T, Lemze D, Itzkovitz S, et al. A conserved abundant cytoplasmic long noncoding RNA modulates repression by Pumilio proteins in human cells. Nat Commun. 2016 Jul 13;7(1):12209.

55. Soghli N, Yousefi T, Abolghasemi M, Qujeq D. NORAD, a critical long non-coding RNA in human cancers. Life Sci. 2021 Jan 1;264:118665.

56. Yang Z, Zhao Y, Lin G, Zhou X, Jiang X, Zhao H. Noncoding RNA activated by DNA damage (NORAD): Biologic function and mechanisms in human cancers. Clin Chim Acta. 2019 Feb;489(October 2018):5–9.

57. Mattick JS, Amaral PP, Carninci P, Carpenter S, Chang HY, Chen L-L, et al. Long non-coding RNAs: definitions, functions, challenges and recommendations. Nat Rev Mol Cell Biol. 2023 Jun 3;24(6):430–47.

58. Zhang Y, Liu Q, Liao Q. Long noncoding RNA: a dazzling dancer in tumor immune microenvironment. J Exp Clin Cancer Res. 2020 Dec 4;39(1):231.

59. Gutschner T, Diederichs S. The hallmarks of cancer. RNA Biol. 2012 Jun 27;9(6):703–19.

60. Park E-G, Pyo S-J, Cui Y, Yoon S-H, Nam J-W. Tumor immune microenvironment lncRNAs. Brief Bioinform. 2022 Jan 17;23(1):1–25.

61. Quinn JJ, Chang HY. Unique features of long non-coding RNA biogenesis and function. Nat Rev Genet. 2016 Jan 15;17(1):47–62.

62. Ventura A. NORAD: Defender of the Genome. Trends Genet. 2016 Jul 1;32(7):390–2.

63. Lee S, Kopp F, Chang T-C, Sataluri A, Chen B, Sivakumar S, et al. Noncoding RNA NORAD Regulates Genomic Stability by Sequestering PUMILIO Proteins. Cell. 2016 Jan;164(1–2):69–80.

64. Elguindy MM, Kopp F, Goodarzi M, Rehfeld F, Thomas A, Chang T-C, et al. PUMILIO, but not RBMX, binding is required for regulation of genomic stability by noncoding RNA NORAD. Elife. 2019 Jul 25;8:1–16.

65. Elguindy MM, Mendell JT. NORAD-induced Pumilio phase separation is required for genome stability. Nature. 2021 Jul 8;595(7866):303–8.

66. Guh C-Y, Hsieh Y-H, Chu H-P. Functions and properties of nuclear lncRNAs-from systematically mapping the interactomes of lncRNAs. J Biomed Sci. 2020 Mar 17;27(1):44.

67. Fan N, Fu H, Feng X, Chen Y, Wang J, Wu Y, et al. Long non-coding RNAs play an important regulatory role in tumorigenesis and tumor progression through aerobic glycolysis. Front Mol Biosci. 2022 Aug 22;9(August):1–19.

68. Erson-Bensan AE. RNA-biology ruling cancer progression? Focus on 3′UTRs and splicing. Cancer Metastasis Rev. 2020 Sep 2;39(3):887–901.

69. Mendell JT. Targeting a Long Noncoding RNA in Breast Cancer. Phimister EG, editor. N Engl J Med. 2016 Jun 9;374(23):2287–9.

70. Liu H, Luo J, Luan S, He C, Li Z. Long non-coding RNAs involved in cancer metabolic reprogramming. Cell Mol Life Sci. 2019 Feb 15;76(3):495–504.

71. Chandra Gupta S, Nandan Tripathi Y. Potential of long non-coding RNAs in cancer patients: From biomarkers to therapeutic targets. Int J Cancer. 2017 May 30;140(9):1955–67.

72. Beermann J, Piccoli M-T, Viereck J, Thum T. Non-coding RNAs in Development and Disease: Background, Mechanisms, and Therapeutic Approaches. Physiol Rev. 2016 Oct 1;96(4):1297–325.

73. Barth DA, Juracek J, Slaby O, Pichler M, Calin GA. lncRNA and Mechanisms of Drug Resistance in Cancers of the Genitourinary System. Cancers (Basel). 2020 Aug 3;12(8):2148.

74. Ding M, Cao X, Xu H, Fan J, Huang H, Yang D, et al. Prostate Cancer-Specific and Potent Antitumor Effect of a DD3-Controlled Oncolytic Virus Harboring the PTEN Gene. Ulasov I, editor. PLoS One. 2012 Apr 11;7(4):e35153.

75. Wei S, Wang K, Huang X, Zhao Z, Zhao Z. LncRNA MALAT1 contributes to non-small cell lung cancer progression via modulating miR-200a-3p/programmed death-ligand 1 axis. Int J Immunopathol Pharmacol. 2019 Jun 26;33:2058738419859699.

76. Chang J, Xu W, Du X, Hou J. MALAT1 silencing suppresses prostate cancer progression by upregulating miR-1 and downregulating KRAS. Onco Targets Ther. 2018 Jun 15;Volume 11:3461–73.

77. Zheng T, Ma G, Tang M, Li Z, Xu R. IL-8 Secreted from M2 Macrophages Promoted Prostate Tumorigenesis via STAT3/MALAT1 Pathway. Int J Mol Sci. 2018 Dec 27;20(1):98.

78. Huang J, Ma L, Song W, Lu B, Huang Y, Dong H, et al. LncRNA-MALAT1 Promotes Angiogenesis of Thyroid Cancer by Modulating Tumor-Associated Macrophage FGF2 Protein Secretion. J Cell Biochem. 2017 Dec 13;118(12):4821–30.

79. Kan J-Y, Wu D-C, Yu F-J, Wu C-Y, Ho Y-W, Chiu Y-J, et al. Chemokine (C-C Motif) Ligand 5 is Involved in Tumor-Associated Dendritic Cell-Mediated Colon Cancer

Progression Through Non-Coding RNA MALAT-1. J Cell Physiol. 2015 Aug 1;230(8):1883–94.

80. Wang Q-M, Lian G-Y, Song Y, Huang Y-F, Gong Y. LncRNA MALAT1 promotes tumorigenesis and immune escape of diffuse large B cell lymphoma by sponging miR-195. Life Sci. 2019 Aug 15;231:116335.

81. Wu L, Zhang L, Zheng S. Role of the long non-coding RNA HOTAIR in hepatocellular carcinoma (review). Oncol Lett. 2017 Aug 1;14(2):1233–9.

82. Gao JZ, Li J, Du JL, Li XL. Long non-coding RNA HOTAIR is a marker for hepatocellular carcinoma progression and tumor recurrence. Oncol Lett. 2016 Mar 1;11(3):1791–8.

83. Sun J, Chu H, Ji J, Huo G, Song Q, Zhang X. Long non-coding RNA HOTAIR modulates HLA-G expression by absorbing miR-148a in human cervical cancer. Int J Oncol. 2016 Sep 1;49(3):943–52.

84. Song B, Guan Z, Liu F, Sun D, Wang K, Qu H. Long non-coding RNA HOTAIR promotes HLA-G expression via inhibiting miR-152 in gastric cancer cells. Biochem Biophys Res Commun. 2015 Aug 28;464(3):807–13.

85. Wu X, Dinglin X, Wang X, Luo W, Shen Q, Li Y, et al. Long noncoding RNA XIST promotes malignancies of esophageal squamous cell carcinoma via regulation of miR-101/EZH2. Oncotarget. 2017 Sep 29;8(44):76015–28.

86. Ma L, Zhou Y, Luo X, Gao H, Deng X, Jiang Y. Long non-coding RNA XIST promotes cell growth and invasion through regulating miR-497/MACC1 axis in gastric cancer. Oncotarget. 2017 Jan 17;8(3):4125–35.

87. Zhang X-T, Pan S-X, Wang A-H, Kong Q-Y, Jiang K-T, Yu Z-B. Long Non-Coding RNA (lncRNA) X-Inactive Specific Transcript (XIST) Plays a Critical Role in Predicting Clinical Prognosis and Progression of Colorectal Cancer. Med Sci Monit. 2019 Aug 27;25:6429–35.

88. Sun Z, Zhang B, Cui T. Long non-coding RNA XIST exerts oncogenic functions in pancreatic cancer via miR-34a-5p. Oncol Rep. 2018 Feb 2;39(4):1591–600.

89. Liu W-G, Xu Q. Long non-coding RNA XIST promotes hepatocellular carcinoma progression by sponging miR-200b-3p. Eur Rev Med Pharmacol Sci. 2019 Nov;23(22):9857–62.

90. Yan K, Fu Y, Zhu N, Wang Z, Hong J, Li Y, et al. Repression of lncRNA NEAT1 enhances the antitumor activity of CD8+T cells against hepatocellular carcinoma via regulating miR-155/Tim-3. Int J Biochem Cell Biol. 2019 May 1;110:1–8.

91. Li Z, Feng C, Guo J, Hu X, Xie D. GNAS-AS1/miR-4319/NECAB3 axis promotes migration and invasion of non-small cell lung cancer cells by altering macrophage polarization. Funct Integr Genomics. 2020 Jan 1;20(1):17–28.

92. Chu Z, Huo N, Zhu X, Liu H, Cong R, Ma L, et al. FOXO3A-induced LINC00926 suppresses breast tumor growth and metastasis through inhibition of PGK1-mediated Warburg effect. Mol Ther. 2021 Sep 9;29(9):2737–53.

93. Yu Z, Zhao H, Feng X, Li H, Qiu C, Yi X, et al. Long Non-coding RNA FENDRR Acts as

a miR-423-5p Sponge to Suppress the Treg-Mediated Immune Escape of Hepatocellular Carcinoma Cells. Mol Ther - Nucleic Acids. 2019 Sep 6;17:516–29.

94. Filippova EA, Fridman M V., Burdennyy AM, Loginov VI, Pronina I V., Lukina SS, et al. Long Noncoding RNA GAS5 in Breast Cancer: Epigenetic Mechanisms and Biological Functions. Int J Mol Sci. 2021 Jun 24;22(13):6810.

95. Li Y, Li Y, Huang S, He K, Zhao M, Lin H, et al. Long non-coding RNA growth arrest specific transcript 5 acts as a tumour suppressor in colorectal cancer by inhibiting interleukin-10 and vascular endothelial growth factor expression. Oncotarget. 2017 Feb 21;8(8):13690–702.

96. Wang C, Ke S, Li M, Lin C, Liu X, Pan Q. Downregulation of LncRNA GAS5 promotes liver cancer proliferation and drug resistance by decreasing PTEN expression. Mol Genet Genomics. 2020 Jan 8;295(1):251–60.

97. Heidari R, Akbariqomi M, Asgari Y, Ebrahimi D, Alinejad-Rokny H. A systematic review of long non-coding RNAs with a potential role in breast cancer. Mutat Res Mutat Res. 2021 Jan 1;787:108375.

98. Kopp F, Elguindy MM, Yalvac ME, Zhang H, Chen B, Gillett FA, et al. PUMILIO hyperactivity drives premature aging of Norad-deficient mice. Elife. 2019 Feb 8;8:1–31.

99. Miao Z, Guo X, Tian L. The long noncoding RNA NORAD promotes the growth of gastric cancer cells by sponging miR-608. Gene. 2019 Mar 1;687(16):116–24.

100. Ghafouri-Fard S, Azimi T, Hussen BM, Abak A, Taheri M, Dilmaghani NA. Non-coding RNA Activated by DNA Damage: Review of Its Roles in the Carcinogenesis. Front Cell Dev Biol. 2021 Aug 13;9:714787.

101. Zhao W, Wang L, Xu F. LncRNA NORAD stimulates proliferation and migration of renal cancer via activating the miR-144-3p/MYCN axis. Eur Rev Med Pharmacol Sci. 2020 Oct;24(20):10426–32.

102. Wang X, Zou J, Chen H, Zhang P, Lu Z, You Z, et al. Long noncoding RNA NORAD regulates cancer cell proliferation and migration in human osteosarcoma by endogenously competing with miR-199a-3p. IUBMB Life. 2019 Oct 6;71(10):1482–91.

103. Shi P, Zhang J, Li X, Li W, Li H, Fu P. Long non-coding RNA NORAD inhibition upregulates microRNA-323a-3p to suppress tumorigenesis and development of breast cancer through the PUM1/eIF2 axis. Cell Cycle. 2021 Jul 3;20(13):1295–307.

104. Zhou K, Ou Q, Wang G, Zhang W, Hao Y, Li W. High long non-coding RNA NORAD expression predicts poor prognosis and promotes breast cancer progression by regulating TGF-β pathway. Cancer Cell Int. 2019 Dec 20;19(1):63.

105. Liu W, Zhou X, Li Y, Jiang H, Chen A. Long Non-Coding RNA NORAD Inhibits Breast Cancer Cell Proliferation and Metastasis by Regulating miR-155-5p/SOCS1 Axis. J Breast Cancer. 2021 Jun 1;24(3):330.

106. Tan B-S, Yang M-C, Singh S, Chou Y-C, Chen H-Y, Wang M-Y, et al. LncRNA NORAD is repressed by the YAP pathway and suppresses lung and breast cancer metastasis by sequestering S100P. Oncogene. 2019 Jul 9;38(28):5612–26.

107. Tao W, Li Y, Zhu M, Li C, Li P. LncRNA NORAD Promotes Proliferation And Inhibits Apoptosis Of Gastric Cancer By Regulating miR-214/Akt/mTOR Axis. Onco Targets Ther. 2019 Oct 30;Volume 12:8841–51.

108. Yu S-Y, Peng H, Zhu Q, Wu Y-X, Wu F, Han C-R, et al. Silencing the long noncoding RNA NORAD inhibits gastric cancer cell proliferation and invasion by the RhoA/ROCK1 pathway. Eur Rev Med Pharmacol Sci. 2019 May;23(9):3760–70.

109. Li Q, Li C, Chen J, Liu P, Cui Y, Zhou X, et al. High expression of long noncoding RNA NORAD indicates a poor prognosis and promotes clinical progression and metastasis in bladder cancer. Urol Oncol Semin Orig Investig. 2018 Jun 1;36(6):310.e15-310.e22.

110. Yang X, Cai J, Peng R, Wei C, Lu J, Gao C, et al. The long noncoding RNA NORAD enhances the TGF-β pathway to promote hepatocellular carcinoma progression by targeting miR-202-5p. J Cell Physiol. 2019 Jul 10;234(7):12051–60.

111. Tian Q, Yan X, Yang L, Liu Z, Yuan Z, Shen Z, et al. lncRNA NORAD promotes hepatocellular carcinoma progression via regulating miR-144-3p/SEPT2. Am J Transl Res. 2020;12(5):2257–66.

112. Li H, Wang X, Wen C, Huo Z, Wang W, Zhan Q, et al. Long noncoding RNA NORAD, a novel competing endogenous RNA, enhances the hypoxia-induced epithelial-mesenchymal transition to promote metastasis in pancreatic cancer. Mol Cancer. 2017 Dec 9;16(1):169.

113. Wu X, Lim Z-F, Li Z, Gu L, Ma W, Zhou Q, et al. NORAD Expression Is Associated with Adverse Prognosis in Esophageal Squamous Cell Carcinoma. Oncol Res Treat. 2017;40(6):370–4.

114. Wang L, Du L, Duan W, Yan S, Xie Y, Wang C. Overexpression of long noncoding RNA NORAD in colorectal cancer associates with tumor progression. Onco Targets Ther. 2018 Oct;Volume 11:6757–66.

115. Zhang J, Li X-Y, Hu P, Ding Y-S. lncRNA NORAD Contributes to Colorectal Cancer Progression by Inhibition of miR-202-5p. Oncol Res Featur Preclin Clin Cancer Ther. 2018 Oct 17;26(9):1411–8.

116. Shaker OG, Ali MA, Ahmed TI, Zaki OM, Ali DY, Hassan EA, et al. Association between LINC00657 and <scp>miR-106a</scp> serum expression levels and susceptibility to colorectal cancer, adenomatous polyposis, and ulcerative colitis in Egyptian population. IUBMB Life. 2019 Sep 29;71(9):1322–35.

117. Lei Y, Wang Y-H, Wang X-F, Bai J. LINC00657 promotes the development of colon cancer by activating PI3K/AKT pathway. Eur Rev Med Pharmacol Sci. 2018 Oct;22(19):6315–23.

118. Xu C, Zhu L-X, Sun D-M, Yao H, Han D-X. Regulatory mechanism of lncRNA NORAD on proliferation and invasion of ovarian cancer cells through miR-199a-3p. Eur Rev Med Pharmacol Sci. 2020 Feb;24(4):1672–81.

119. Huo H, Tian J, Wang R, Li Y, Qu C, Wang N. Long non-coding RNA NORAD upregulate SIP1 expression to promote cell proliferation and invasion in cervical cancer. Biomed Pharmacother. 2018 Oct 1;106:1454–60.

120. Chen Y, Cao K, Li J, Wang A, Sun L, Tang J, et al. Overexpression of long non-coding RNA NORAD promotes invasion and migration in malignant melanoma via regulating the MIR-205-EGLN2 pathway. Cancer Med. 2019 Apr 7;8(4):1744–54.

121. Chen F, Liu L, Wang S. Long non-coding RNA NORAD exhaustion represses prostate cancer progression through inhibiting TRIP13 expression via competitively binding to miR-495-3p. Cancer Cell Int. 2020 Jul 18;20(1):1–15.

122. Wu Y, Shen Q-W, Niu Y-X, Chen X-Y, Liu H-W, Shen X-Y. LncNORAD interference inhibits tumor growth and lung cancer cell proliferation, invasion and migration by down-regulating CXCR4 to suppress RhoA/ROCK signaling pathway. Eur Rev Med Pharmacol Sci. 2020 May;24(10):5446–55.

123. Han T, Wu Y, Hu X, Chen Y, Jia W, He Q, et al. NORAD orchestrates endometrial cancer progression by sequestering FUBP1 nuclear localization to promote cell apoptosis. Cell Death Dis. 2020 Jun 18;11(6):473.

124. Utnes P, Løkke C, Flægstad T, Einvik C. Clinically Relevant Biomarker Discovery in High-Risk Recurrent Neuroblastoma. Cancer Inform. 2019 Jan 11;18:117693511983291.

125. Song Q, Geng Y, Li Y, Wang L, Qin J. Long noncoding RNA NORAD regulates MPP+-induced Parkinson's disease model cells. J Chem Neuroanat. 2019 Nov 1;101:101668.

126. He H, Yang H, Liu D, Pei R. LncRNA NORAD promotes thyroid carcinoma progression through targeting miR-202-5p. Am J Transl Res. 2019 Jan 1;11(1):290–9.

127. Munschauer M, Nguyen CT, Sirokman K, Hartigan CR, Hogstrom L, Engreitz JM, et al. The NORAD lncRNA assembles a topoisomerase complex critical for genome stability. Nature. 2018 Sep 27;561(7721):132–6.

128. Hu J, Zhou Y, Obayemi JD, Du J, Soboyejo WO. An investigation of the viscoelastic properties and the actin cytoskeletal structure of triple negative breast cancer cells. J Mech Behav Biomed Mater. 2018 Oct;86:1–13.

129. Holliday DL, Speirs V. Choosing the right cell line for breast cancer research. Breast Cancer Res. 2011 Aug 12;13(4):215.

130. Alves-Vale C, Capela AM, Tavares-Marcos C, Domingues-Silva B, Pereira B, Santos F, et al. Expression of NORAD correlates with breast cancer aggressiveness and protects breast cancer cells from chemotherapy. Mol Ther - Nucleic Acids. 2023 Sep 12;33:910–24.

131. Olive PL, Banáth JP. The comet assay: a method to measure DNA damage in individual cells. Nat Protoc. 2006 Jun 27;1(1):23–9.

132. Li X, Yang J, Peng L, Sahin AA, Huo L, Ward KC, et al. Triple-negative breast cancer has worse overall survival and cause-specific survival than non-triple-negative breast cancer. Breast Cancer Res Treat. 2017 Jan 25;161(2):279–87.

133. Huarte M. The emerging role of lncRNAs in cancer. Nat Med. 2015 Nov 5;21(11):1253–61.

134. Wang Z, Yang B, Zhang M, Guo W, Wu Z, Wang Y, et al. lncRNA Epigenetic Landscape Analysis Identifies EPIC1 as an Oncogenic lncRNA that Interacts with MYC and Promotes Cell-Cycle Progression in Cancer. Cancer Cell. 2018 Apr 9;33(4):706-720.e9.

135. Rodrıguez-Gonzalez FG, Mustafa DAM, Mostert B, Sieuwerts AM. The challenge of gene expression profiling in heterogeneous clinical samples. Methods. 2013 Jan 1;59(1):47–58.

136. Silva ILZ, Kohata AA, Shigunov P. Modulation and function of Pumilio proteins in cancer. Semin Cancer Biol. 2022 Nov 1;86:298–309.

137. Tichon A, Perry RB-T, Stojic L, Ulitsky I. SAM68 is required for regulation of Pumilio by the NORAD long noncoding RNA. Genes Dev. 2018 Jan 1;32(1):70–8.

138. Banani SF, Lee HO, Hyman AA, Rosen MK. Biomolecular condensates: organizers of cellular biochemistry. Nat Rev Mol Cell Biol. 2017 May 22;18(5):285–98.

139. Huber D, Voith von Voithenberg L, Kaigala GV. Fluorescence in situ hybridization (FISH): History, limitations and what to expect from micro-scale FISH? Micro Nano Eng. 2018 Nov 1;1:15–24.

140. Blumberg A, Zhao Y, Huang YF, Dukler N, Rice EJ, Chivu AG, et al. Characterizing RNA stability genome-wide through combined analysis of PRO-seq and RNA-seq data. BMC Biol. 2021 Dec 1;19(1):1–17.

141. Graf J, Kretz M. From structure to function: Route to understanding lncRNA mechanism. BioEssays. 2020 Dec 9;42(12):2000027.

142. Sajek M, Janecki DM, Smialek MJ, Ginter-Matuszewska B, Spik A, Oczkowski S, et al. PUM1 and PUM2 exhibit different modes of regulation for SIAH1 that involve cooperativity with NANOS paralogues. Cell Mol Life Sci. 2019 Jan 29;76(1):147–61.

143. Goldstrohm AC, Hall TMT, McKenney KM. Post-transcriptional Regulatory Functions of Mammalian Pumilio Proteins. Trends Genet. 2018 Dec 1;34(12):972–90.

144. Zhang L, Chen Y, Li C, Liu J, Ren H, Li L, et al. RNA binding protein PUM2 promotes the stemness of breast cancer cells via competitively binding to neuropilin-1 (NRP-1) mRNA with miR-376a. Biomed Pharmacother. 2019 Jun 1;114:108772.

145. Maier T, Güell M, Serrano L. Correlation of mRNA and protein in complex biological samples. FEBS Lett. 2009 Dec 17;583(24):3966–73.

146. Smialek MJ, Ilaslan E, Sajek MP, Jaruzelska J. Role of PUM RNA-Binding Proteins in Cancer. Cancers (Basel). 2021 Jan 3;13(1):129.

147. Uyhazi KE, Yang Y, Liu N, Qi H, Huang XA, Mak W, et al. Pumilio proteins utilize distinct regulatory mechanisms to achieve complementary functions required for pluripotency and embryogenesis. Proc Natl Acad Sci U S A. 2020 Apr 7;117(14):7851–62.

148. Zeng T, Guan Y, Li Y, Wu Q, Tang X, Zeng X, et al. The DNA replication regulator MCM6: An emerging cancer biomarker and target. Clin Chim Acta. 2021 Jun 1;517:92–8.

149. Zhang S, Xiao M, Liu Z, Mo Y, Liu H, Xu B. The functional significance of ATM phosphorylation of Bub3 on Serine 135 in sensitivity to DNA damaging agents. J Clin Oncol. 2021 May 20;39(15_suppl):e15048–e15048.

150. Wang Y, Luo W, Wang Y. PARP-1 and its associated nucleases in DNA damage response. DNA Repair (Amst). 2019 Sep 1;81:102651.

151. Sunada S, Saito H, Zhang D, Xu Z, Miki Y. CDK1 inhibitor controls G2/M phase transition and reverses DNA damage sensitivity. Biochem Biophys Res Commun. 2021 Apr 23;550:56–61.

152. BOZGEYİK İ. The Possible Role of the Long Non-coding RNA NORAD in Mitomycin C-Related Chemoresistance. Namık Kemal Tıp Derg. 2022 Sep 16;10(3):255–9.

153. Wang B, Xu L, Zhang J, Cheng X, Xu Q, Wang J, et al. LncRNA NORAD accelerates the progression and doxorubicin resistance of neuroblastoma through up-regulating HDAC8 via sponging miR-144-3p. Biomed Pharmacother. 2020 Sep 1;129:110268.

154. Zhang L, Wu H, Zhang Y, Xiao X, Chu F, Zhang L. Induction of lncRNA NORAD accounts for hypoxia-induced chemoresistance and vasculogenic mimicry in colorectal cancer by sponging the miR-495-3p/ hypoxia-inducible factor-1α (HIF-1α). Bioengineered. 2022 Jan 1;13(1):950–62.

155. Yang Y, Zhang G, Li J, Gong R, Wang Y, Qin Y, et al. Long noncoding RNA NORAD acts as a ceRNA mediates gemcitabine resistance in bladder cancer by sponging miR-155–5p to regulate WEE1 expression. Pathol - Res Pract. 2021 Dec 1;228:153676.

Annex

Molecular Therapy
Nucleic Acids
Original Article

Expression of *NORAD* correlates with breast cancer aggressiveness and protects breast cancer cells from chemotherapy

Catarina Alves-Vale,[1,2,9] Ana Maria Capela,[3,9] Carlota Tavares-Marcos,[3,9] Beatriz Domingues-Silva,[1] Bruno Pereira,[4,5] Francisco Santos,[3] Carla Pereira Gomes,[1] Guadalupe Espadas,[6,7] Rui Vitorino,[3] Eduard Sabidó,[6,7] Paula Borralho,[2,8] Sandrina Nóbrega-Pereira,[3] and Bruno Bernardes de Jesus[3]

[1]Instituto de Medicina Molecular João Lobo Antunes, Faculdade de Medicina, Universidade de Lisboa, Av. Professor Egas Moniz, 1649-028 Lisboa, Portugal; [2]Hospital CUF Descobertas, CUF Oncologia, 1998-018 Lisbon, Portugal; [3]Department of Medical Sciences and Institute of Biomedicine – iBiMED, University of Aveiro, 3810-193 Aveiro, Portugal; [4]i3S – Instituto de Investigação e Inovação em Saúde, Universidade do Porto, Porto, Portugal; [5]IPATIMUP – Instituto de Patologia e Imunologia Molecular da Universidade do Porto, Porto, Portugal; [6]Center for Genomic Regulation, Barcelona Institute of Science and Technology (BIST), Barcelona, Spain; [7]Universitat Pompeu Fabra, Barcelona, Spain; [8]Faculdade de Medicina, Universidade de Lisboa, Av. Professor Egas Moniz, 1649-028 Lisboa, Portugal

The recently discovered human lncRNA *NORAD* is induced after DNA damage in a p53-dependent manner. It plays a critical role in the maintenance of genomic stability through interaction with Pumilio proteins, limiting the repression of their target mRNAs. Therefore, *NORAD* inactivation causes chromosomal instability and aneuploidy, which contributes to the accumulation of genetic abnormalities and tumorigenesis. *NORAD* has been detected in several types of cancer, including breast cancer, which is the most frequently diagnosed and the second-leading cause of cancer death in women. In the present study, we confirmed upregulated *NORAD* expression levels in a set of human epithelial breast cancer cell lines (MDA-MB-231, MDA-MB-436, and MDA-MB-468), which belong to the most aggressive subtypes (triple-negative breast cancer). These results are in line with previous data showing that high *NORAD* expression levels in basal-like tumors were associated with poor prognosis. Here, we demonstrate that *NORAD* downregulation sensitizes triple-negative breast cancer cells to chemotherapy, through a potential accumulation of genomic aberrations and an impaired capacity to signal DNA damage. These results show that *NORAD* may represent an unexploited neoadjuvant therapeutic target for chemotherapy-unresponsive breast cancer.

INTRODUCTION

The Human Genome Project provided scientists and society with transformational insights into the intriguing complexity of the transcriptome of human cells.[1] Long non-coding RNAs (lncRNAs) constitute the broadest class of non-coding RNAs, displaying a tissue-specific spatiotemporal expression profile,[2] with numerous biological roles identified, spanning from development to aging, in both normal and pathological conditions, such as age-related diseases.[3–5] The study of differential gene expression in cancer has led to the identification of thousands of associated lncRNAs[2] involved in several cancer hallmarks including genomic instability, tumor-promoting inflammation, and evasion of immune detection.[6,7] LncRNA *NORAD*[8] is a 5.3 kb transcript, annotated as *LINC00657*, localized on chromosome 20 (20q11.23).[9] *NORAD* shows strong evolutionary conservation and is widely expressed in human tissues and cell lines.[9,10] *NORAD* seems to play a crucial role in the maintenance of genomic stability: its inactivation triggers chromosomal instability in previously karyotypically stable cell lines, and expression levels of this lncRNA seem to increase after inducing DNA damage with doxorubicin.[9] One of the possible mechanisms involves *NORAD* sequestering PUMILIO-1 and PUMILIO-2 RNA-binding proteins that target mRNAs and reduce their stability.[9,11–13] PUMILIO interaction seems to be mediated by SAM68, an abundant and multifunctional cell-cycle-regulated RNA-binding protein.[14] Therefore, *NORAD* levels directly influence the availability of PUMILIO to downregulate a set of factors involved in mitosis, DNA repair, and DNA replication.[9] Nonetheless, many genes regulated by *NORAD* are not PUMILIO targets, suggesting that other mechanistic events are involved, such as miRNA sponging. Considering the complexity of the *NORAD* network, *NORAD* appears to have a dual effect depending on the tumor type.[9,15,16] Among those interactors, there was shown to be enrichment of DNA damage response (DDR)-associated proteins, mitotic cell cycle and mini-chromosome maintenance (MCM) complex.[17] Some previously identified *NORAD* interactors are nucleosome assembly protein 1-like 4 (NAP1L4),[17] a histone chaperone[18] involved in the chromatin assembly step related to DNA replication and repair.[19] The nucleosome assembly protein 1 is an H2A-H2B chaperone,[20]

Received 23 February 2023; accepted 16 August 2023;
https://doi.org/10.1016/j.omtn.2023.08.019.

[9]These authors contributed equally

Correspondence: Bruno Bernardes de Jesus, Department of Medical Sciences and Institute of Biomedicine – iBiMED, University of Aveiro, 3810-193 Aveiro, Portugal.
E-mail: brunob.jesus@ua.pt

preventing excessive accumulation of these chromatin marks.[21] *NORAD* also binds to the RNA binding motif protein X-linked (RBMX), which participates in the DDR, inducing the assembly of the *NORAD*-activated ribonucleoprotein complex 1 nucleic complex, through RBMX, promoting genomic and chromosomal stability.[22]

The intrinsic resistance of neoplastic disorders to chemotherapy and targeted therapy represents a major clinical concern.[23] The underlying causes of resistance can be attributed to intratumor heterogeneity,[23,24] in part due to genomic instability.[25] Chromosomal instability, a hallmark of cancer, is often associated with cancer progression, correlating with poor breast cancer prognosis.[26] Paradoxically, by affecting cancer cell fitness, chromosomal instability may be exploited and have beneficial roles against cancer, namely in estrogen receptor (ER)-negative tumors, which were found to be associated with a better long-term survival when extreme levels of chromosome instability were present.[27]

Considering the correlation between *NORAD* and genome instability, as well as the contradictory effect of chromosomal instability in tumor progression, we investigate whether targeting *NORAD* could act synergistically with cytotoxic agents.[27,28] Here, we demonstrate that downregulation of *NORAD* sensitizes human breast cancer cells to doxorubicin. *NORAD* expression was shown to be needed to signal the DNA damage after doxorubicin treatment. Our results underline the potential contribution of *NORAD* in chemotherapy-resistant cancer cells.

RESULTS

NORAD is highly expressed in triple-negative breast cancer

Breast cancer is a heterogeneous disease and four main clinicopathological groups (luminal A-like, luminal B-like, HER2-positive (non-luminal), and triple-negative) are defined based on the expression of ERs, progesterone receptors (PRs), human epidermal growth factor receptor 2 (ERBB2/HER2), and Ki67.[29]

Initially, we determined the basal mRNA levels of *NORAD* in a set of human breast cancer cell lines (MCF-7, MDA-MB-231, -436, and -468) and in a non-malignant human mammary epithelial cell line (MCF-10A) by real-time quantitative reverse transcriptase polymerase chain reaction (qRT-PCR). We observed that MDA-MB-231, -436, and -468 cell lines, corresponding to triple-negative breast cancer (TNBC), express higher levels of *NORAD*. On the other hand, the luminal A-like subtype MCF-7 cell line expresses *NORAD* at comparable levels with control MCF-10A cell line (Figure 1A). The same pattern could be detected when we compared *NORAD* levels through fluorescence *in situ* hybridization (FISH) using Stellaris-specific probes (Figure 1B).

TNBC, considered the most aggressive breast cancer subtype, is defined by the absence of ER, PR, and HER2, detected through immunohistochemical staining, which limits targeted hormonal therapeutic options.[30] On the contrary, luminal-like breast cancer is characterized by the expression of hormonal receptors (ER and/or PR) and a more indolent clinical behavior. Therefore, our findings suggest that high expression of *NORAD* may be indicative of a more aggressive form of breast cancer. These results align with those obtained by analyzing formalin-fixed paraffin-embedded (FFPE) human breast samples using single-molecule RNA *in situ* hybridization (RNAscope), which revealed higher *NORAD* expression in TNBC compared with the luminal-like tumor and normal mammary epithelium (Figure 1C). Neither patient had received previous chemotherapy. Despite the low level of evidence to recommend p53 immunohistochemical assessment for routine use, some studies suggest that abnormal staining correlates with aggressiveness features.[31] The p53 expression pattern strongly differed between the two neoplasms, being heterogeneous ("wild-type" pattern) in the luminal-like tumor, with strong and diffuse staining (overexpression/accumulation, "mutated-type" pattern) in TNBC. This observation is concordant with the higher frequency of *TP53* mutations in tumors classified as basal-like, which are a subtype of TNBC defined by specific gene expression patterns (Figure 1C).

Next, we asked how *NORAD* expression levels correlated with cancer patients' outcome. We used the Kaplan-Meier Plotter Tool to correlate *NORAD* levels with prognosis of breast cancer patients. The KMPlotter database incorporates several gene expression profiles; breast cancer samples are stratified into high- and low-expression groups using the median gene expression level as a cutoff.[32] Considering all breast cancer subtypes as a group, *NORAD* levels do not correlate with relapse-free survival ($n = 2032$, $p = 0.057$) (Figure 1D) nor overall survival ($n = 943$, $p = 0.25$) (Figures S1A and S1B). However, there is a statistically significant negative correlation between *NORAD* levels and relapse-free survival ($n = 953$, $p = 0.002$) when considering, in isolation, basal-like tumors (defined by PAM50 genetic profiling) (Figure 1E). Even though high *NORAD* levels are correlated with a lower relapse-free survival in poorly differentiated (grade 3) tumors ($n = 417$, $p = 0.026$), no association between *NORAD* expression and survival for the remaining tumor subtypes (luminal or HER2+) was found (Figures S1C–S1F). Therefore, high *NORAD* levels seem to be a survival prognostic factor specifically for patients with TNBC.

NORAD knockdown affects relevant tumor-specific phenotypes and sensitizes TNBC cells to chemotherapy

To unveil the role of *NORAD* in breast cancer, we used LNA GapmeRs and siRNAs targeting both the nuclear and cytoplasmic fractions of *NORAD*. Two LNA GapmeRs that target different regions of *NORAD* were tested individually and in combination in the MDA-MB-231 and MDA-MB-468 (Figures S2A–S2C) at final concentrations of 25 and 50 nM. We observed the most significant and consistent reduction of *NORAD*, confirmed by smRNA FISH in MDA-MB-468, using LNA GapmeRs in combination with siRNAs, at a final concentration of 25 nM, with an interval of 24 h between transfections (Figure 2A).

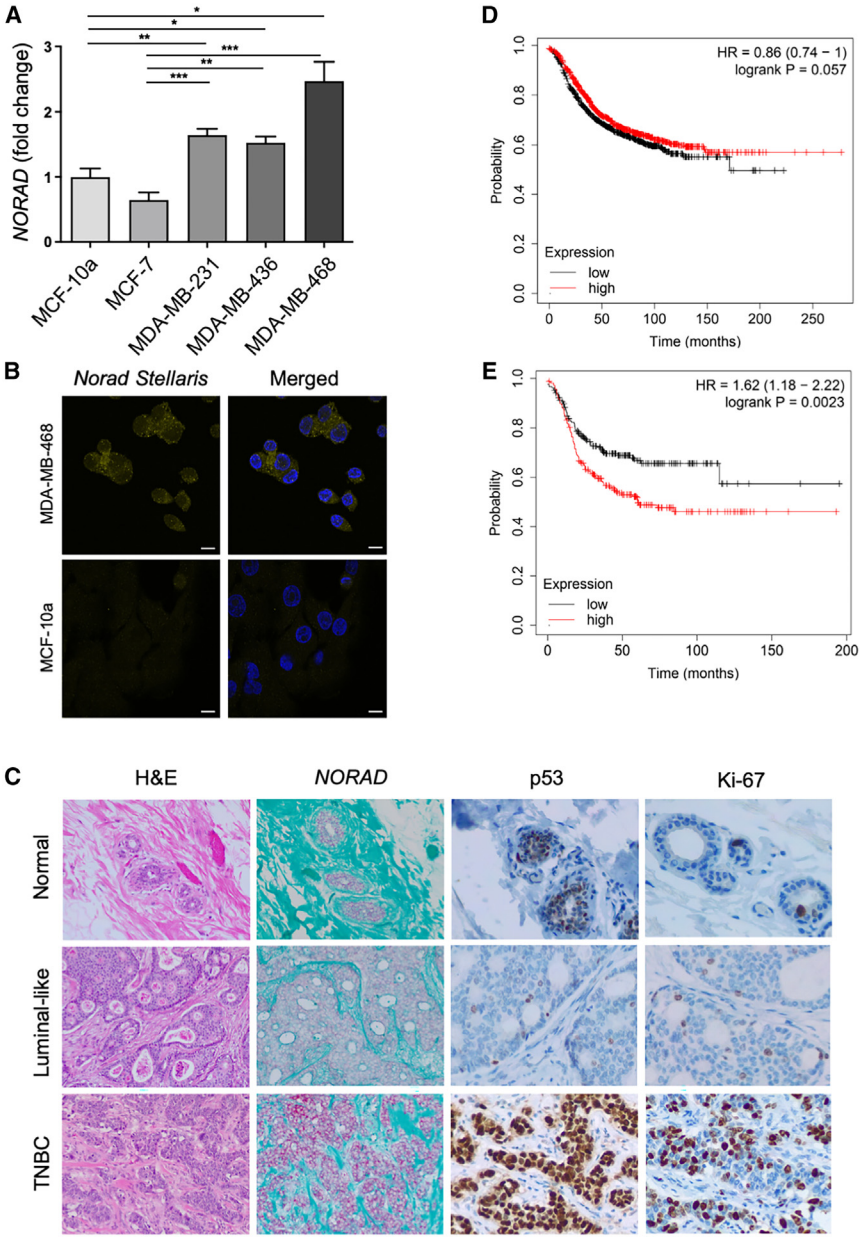

Figure 1. *NORAD* characterization

(A) *NORAD* mRNA basal levels in human epithelial breast cancer cell lines (qRT-PCR) (n = 3). (B) *NORAD* subcellular localization in the MDA-MB-468 and MCF10a cell lines (smRNA FISH). Scale bar, 10 μm). (C) Higher *NORAD* expression (by RNA *in situ* hybridization, RNAscope) in triple-negative breast invasive carcinoma (TNBC) (lower) compared with luminal-like invasive (cribriform) carcinoma (middle) and human normal mammary tissue (upper) (n = 1, each); strong and diffuse p53 immunostaining and higher proliferative index (Ki67) in TNBC; hematoxylin and eosin (H&E) staining and *NORAD in situ* hybridization at 100×; p53 and Ki67 immunostaining at 200× magnification. (D and E) Correlation between *NORAD* expression and prognosis of breast cancer patients (Kaplan-Meier Plotter): relapse-free survival irrespective of breast cancer subtype (A) and for basal-like breast cancer (E) (curves show the probability of survival over time and are colored based on the *NORAD* levels, the x axis represents time in months, and the y axis represents the proportion of patients who are still alive without relapse). For statistical analysis we used one-way ANOVA with a control condition for multiple comparisons. No symbol, $p > 0.05$, *$p < 0.05$, **$p < 0.01$, ***$p < 0.001$.

Characterization of breast cancer cells was performed 48 h after *NORAD* downregulation, the time at which we detected lower *NORAD* levels. In addition, it has been demonstrated previously that 24 h after *NORAD* knockdown (KD) is not sufficient to affect PUMILIO-targeted mRNAs related to cell cycle and mitosis.[12] We first tested whether *NORAD* affected the capacity of TNBC cells to migrate through the wound healing assay. After *NORAD* KD, a reduction in the migration rates of cells was evident, in comparison with the controls (Figures 2B, 2C, and S3). This result supports the role of *NORAD* in tumorigenesis, since invasiveness is one of the hallmarks of cancer.[6,7] Considering the higher expression levels of *NORAD* in aggressive tumors, we addressed whether this transcript might be associated with chemoresistance. We tested the chemotherapeutic agent doxorubicin, an anthracycline commonly used in breast cancer treatment,[33,34] which disrupts topoisomerase II-dependent DNA repair and mitochondrial function.[35] Initially, we determined the half-maximal inhibitory concentration (IC_{50}) for MCF-10A (Figure S4A) and MDA-MB-231 (Figure S4B) cell lines, confirming the higher values for non-malignant human mammary epithelial cells and demonstrating the chemotherapy selectivity toward cancer cells with higher proliferation rates. Then, we evaluated the effects of combining *NORAD* KD with chemotherapy. We observed a reduction in doxorubicin IC_{50} upon *NORAD* KD through alamarBlue cellular viability assay (Figures 2D and S5, IC_{50} shifted from 0.3779 to 0.05680 μM), indicating that *NORAD* KD sensitizes breast cancer cells to chemotherapy. This was accompanied by an increase in Annexin V^+ cells (Figures 2E and 2F), something previously observed after doxorubicin treatment.[36]

NORAD dowregulation impairs DNA damage pathways

To identify *NORAD*-associated proteins that could be mediating the increased sensitivity to doxorubicin we performed liquid chromatography-tandem mass spectrometry (LC-MS/MS) for quantitative comparison between groups (*NORAD* wild-type vs. *NORAD* KD) in the MDA-MB-231 cell line. Four independent conditions

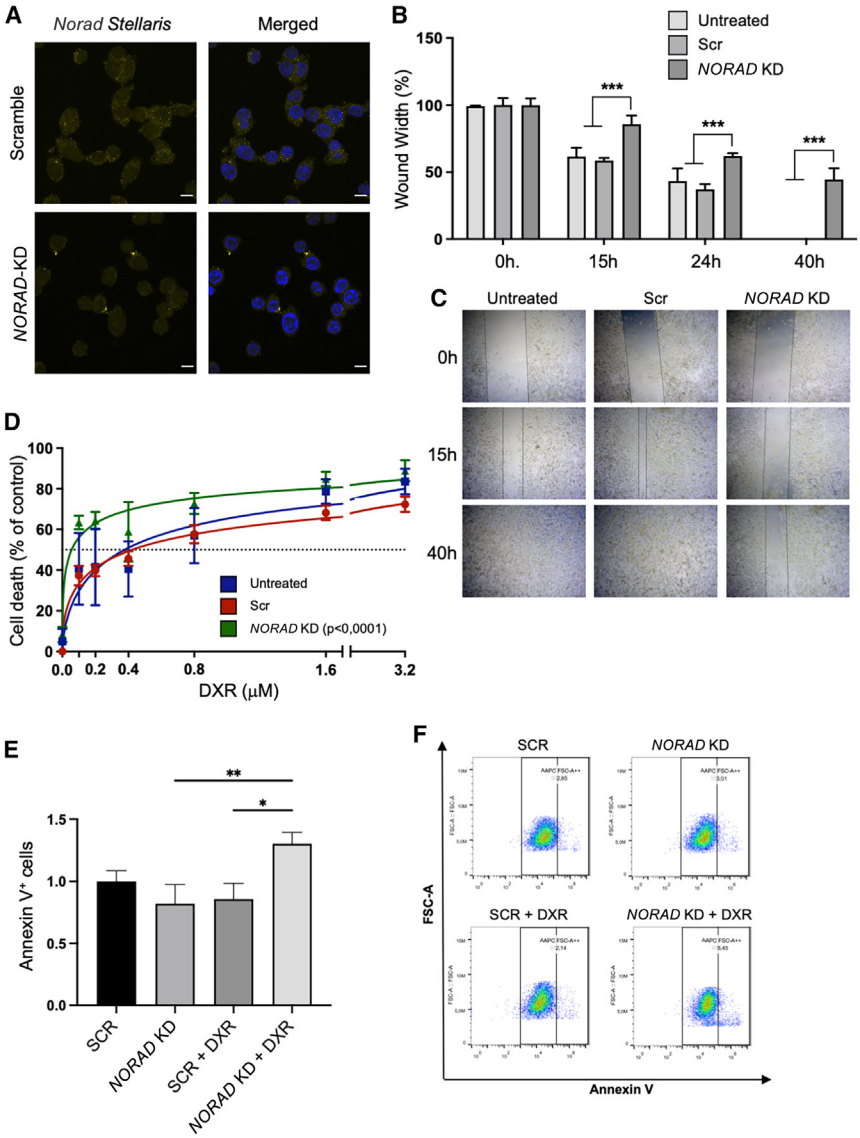

Figure 2. *NORAD* KD effects on tumor-relevant phenotypes

(A) *NORAD* levels in the MDA-MB-468 cell line (smRNA FISH) treated with control siRNA + LNA or *NORAD*-specific siRNA + LNA. (B and C) *NORAD* KD effect on cell migration in the MDA-MB-231 cell line (wound healing assay); (B) is the gap quantification at the indicated time points (n = 3), (C) is a representative image of the wound healing. (D) *NORAD* KD sensitizes cells to doxorubicin (DXR), measured through the alamarBlue reduction assay (n = 3). (E and F) *NORAD* KD and doxorubicin effects on cell apoptosis in the MDA-MB-231 cell line (n = 3) as measured through the increase in Annexin V^+ cells and as visualized in the representative plots (F). No symbol, $p > 0.05$, *$p < 0.05$, **$p < 0.01$, ***$p < 0.001$.

were individually analyzed. Whole proteome analysis by LC-MS/MS retrieved 4,167 unique proteins with at least two unique peptides. Of all proteins detected, 1,464 were common to all the conditions studied, leading to 35% of common proteins. Partial least-squares discriminant analysis (PLS-DA) was used to visualize group separation based on proteome datasets by means of dimensionality reduction. PLS-DA showed a clear separation of the experimental groups (Figure 3A). *NORAD* KD appeared, however, to increase the heterogeneity of the proteome, which was probably related with the KD efficiency (Figure 3A). To find quantitative patterns between the experimental groups, comparative and grouped analysis was performed (Figure 3B). When looking at experimental groups, two main clusters were apparent with a different profile of proteins being either overexpressed or repressed in the different experimental conditions (adjusted $p < 0.05$). *NORAD* KD downregulated proteins that were predominantly involved in biological processes related with G1/S transition of mitotic cell cycle and DDR (Figure 3C). The analysis revealed a preponderant altered modulation of proteins involved in the regulation of DNA repair, chromatin remodeling, and epigenetic regulation (Figure S6), suggesting that *NORAD* KD could affect the sensitivity of the MDA-MB-231 cells to doxorubicin by modulating the activity of proteins involved in DNA repair and epigenetic regulation. One example is MCM protein 6 (MCM6), the levels of which strongly decrease after *NORAD* KD. MCM6 is involved in the initiation of DNA replication and is a strong predictor of survival in cancer patients,[37] or ALYREF, a known interactor of *NORAD*,[22] a factor associated with poor survival in breast cancer patients.[38] The lower expression of some detected proteins could be moderately confirmed by qPCR, demonstrating that *NORAD* may regulate the level of these proteins by other pathways, not only at the transcriptional level (Figures S6B–S6D).

NORAD in the response to DNA damage

In line with previous observations on the role of *NORAD* in DDR, and our own results supporting the sensitivity of *NORAD* KD cells to doxorubicin, we wondered how MDA-MB-231 or MDA-MB-468 cells with silenced *NORAD* would recognize and repair DNA lesions. Immediately after DNA double-strand breaks (DSBs) occur, histone H2AX is phosphorylated (γH2AX) mainly by ATM at C-terminal Ser136 and Ser139 residues,[39] leading to signal amplification that ends with chromatin remodeling and recruitment of DNA repair proteins, such as BRCA1 and 53BP1. Using immunofluorescence (IF) we observed that *NORAD* KD resulted in an exacerbated accumulation of γH2AX in the

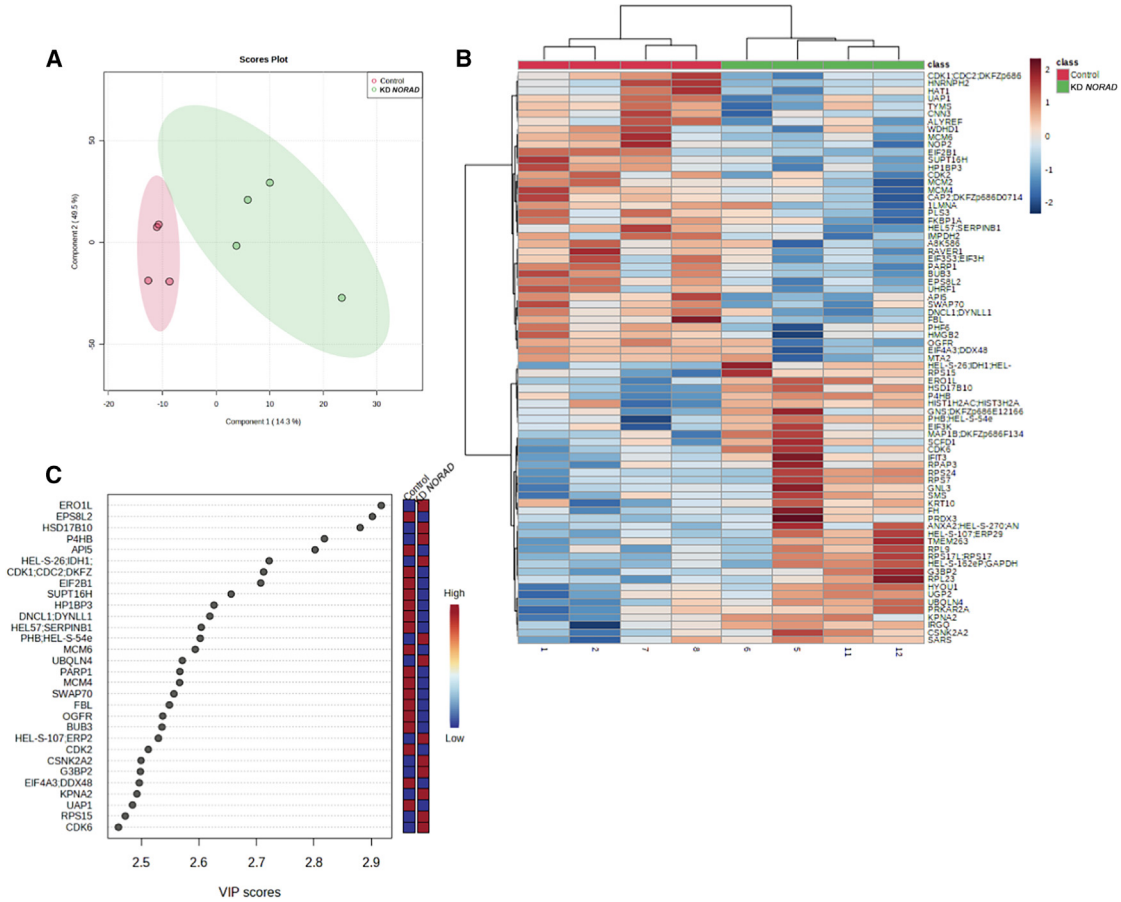

Figure 3. *NORAD* KD alters the proteome balance toward genetic instability

(A) Partial least-squares discriminant analysis (PLS-DA) of the different variables tested (control vs. *NORAD* KD). (B) Heatmap showing the hierarchical clustering of the top 100 hits contributing to the separation of the variables control vs. *NORAD* KD. (C) Variable importance in projection (VIP) scores of the top 30 genes between the conditions control vs. *NORAD* KD.

MDA-MB-231 cells exposed to different concentrations of doxorubicin (Figures 4A, 4C, S7, and S8). This effect was not exacerbated when the Pumilio 1 and 2 proteins were concomitantly targeted with *NORAD*. Targeting Pumilio proteins separately (Figure S9) also resulted in some accumulation of γH2AX, although not equivalent to *NORAD* KD (Figures 4A and 4C), demonstrating a multifaceted role for Pumilio family of proteins in the setting of doxorubicin-induced DNA damage in breast cancer cells. Pumilio proteins have crucial roles in several cellular pathways, spanning mitosis and DNA repair. Whether DNA damage may induce Pumilio expression was also assessed by IF (Figures 4B and 4D). The presence of doxorubicin was shown to significantly decrease the presence of Pumilio 1 proteins independently of *NORAD* in cancer cells. Interestingly, in the absence of Pumilio 2 there is a compensatory expression of Pumilio 1, previously observed in the context of stemness and embryogenesis.[40] Still, this increased expression does not impact on the signaling of DNA damage (Figures 4A and 4C). To further explore these results we evaluated γH2AX, H2AX, and Pum1 expression by western blot (WB) (Figures 5A and 5B). Similarly to IF, we could detect an increased expression of γH2AX in the conditions where *NORAD* was absent. Interestingly, the same compensatory role of Pumilio could be observed, since Pum2 levels greatly increased when Pum1 was targeted (Figures 5A and 5B). Of note, *NORAD*/PUM1/2 KD has a comparable level of γH2AX levels as SCR + DXR alone by WB, showing an impact of these proteins on DDR.

To understand whether this increase in DNA damage signaling correlated with an accumulation of DNA breaks, Comet assay was performed to explore different cellular conditions. DNA damage is measured by the presence of DNA in the comet tail, indicative of DNA break intensity.[41,42] As expected, DNA breaks have been detected in the presence of doxorubicin. KD of *NORAD* increased the amount of DNA damage at 0.6 μM of DXR (Figures 5C and 5D), supporting previous results showing an increased accumulation of γH2Ax or cell death in the *NORAD* KD condition. Again, the condition *NORAD*/PUM1/2 KD had an increased amount of DNA damage even in the absence of DXR.

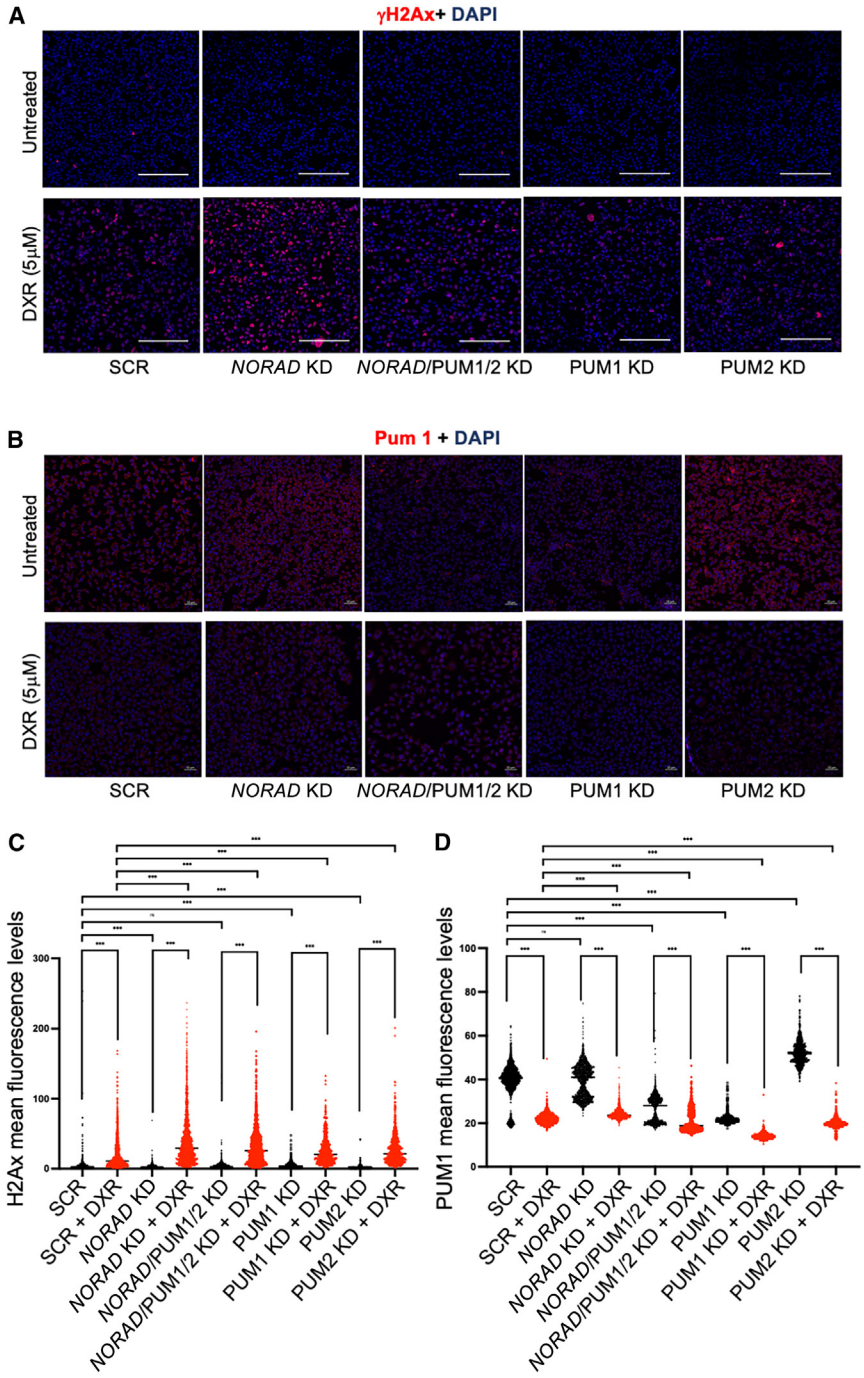

Figure 4. *NORAD* KD alters γH2Ax accumulation after DNA damage

(A and B) Immunofluorescence (A) for γH2Ax and (B) for Pum1 in the depicted experimental conditions in the MDA-MB-231 cell line. Scale bars, 200 μm (A) and 50 μm (B). (C and D) Quantification of the signal corresponding to γH2Ax (C) and Pum1 (D) in the depicted experimental conditions in the MDA-MB-231 cell line (see materials and methods). No symbol, $p > 0.05$, *$p < 0.05$, **$p < 0.01$, ***$p < 0.001$.

To further explore the involvement of the DDR proteins in the *NORAD*-mediated accumulation of γH2Ax we used siRNAs to KD (Figures 6A and 6B) two of the hits identified in the *NORAD*-associated proteome (LC-MS/MS experiment, Figure 3), namely PARP1 and CDK1, both proteins being extensively linked to cancer and DXR response.[43–47] Although *NORAD* KD already impacted on the levels of PARP1 and CDK1 (Figure 3), siRNA-mediated KD showed a more consistent and severe reduction of their levels. Using IF we observed that *NORAD*/PARP1 KD, in the presence of DXR, resulted in a higher level of accumulation of γH2Ax, demonstrating the synergistic role of these two factors (Figures 6C and 6D). PARP1 alone, in the absence of DXR, increased the mean γH2Ax intensity (SCR, 105, to PARP1 KD, 189). Although CDK1-KD increased the 75th percentile of mean γH2Ax intensity (*NORAD* KD + DXR, 614; *NORAD*/PARP1 KD + DXR, 692; and *NORAD*/CDK1 KD + DXR, 692), the average intensity was not altered, probably due to an incomplete reduction of CDK1 levels, as depicted by WB (Figure 6B).

DISCUSSION

In this study, we reported that *NORAD* is overexpressed in breast cancer, conferring resistance to chemotherapy, and interfering with γH2AX signaling upon DNA damage.

It was described previously in esophageal, breast, lung, pancreatic, bladder, and colorectal cancers that *NORAD* functions as a potential oncogenic factor, suggesting that it may constitute a tumor biomarker, defining patient prognosis, predicting therapy response, and/or be used as a therapeutic target.[16,28,48–50] Our results support this scenario where higher *NORAD* levels are associated with an aggressive breast cancer subtype (TNBC) and poor relapse-free survival of patients, while *NORAD* KD inhibits cancer cell viability and migration. Despite this association, it was also described previously in liver cancer that *NORAD* functions as a potential tumor suppressor.[51] These opposing results may be explained by the distinctive interacting partners of *NORAD*, as it is known to sponge a myriad of miRNAs, albeit binding preferentially to PUMILIO proteins known to repress mRNAs involved in mitosis, DNA repair, and replication (e.g., PRC1, PARP1, and WDHD1),[9,12] but also repress mRNAs involved in various cancer pathways (e.g.,

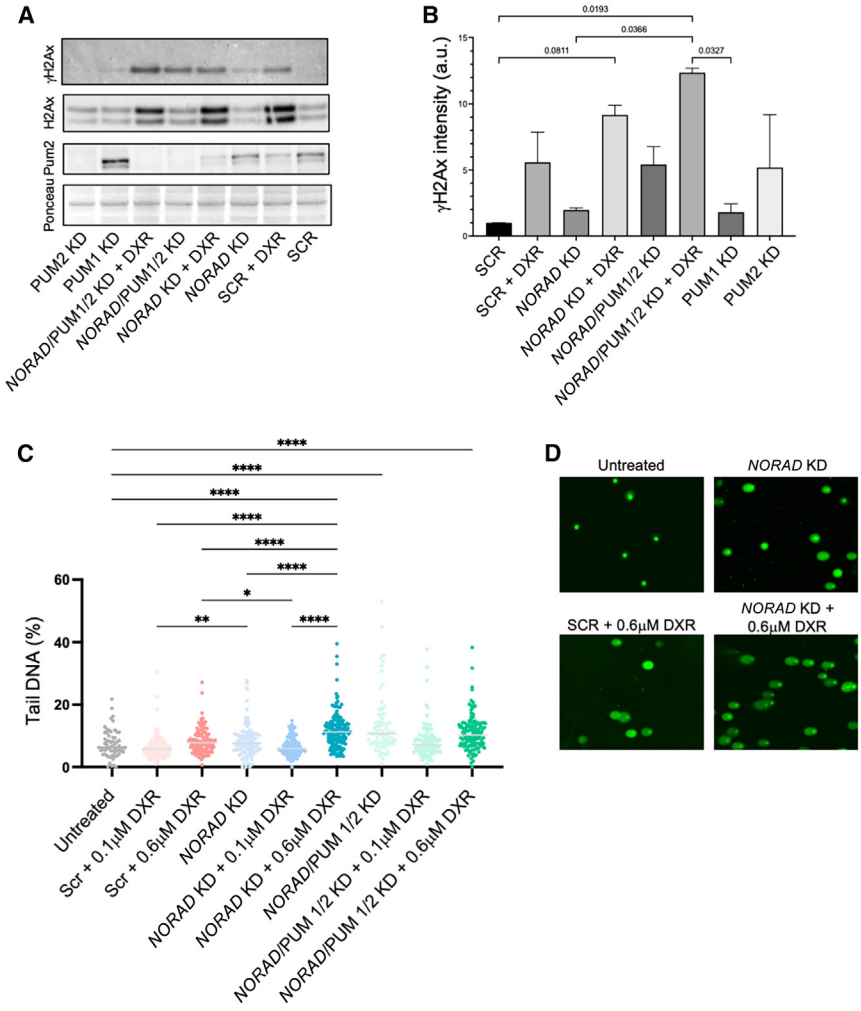

Figure 5. *NORAD* KD alters the DDR

(A) Western blot analysis of γH2Ax, H2Ax, and Pum2 in the depicted experimental conditions in the MDA-MB-231 cell line. Ponceau was used as loading control. (B) Quantification of the western blot bands for the depicted proteins and conditions using the Ponceau band as loading control (n = 3). (C and D) DNA damage detection in the MDA-MB-231 cell line through comet assay (see materials and methods) in the depicted conditions. Quantification (C) and representative images (D) of the Comet assay is depicted. No symbol, $p > 0.05$, *$p < 0.05$, **$p < 0.01$, ***$p < 0.001$.

E2F3).[52] Alternatively, SAM68 binds to conserved secondary structures immediately downstream of the PUMILIO response elements in *NORAD*.[12] Of note, SAM68 is upregulated in several cancer types including breast cancer and could be involved in the deregulation of the AKT pathway.[53] Interestingly, SAM68 also presents tumor suppressor-like activities as a transcriptional coactivator of p53.[14] Nevertheless, it is still debated whether *NORAD* action is solely mediated through PUMILIO proteins. One example is the role of RBMX, a component of the DDR that may be mediating *NORAD* function in genomic (in)stability, whose role has been discussed by different authors.[13,22] Given the complexity of *NORAD* and the different molecules that can associate with it, one would expect that different binding molecules may cooperate to different responses.[10,54] Here, we demonstrate that the absence of PUMILIO did not synergize with *NORAD* in the intensity of γH2Ax signal or the levels of DNA damage after DXR. *NORAD* KD is somehow destabilizing the DDR complex, as supported by the LC-MS/MS data where we see, for instance, lower levels of PARP1, MCM6, or ALYREF (previously shown to be in a complex with *NORAD*[22] and involved in carcinogenesis[38]). Whether PUMILIO may have a compensatory role in the response to DXR, in the *NORAD* KD scenario, later in time, or whether DXR may induce changes in the transcriptional program evading some of the PUMILIO regulated genes, is still unknown. It is known, however, that PUMILIO proteins need to be tightly regulated to maintain genome stability in human cells.[9] The need for such a tight regulation of PUMILIO activity might be also the case for the *NORAD*-PUMILIO axis in DDR and could explain why the *NORAD*/PUM1/PUM2 triple KD does not rescue the phenotypes observed in *NORAD* KD cells.

Breast cancer is the most frequently diagnosed malignancy in women, accounting for about one-third of female cancers. Systemic therapies have been shown to be successful in treating early breast cancer; however, once the disease recurs, it tends to be more aggressive and resistant to therapy. The combination of conventional chemotherapeutic agents with novel molecular-targeted agents is a promising therapeutic approach. First, since the targets and mechanisms of action of these agents are different, there is no cross-resistance. Second, in combinatorial approaches, lower concentrations of chemotherapeutic agents may be considered, reducing both their side effects and off-target effects. Third, alterations in expression and/or activity of genes that regulate mitogenic signals caused by molecular-targeted agents may not only disturb cell growth, but also sensitize cancer cells to chemotherapeutic agents.[55–57] For example, lncRNA *HOTAIR* contributes to colorectal cancer and 5-FU resistance through the recruitment of EZH2 and subsequent silencing of *miR-218*, upregulation of VOPP1 expression and subsequent activation of the NF-κB/TS pathway.[58] Similarly, *H19* lncRNA plays a leading role in breast cancer chemoresistance, mediated mainly through a *H19-CUL4A-ABCB1/MDR1* pathway. *H19* expression was greatly upregulated in doxorubicin-resistant breast cancer cells (MCF-7) and its KD sensitizes them to chemotherapy.[59]

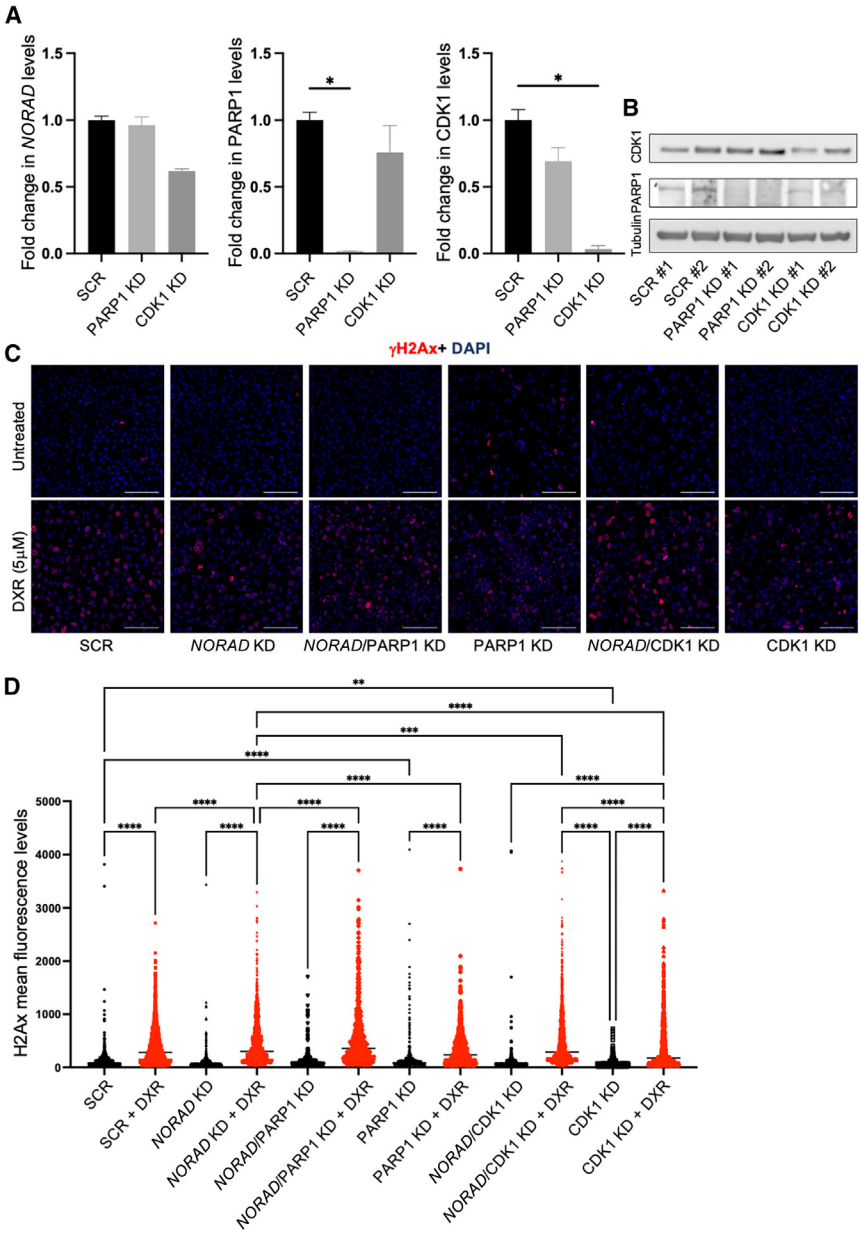

Figure 6. *NORAD* KD synergizes with PARP1 in the DDR

(A) *NORAD*, PARP1, and CDK1 mRNA levels after KD of the conditions represented, using siRNAs (n = 3). (B) Western blot analysis of PARP1 and CDK1 in the depicted experimental conditions in the MDA-MB-231 cell line. Tubulin was used as loading control. (C) Immunofluorescence for γH2Ax in the depicted experimental conditions in the MDA-MB-231 cell line. Scale bar, 100 μm. (D) Quantification of the signal corresponding to γH2Ax in the experimental conditions represented in the MDA-MB-231 cell line (see materials and methods). No symbol, $p > 0.05$, *$p < 0.05$, **$p < 0.01$, ***$p < 0.001$.

Our results show that the DNA damage induced by doxorubicin is enduringly signaled by γH2AX in the absence of *NORAD*. Faulty DNA damage signaling may be caused by an error downstream or upstream of *NORAD*. Upon DNA damage, SAM68 is recruited and stimulates the catalytic activity of PARP1.[60] Defective ATM activity and reduced γH2AX foci formation in response to γ-irradiation were observed in PARP1-deficient cells. In a *NORAD* KD background as presented here, PARP1 inhibition leads to an increase in γH2Ax deposition, demonstrating a synergistic role of *NORAD* and PARP1 in DDR. In addition, PARP1 is thought to recruit Nbs1 and Mre11 to DSBs in a γH2AX- and MDC1-independent manner.[61] It is important to know exactly at which point the DNA damage signaling is compromised, especially considering that PARP inhibitors are currently used in patients with advanced-stage breast cancer, in the context of germline mutations in *BRCA1* or *BRCA2* genes, which frequently belong to the triple-negative subtype.[62]

In summary, we demonstrated that *NORAD* confers resistance of breast cancer cells to a chemotherapeutic agent. Therefore, *NORAD* may represent an actionable molecular target and could be used in a combinatorial approach.

MATERIALS AND METHODS

Cell lines and culture conditions

The following human breast cell lines and control were used in this study: MCF-10A (non-tumoral, mammary epithelial cell line), MCF-7 (breast carcinoma cell line, luminal A subtype), and MDA-MB-231, MDA-MB-436, and MDA-MB-468 (breast carcinoma cell lines, triple-negative subtype). The MCF-10A cell line was cultured in DMEM/F-12 (Dulbecco's modified Eagle's medium/nutrient mixture F-12, Gibco by Life Technologies), supplemented with 5% (v/v) horse serum, epidermal growth factor (20 ng/mL), hydrocortisone (0.5 μg/mL), cholera toxin (100 ng/mL), insulin (10 μg/mL), and 1% (v/v) penicillin-streptomycin. The MCF-7, MDA-MB-231, MDA-MB-436, and MDA-MB-468 cell lines were cultured in DMEM (Gibco by Life Technologies), supplemented with 10% (v/v) heat-inactivated fetal bovine serum and 1% (v/v) penicillin-streptomycin. All cell lines were grown under adherent conditions at 37°C in a humidified incubator with 5% CO_2. MCF-10A and MCF-7 cell lines were a kind gift from Dr. Sérgio de Almeida (Instituto de Medicina Molecular João Lobo Antunes, Lisbon, Portugal), while MDA-MB-231, MDA-MB-436, and MDA-MB-468 were generously offered by Dr. Sérgio Dias (Instituto de Medicina Molecular João Lobo Antunes, Lisbon, Portugal).

Table 1. List of siRNAs and Gapmers

siRNAs			
Target mRNA	Sequence (5′–3′)	Reference	
NORAD	CUGUGUAUAUAGCGGACAA	siRNA N038095-17	Lincode SMARTpool Human LOC647979 038095-00-0010 (Dharmacon)
	CAUCUAAGCUUUACGAAUG	siRNA N038095-18	
	AGUGCACAAUGUAGGUUAA	siRNA N038095-19	
	CGACCCAAGCCUCGACGAA	siRNA N038095-20	
PUM1	GGUCAGAGUUUCCAUGUGA	siRNA J-014179-05	ON-TARGETplus SMARTpool L-014179-00-0005 (Dharmacon)
	GGAGGAGGCGGCUAUAAUA	siRNA J-014179-06	
	GGAGAUAAGCUAGGAGAUU	siRNA J-014179-07	
	CGGAAGAUCGUCAUGCAUA	siRNA J-014179-08	
PUM2	CUGAAGUAGUUGAGCGCUU	siRNA J-014031-17	ON-TARGETplus SMARTpool L-014031-02-0005 (Dharmacon)
	GCAGAGUAAUUCAGCGCAU	siRNA J-014031-18	
	GACAAAUGGUAGUGGUCGA	siRNA J-014031-19	
	AGACAUAACAGUAACACGA	siRNA J-014031-20	

Obtaining patient tissue samples

After study approval (Project "Ref[a]CE – JMS/is – Estudo 64") by the Ethics Committee of CUF Descobertas Hospital (Lisbon, Portugal), a retrospective analysis of breast cancer cases diagnosed between 2019 and 2021 at the Pathology Department (CUF Descobertas Hospital) was performed. Clinicopathological information was retrieved, and both hematoxylin and eosin-stained and immunohistochemistry (IHC) slides from selected cases were reviewed by a pathologist with experience in breast pathology. After validating tissue quality and confirming diagnosis, representative tumor and control sections were obtained from FFPE samples.

RNAscope in tissue samples

Selected FFPE samples were cut to 3 μm sections on positively charged slides. For the RNAscope of the clinical tissue samples, the manufacturer protocol for RNAscope 2.5 Assay was followed, starting with FFPE drying in an oven at 60°C for 1 h. Sequential incubations in xylene and 100% alcohol, accompanied by air drying, were used to deparaffinize the sections. Next, RNAscope Hydrogen Peroxide was applied for 10 min at room temperature (RT), and the slides were rinsed. The RNAscope 1X Target Retrieval Reagent was used for target retrieval for 15 min at 100°C, following standard instructions. After rinsing, the slides were incubated in 100% alcohol for 3 min, and dried at RT, and the tissue area delimited using an Immedge hydrophobic barrier pen to delimit the tissue section. In the HybEz Humidity Control Tray, the slides were incubated with RNAscope Protease Plus at 40°C for the standard time of 30 min. At this point, the tissues were incubated with the probes that could be hybridized to the negative (dapB) or positive (PPIB) controls, or *NORAD* itself. This took place in a HybEz Oven for 2 h at 40°C. The kit contained probes for six sequential amplifications to amplify the hybridization signal. The signal was then ready to be detected after incubating with the Fast RED solutions mix for 10 min at RT. Fast Green Stain Solution (Thermo Scientific, 88024) was applied to the slides. To mount the samples, 1–2 drops of VectaMount Permanent Mounting Medium (Vector Laboratories, H-5000-60) were placed on the slides and the coverslips were dipped in xylene and placed over the sections carefully. Once dry, the samples were evaluated in Nikon ecliplse Ti-U, an inverted wide-field microscope with a CCD color digital camera, at 10× magnification (Achno ADL objective).

IHC in tissue samples

Tissue sections with a thickness of 3 μm were cut from FFPE samples to positively charged slides for IHC with p53 (clone DO-7, Roche, Switzerland, cat. no. 800–2912) and Ki67 (clone 30-9, Roche, cat. no. 790–4286) antibodies. All IHC was performed on the Ventana BenchMark ULTRA automated staining platform. Antibodies were pre-diluted and run using the OptiView DAB IHC Detection Kit (Roche, cat. no. 760-700) with ULTRA CC1 antigen retrieval (Roche, cat. no. 950-224), and slides evaluated using the optical microscope Leica DM1000 Led, at 200× magnification.

LNA GapmeR and siRNA transfection

NORAD downregulation was performed using RNase H-activating LNA GapmeRs (Exiqon), consisting of chimeric antisense oligonucleotides that contain a central block of DNA, which activates RNase H-dependent cleavage of complementary RNA targets, and are flanked by modified nucleotides (hence LNA [locked nucleic acid]) to offer higher protection of the oligonucleotides against nuclease degradation[63,64] and siRNA (Table 1).

Cells were transfected with either control (non-specific) LNA GapmeRs or LNA GapmeRs directed against *NORAD*, using Lipofectamine RNAiMAX transfection reagent (Invitrogen), with 24 or 48 h between the two transfections, following standard procedures (final concentration of 25 nM). Two different GapmeRs were designed using the Antisense LNA GapmeR design tool, with the following central sequences: 5′-CTAGACGTAAATTAGG-3' (human *NORAD*

GapmeR 1) and 5′- ACTTTACTAAAAACGC-3' (human *NORAD* GapmeR 2). siRNAs used for NORAD, PUM1 and PUM2 were the same as in Tichon et al.[12] KD efficiency was assessed by qRT-PCR. siRNAs used for PARP1 (Santa Cruz, sc-29437) and CDK1 (Thermo Fisher Scientific, AM16704 103821) were used at 25 nM. KD efficiency was assessed by qRT-PCR and WB. A combination of unspecific siRNA + scrambled LNA Gapmer was used as a control at the same concentrations.

Single-molecule RNA FISH

Stellaris FISH probes recognizing *NORAD* and labeled with Quasar 570 dye were purchased from Biosearch Technologies. The probe set sequences utilized in the experiments had been described previously and each set comprises 48 different oligonucleotides (20 nucleotides in length).[9]

Cells were seeded on gelatin-coated glass coverslips in flat-bottom 24-well cell culture plates (TPP), washed in phosphate-buffered saline (PBS), and fixed with 3.7% paraformaldehyde for 10 min at RT. Fixed cells were then washed in PBS, permeabilized in 70% ethanol for 1 h at RT, and washed with a solution containing 20× saline sodium citrate (SSC), deionized formamide, and nuclease-free water. Within a humidified chamber, coverslips were transferred onto drops of hybridization buffer (containing probe, 50% dextran sulfate, 20× SSC, deionized formamide, 100% formaldehyde, and nuclease-free water), and hybridized overnight at 37°C. Coverslips were washed with the previsouly detailed buffer and with 2× SSC, following which they were mounted with VECTASHIELD and 4′,6-diamidino-2-phenylindole mounting medium. Images were acquired using a laser scanning confocal inverted microscope (LSM710, Carl Zeiss).

Cellular viability assay

Cells were seeded in 48-well plates (TPP), at a density of 20,000–60,000 cells/well and incubated at 37°C in a humidified incubator with 5% CO_2. When applicable, *NORAD* downregulation was performed at the time of seeding and 24 h later, as mentioned above or in the figure legend.

Seventy-two hours after plating, cells were incubated with doxorubicin (Sigma-Aldrich, D2975000) for 24 h, in a range of concentrations. Specific culture medium containing 10% (v/v) alamarBlue Cell Viability Reagent (Thermo Fisher Scientific) was then added to the cells and resazurin assay performed. Plates were incubated for 2 h at 37°C protected from light and the fluorescence intensity was then quantified using a plate-reading fluorometer (Microplate Reader Infinite M200, Tecan) with excitation wavelength at 560 nm and emission wavelength at 590 nm. The relative viable cell number was standardized to untreated cells and the IC_{50} for each drug determined from dose-response curves using GraphPad Prism software.

Cell apoptosis analysis

Analysis of apoptosis was performed using the Annexin V Apoptosis Detection Conjugate (Thermo Fisher Scientific, A35110). Cells were trypsinized, centrifuged at 1,200 rpm for 5 min, washed with 1× PBS and resuspended in 1× Binding Buffer Solution at a final concentration of 1×10^6 cells/mL. To each 100 μL of cell suspension were added 2.5 μL of Annexin V-CF blue conjugate and 5 μL of 7-AAD staining solution. After incubation at RT for 15 min in the dark, 400 μL of 1× binding buffer solution was added, cells were transferred to FACS tubes and analyzed in a BD LSRFortessaTM X-20 cytometer. Results were analyzed using the FlowJo software.

qPCR analysis of gene expression

Total RNA was isolated using NZYol following manufacturer's instructions (NZYTech). RNA quality was verified using a NanoDrop 2000 Spectrophotometer (Thermo Fisher Scientific). cDNA was synthesized with random primers using the Roche Transcriptor High Fidelity cDNA Synthesis Kit. qRT-PCR analysis was performed in the ViiA 7 Real-Time PCR System (Thermo Fisher Scientific) using SYBR Green PCR master mix (Thermo Fisher Scientific). Gene-specific primer pairs (Sigma) were used as follows:

NORAD forward 5′-TGTTTGTGCAGTGGTTCAGG-3′

reverse: 5′-TCTTGCCTCGCTGTAAACAG-3′

p53 forward: 5′-CCCCTCCTGGCCCCTGTCATCTTC-3′

reverse: 5′-GCAGCGCCTCACAACCTCCGTCAT-3′

18s forward: 5′-GGATGTAAAGGATGGAAAATACA-3′

reverse: 5′-TCCAGGTCTTCACGGAGCTTGTT-3′

GAPDH forward: 5′-GACAGTCAGCCGCATCTTCT-3′

reverse: 5′-TTAAAAGCAGCCCTGGTGAC-3′

PUM1 forward: 5′- CCGGGCGATTCCTGTCTAA-3′

reverse: 5′- CCTTTGTCGTTTTCATCACTGTCT-3′

PUM2 forward: 5′- GGGAGCTTCTCACCATTCA-3′

reverse: 5′- CCATGAAAACCCTGTCCAGATC-3′

MCM6 forward: 5′- GAGGAACTGATTCGTCCTGAGA

reverse: 5′- CAAGGCCCGACACAGGTAAG

PARP1 forward: 5′-GCAGAGTATGCCAAGTCCAACAG-3′

reverse: 5′-ATCCACCTCATCGCCTTTTC-3′

BUB3. forward: 5′- GGTTCTAACGAGTTCAAGCTGA

reverse: 5′- GGCACATCGTAGAGACGCAC

Relative fold changes in gene expression were calculated based on the threshold cycle (Ct), using the $2^{-\Delta\Delta Ct}$ method, considering GAPDH exclusively or in combination with 18S ribosomal RNA as endogenous controls.

Correlation analysis between *NORAD* expression and survival: KM Plotter Online

The open access KM Plotter Online Tool was used to explore the association between *NORAD* expression and the clinical outcome for breast cancer patients, namely overall survival and relapse-free survival.[32,65] This platform integrates information available at Gene Expression Omnibus, European Genome-phenome Archive and The Cancer Genome Atlas, incorporating high-throughput data with clinical information.[32,65] After selecting the genes of interest and the characteristics of the study sample, a Kaplan-Meier survival curve, the hazard ratio with 95% confidence intervals, and log rank p values are displayed for each combination.

Sample preparation for spectrometric analysis

Samples (10 μg) were reduced with dithiothreitol (30 nmol, 37°C, 60 min) and alkylated in the dark with iodoacetamide (60 nmol, 25°C, 30 min). The resulting protein extract was diluted to 2 M urea with 200 mM ammonium bicarbonate for digestion with endoproteinase LysC (1:10 w:w, 37°C, 6 h, Wako, cat. no. 129–02541), and then diluted 2-fold with 200 mM ammonium bicarbonate for trypsin digestion (1:10 w:w, 37°C, o/n, Promega cat. mo. V5113).

After digestion, peptide mix was acidified with formic acid and desalted using a MicroSpin C18 column (The Nest Group) prior to LC-MS/MS analysis.

LC-MS

Samples were analyzed using an LTQ-Orbitrap Fusion Lumos mass spectrometer (Thermo Fisher Scientific, San Jose, CA) coupled to an EASY-nLC 1200 (Thermo Fisher Scientific [Proxeon], Odense, Denmark). Peptides were loaded directly onto the analytical column and were separated by reversed-phase chromatography using a 50 cm column with an inner diameter of 75 μm, packed with 2 μm C18 particles (Thermo Scientific).

Chromatographic gradients started at 95% buffer A and 5% buffer B with a flow rate of 300 nL/min for 5 min and gradually increased to 25% buffer B and 75% A in 79 min and then to 40% buffer B and 60% A in 11 min. After each analysis, the column was washed for 10 min with 10% buffer A and 90% buffer B. Buffer A: 0.1% formic acid in water. Buffer B: 0.1% formic acid in 80% acetonitrile.

The mass spectrometer was operated in positive ionization mode with nanospray voltage set at 2.4 kV and source temperature at 305°C. The acquisition was performed in data-dependent acquisition mode and full MS scans with one micro scan at resolutions of 120,000 were used over a mass range of m/z 350–1,400 with detection in the Orbitrap mass analyzer. Auto gain control (AGC) was set to "standard" and injection time to "auto." In each cycle of data-dependent acquisition analysis, following each survey scan, the most intense ions above a threshold ion count of 10,000 were selected for fragmentation. The number of selected precursor ions for fragmentation was determined by the "Top Speed" acquisition algorithm and a dynamic exclusion of 60 s. Fragment ion spectra were produced via high-energy collision dissociation at a normalized collision energy of 28% and acquired in the ion trap mass analyzer. AGC was set to 2E4, and an isolation window of 0.7 m/z and a maximum injection time of 12 ms were used.

Digested bovine serum albumin (New England Biolabs, cat. no. P8108S) was analyzed between each sample to avoid sample carryover and to assure stability of the instrument, and QCloud[66] was used to control instrument longitudinal performance during the project.

Proteomic data analysis

The LC-MS/MS raw files were elaborated using MaxQuant (v.1.6.17.0) for the processes of protein identification and quantification according to the LFQ algorithm.[67,68] Runs were analyzed using the Andromeda search engine against the freely available reference proteome of *Homo sapiens* downloaded from the UniProtKB database (January 2021). The allowable tolerance for precursor mass and fragment mass was set at 4.5 and 20 ppm, respectively. The minimum peptide length was set at seven amino acids and trypsin and LysC were selected as the proteolytic enzyme allowing up to two missing cleavage sites. Carbamidomethylation (Cys) was set as the fixed modification, while oxidation (Met), deamidation (ND), and N-terminal protein acetylation were the variable modifications. The false discovery rate was set at 1% at both the protein and peptide levels. In this analysis, the inter-run agreement option was selected. According to the MaxLFQ algorithm, proteins were quantified based on the extracted ion currents of the precursor ion peptides. The results of this analysis were first imported into Perseus (v.1.6.14.0) and then into MetaboAnalyst 5.0 for univariate and multivariate statistical data analysis and visualization. In brief, proteins identified as site only, reverse, and contaminants were removed. Expression values were transformed to a logarithmic scale with base 2. Samples were annotated according to their respective groups. Abundance of proteins between two groups were compared using a two-tailed t test, with the adjusted p value set at <0.05. Principal-component analysis (PCA) was performed on the matrix before logarithmic transformation; after filtering valid values, a multistream plot and histogram were generated; after the two-sample t test, a volcano plot was generated. PLSDA and variable importance in projection from the previous analysis were extracted. A heatmap was performed from the top 100 proteins, the 2 clusters (downregulated and upregulated) were extracted and filtered according to the PCA values (>2). Resulting clusters were run on STRING and g:PROFILER to explore the biological functions of the proteins.

The MS proteomics data have been deposited to the ProteomeXchange Consortium via the PRIDE[69] partner repository with the dataset identifier PXD039920.

Table 2. – List of antibodies

Antibody	Type	Reference	Dilution
γH2AX	primary antibody	ab2893 (Abcam)	1:1,000
PUM2	primary antibody	ab92390 (Abcam)	1:10,000
H2AX	primary antibody	10856-1-AP (Proteintech)	1:2,000
PARP1	primary antibody	MA3-950 (Thermo Fisher Scientific)	1:500
CDK1	primary antibody	Ab131450 (Abcam)	1:500
Anti-mouse	cross-adsorbed secondary antibody, HRP	G21040 (Invitrogen)	1:10,000
Anti-rabbit	cross-adsorbed secondary antibody, HRP	G21234 (Invitrogen)	1:10,000

WB analysis

Proteins were extracted on ice after cell washing in PBS (Fisher Bioreagents, BP399-1), with RIPA buffer containing protease and phosphatase inhibitors (RIPA, Thermo Scientific, 89901; EDTA 100×, Thermo Scientific, 1861275; Cocktail protease inhibitor 100×, Thermo Scientific, 1861278; Cocktail phosphatase inhibitor 100×, Thermo Scientific, 1861277). Cell lysates were incubated on ice for 30 min and centrifuged at 15,000 × *g* at 4°C for 15 min. Protein levels were evaluated using the BCA assay according to the manufacturer's protocol (Pierce BCA Protein Assay Kit, Thermo Scientific, 23227). Thirty micrograms of protein from each sample was prepared for loading in NuPAGE LDS Sample Buffer (Invitrogen, NP0004) and separated in a precast gel (Bolt 4%–12%, Bis-Tris, 1.0 mm, Mini Protean Gels, NW04120Box, Thermo Scientific; Running Buffer: 20× Bolt MES SDS Running Buffer, B0002, Thermo Scientific). After wet transfer, the nitrocellulose membranes were stained with Ponceau S (0.1%, w/v) for 15 min to assess gel loading. Prior to immunoblotting, membranes were blocked with 5% bovine serum albumin (BSA), prepared in TBS-T, and then incubated with the indicated antibodies. Membranes were visualized in a chemiluminescence-based system (ChemiDoc Touch [Bio-Rad]), and protein levels were calculated using the Ponceau S staining for normalization. For a list of the antibodies used see Table 2.

Immunofluorescence

Cells previously seeded on 24-well plates in coverslips with gelatin coating were prepared according to the different experimental conditions (see figure legends) and fixed with 4% formaldehyde for 20–25 min, washed with PBS, and permeabilized (0.2% Triton X-100 in PBS) for 10 min. Samples were then washed three times with PBS and blocked for 1 h in PBS containing 1% BSA, incubated overnight at 4°C with primary antibodies diluted in PBS containing 1% BSA, washed with PBS containing 0.05% Triton X, and incubated for 2 h at RT with secondary antibodies conjugated with Alexa 647 (diluted in PBS with 1% BSA), and finally washed again with 0.01% Triton X. Images were acquired using a Zeiss confocal microscope (Zeiss LSM 880).

Wound healing assay

MDA-MB-231 and MDA-MB-468 cells were seeded into 24-well plates and grown to sub-confluence. Cell proliferation was blocked by a 2 h pre-treatment with mitomycin C (100 ng/mL) in serum-free medium. A scratch was made in each well using a 1,000 μL pipette tip and the wounded monolayers washed twice with PBS to remove cell debris and floating cells. Wound width was monitored over time (see corresponding images and figure legends) under an inverted microscope with a digital camera. Percentage wound recovery was expressed compared with the width of the wound at t = 0 (100%).

Comet assay

MDA-MB-231 cells were seeded and exposed to the different experimental conditions as depicted in the corresponding pictures. For the Comet assay we follow the manufacturer's protocol (Fischer Scientific, 13464434). Tail DNA analysis was processed with the Cometscore 2.0 software.

Statistical analysis

Results are presented by the mean along with the standard deviation, and respective p value. Kruskal-Wallis (medians of three or more independent groups) and Mann-Whitney (comparison of two groups) tests were used to calculate statistical significance. A log rank test was used to calculate the statistical differences in the survival curves (KM Plotter Online Tool). Statistical power is detailed in the corresponding figure legends.

DATA AND CODE AVAILABILITY

Data available on request from the authors.

SUPPLEMENTAL INFORMATION

Supplemental information can be found online at https://doi.org/10.1016/j.omtn.2023.08.019.

ACKNOWLEDGMENTS

We thank members of the Carmo-Fonseca, Bernardes de Jesus, and Nóbrega-Pereira laboratories for insightful discussions and advice. We are also grateful to José Rino and Mariana Alves for help with the confocal microscope (a node of PPBI, Portuguese Platform of BioImaging: POCI-01-0145-FEDER-022122). We further acknowledge Sérgio Almeida and Sérgio Dias (IMM-JLA, Lisbon) for providing human cell lines. This work was supported by Fundação para a Ciência e Tecnologia (FCT), and FEDER (EXPL/BIA-CEL/0358/2021, 2022.01199.PTDC and LISBOA-01-0145-FEDER-007391, project co-funded by FEDER, through POR Lisboa 2020 – Programa Operacional Regional de Lisboa, PORTUGAL 2020, and Fundação para a Ciência e a Tecnologia), EPIC-XS (project no. 0000309), and Bolsa de Investigação em Oncologia Dr. Dário Cruz, do Núcleo Regional do Centro da Liga Portuguesa Contra o Cancro 2023. C.A.-V. received funding from Faculdade de Medicina da Universidade de Lisboa (20th "Educação pela Ciência" Program – project no. 20170029). C.T.M. received funding from the Verão com Ciência_i-BiMED BII/UI98/10332/2022 program. F.S. is funded by an FCT individual scholarship (SFRH/BD/146204/2019). S.N.-P. received funding from FCT CEECIND Program (2020.00355.CEECIND). B.P. acknowledges FCT for individual support (CEECIND/03235/2017) and project funding (PTDC/BIA-CEL/0456/2021) used during this

work. A.M.C. received a "Summer with Science 2022" FCT Research Initiation Grant. This project has also received funding from the European Union's Horizon 2020 research and innovation program under grant agreement no. 823839 (EPIC-XS). The CRG/UPF Proteomics Unit is part of the Spanish Infrastructure for Omics Technologies (ICTS OmicsTech) and it is supported by "Secretaria d'Universitats i Recerca del Departament d'Economia i Coneixement de la Generalitat de Catalunya" (2017SGR595). We also acknowledge support of the Spanish Ministry of Science and Innovation to the EMBL partnership, the Centro de Excelencia Severo Ochoa and the CERCA Programme/Generalitat de Catalunya. The funders had no role in study design, data collection and analysis, decision to publish, or preparation of the manuscript.

AUTHOR CONTRIBUTIONS

C.A.-V., A.M.C., and C.T.M. carried out most of the molecular and cell assays. B.P. carried out the tissue RNA-FISH assays. F.S., B.D.-S., and C.P.G. participated in some of the assays represented, namely in Figure 3 and Figure 1. A.M.C., G.E., R.V., and E.S. participated in the acquisition and analysis of mass spectrometry data. S.N.-P. and B.B.d.J. conceived the study, coordinated, and drafted the manuscript. All authors read and approved the final manuscript.

DECLARATION OF INTERESTS

The authors declare no competing interests.

REFERENCES

1. Hood, L., and Rowen, L. (2013). The human genome project: Big science transforms biology and medicine. Genome Med. *5*, 79–88. https://doi.org/10.1186/GM483/METRICS.
2. Huarte, M. (2015). The emerging role of lncRNAs in cancer. Nat. Med. *21*, 1253–1261.
3. Sousa-Franco, A., Rebelo, K., da Rocha, S.T., and Bernardes de Jesus, B. (2019). LncRNAs regulating stemness in aging. Aging Cell *18*, e12870. https://doi.org/10.1111/acel.12870.
4. Gomes, C.P., Nóbrega-Pereira, S., Domingues-Silva, B., Rebelo, K., Alves-Vale, C., Marinho, S.P., Carvalho, T., Dias, S., and Bernardes de Jesus, B. (2019). An antisense transcript mediates MALAT1 response in human breast cancer. BMC Cancer *19*, 1–11. https://doi.org/10.1186/s12885-019-5962-0.
5. De Jesus, B.B., Marinho, S.P., Barros, S., Sousa-Franco, A., Alves-Vale, C., Carvalho, T., and Carmo-Fonseca, M. (2018). Silencing of the lncRNA Zeb2-NAT facilitates reprogramming of aged fibroblasts and safeguards stem cell pluripotency. Nat. Commun. *9*, 1–11. https://doi.org/10.1038/s41467-017-01921-6.
6. Hanahan, D., and Weinberg, R.A. (2011). Hallmarks of cancer: The next generation. Cell *144*, 646–674. https://doi.org/10.1016/j.cell.2011.02.013.
7. Hanahan, D. (2022). Hallmarks of Cancer: New Dimensions. Cancer Discov. *12*, 31–46. https://doi.org/10.1158/2159-8290.CD-21-1059.
8. Hart, T., Komori, H.K., LaMere, S., Podshivalova, K., and Salomon, D.R. (2013). Finding the active genes in deep RNA-seq gene expression studies. BMC Genom. *14*, 778–1471. https://doi.org/10.1186/1471-2164-14-778.
9. Lee, S., Kopp, F., Chang, T.C., Sataluri, A., Chen, B., Sivakumar, S., Yu, H., Xie, Y., and Mendell, J.T. (2016). Noncoding RNA NORAD Regulates Genomic Stability by Sequestering PUMILIO Proteins. Cell *164*, 69–80. https://doi.org/10.1016/j.cell.2015.12.017.
10. Ghafouri-Fard, S., Azimi, T., Hussen, B.M., Abak, A., Taheri, M., and Dilmaghani, N.A. (2021). Non-coding RNA Activated by DNA Damage: Review of Its Roles in the Carcinogenesis. Front. Cell Dev. Biol. *9*, 714787. https://doi.org/10.3389/fcell.2021.714787.
11. Elguindy, M.M., and Mendell, J.T. (2021). NORAD-induced Pumilio phase separation is required for genome stability. Nature *595*, 303–308. https://doi.org/10.1038/S41586-021-03633-W.
12. Tichon, A., Gil, N., Lubelsky, Y., Havkin Solomon, T., Lemze, D., Itzkovitz, S., Stern-Ginossar, N., and Ulitsky, I. (2016). A conserved abundant cytoplasmic long noncoding RNA modulates repression by Pumilio proteins in human cells. Nat. Commun. *7*, 12209. https://doi.org/10.1038/ncomms12209.
13. Elguindy, M.M., Kopp, F., Goodarzi, M., Rehfeld, F., Thomas, A., Chang, T.-C., and Mendell, J.T. (2019). PUMILIO, but not RBMX, binding is required for regulation of genomic stability by noncoding RNA NORAD. Elife *8*, e48625. https://doi.org/10.7554/eLife.48625.
14. Tichon, A., Perry, R.B.T., Stojic, L., and Ulitsky, I. (2018). SAM68 is required for regulation of pumilio by the NORAD long noncoding RNA. Genes Dev. *32*, 70–78. https://doi.org/10.1101/GAD.309138.117/-/DC1.
15. Soghli, N., Yousefi, T., Abolghasemi, M., and Qujeq, D. (2021). NORAD, a critical long non-coding RNA in human cancers. Life Sci. *264*, 118665. https://doi.org/10.1016/J.LFS.2020.118665.
16. Liu, W., Zhou, X., Li, Y., Jiang, H., and Chen, A. (2021). Long Non-Coding RNA NORAD Inhibits Breast Cancer Cell Proliferation and Metastasis by Regulating miR-155-5p/SOCS1 Axis. J. Breast Cancer *24*, 330–343. https://doi.org/10.4048/JBC.2021.24.E32.
17. Spiniello, M., Knoener, R.A., Steinbrink, M.I., Yang, B., Cesnik, A.J., Buxton, K.E., Scalf, M., Jarrard, D.F., and Smith, L.M. (2018). HyPR-MS for Multiplexed Discovery of MALAT1, NEAT1, and NORAD lncRNA Protein Interactomes. J. Proteome Res. *17*, 3022–3038. https://doi.org/10.1021/acs.jproteome.8b00189.
18. Rodriguez, P., Munroe, D., Prawitt, D., Chu, L.L., Bric, E., Kim, J., Reid, L.H., Davies, C., Nakagama, H., Loebbert, R., et al. (1997). Functional Characterization of Human Nucleosome Assembly Protein-2 (NAP1L4) Suggests a Role as a Histone Chaperone. Genomics *44*, 253–265. https://doi.org/10.1006/geno.1997.4868.
19. Rodriguez, P., Pelletier, J., Price, G.B., and Zannis-Hadjopoulos, M. (2000). NAP-2: histone chaperone function and phosphorylation state through the cell cycle. J. Mol. Biol. *298*, 225–238. https://doi.org/10.1006/jmbi.2000.3674.
20. Kimura, H., Takizawa, N., Allemand, E., Hori, T., Iborra, F.J., Nozaki, N., Muraki, M., Hagiwara, M., Krainer, A.R., Fukagawa, T., and Okawa, K. (2006). A novel histone exchange factor, protein phosphatase 2Cγ, mediates the exchange and dephosphorylation of H2A–H2B. J. Cell Biol. *175*, 389–400. https://doi.org/10.1083/jcb.200608001.
21. Chen, X., D'Arcy, S., Radebaugh, C.A., Krzizike, D.D., Giebler, H.A., Huang, L., Nyborg, J.K., Luger, K., and Stargell, L.A. (2016). Histone Chaperone Nap1 Is a Major Regulator of Histone H2A-H2B Dynamics at the Inducible GAL Locus. Mol. Cell Biol. *36*, 1287–1296. https://doi.org/10.1128/MCB.00835-15.
22. Munschauer, M., Nguyen, C.T., Sirokman, K., Hartigan, C.R., Hogstrom, L., Engreitz, J.M., Ulirsch, J.C., Fulco, C.P., Subramanian, V., Chen, J., et al. (2018). The NORAD lncRNA assembles a topoisomerase complex critical for genome stability. Naturen *561*, 132–136. https://doi.org/10.1038/s41586-018-0453-z.
23. Holohan, C., Van Schaeybroeck, S., Longley, D.B., and Johnston, P.G. (2013). Cancer drug resistance: an evolving paradigm. Nat. Rev. Cancer *13*, 714–726. https://doi.org/10.1038/NRC3599.
24. Meacham, C.E., and Morrison, S.J. (2013). Tumour heterogeneity and cancer cell plasticity. Nature *501*, 328–337. https://doi.org/10.1038/nature12624.
25. Fisher, R., Pusztai, L., and Swanton, C. (2013). Cancer heterogeneity: implications for targeted therapeutics. Br. J. Cancer *108*, 479–485. https://doi.org/10.1038/bjc.2012.581.
26. Carter, S.L., Eklund, A.C., Kohane, I.S., Harris, L.N., and Szallasi, Z. (2006). A signature of chromosomal instability inferred from gene expression profiles predicts clinical outcome in multiple human cancers. Nat. Genet. *38*, 1043–1048. https://doi.org/10.1038/NG1861.
27. Roylance, R., Endesfelder, D., Gorman, P., Burrell, R.A., Sander, J., Tomlinson, I., Hanby, A.M., Speirs, V., Richardson, A.L., Birkbak, N.J., et al. (2011). Relationship of extreme chromosomal instability with long-term survival in a retrospective analysis of primary breast cancer. Cancer Epidemiol. Biomarkers Prev. *20*, 2183–2194. https://doi.org/10.1158/1055-9965.EPI-11-0343.

28. Liu, H., Li, J., Koirala, P., Ding, X., Chen, B., Wang, Y., Wang, Z., Wang, C., Zhang, X., and Mo, Y.Y. (2016). Long non-coding RNAs as prognostic markers in human breast cancer. Oncotarget *7*, 20584–20596. 7828 [pii]10.18632/oncotarget.7828.

29. Schettini, F., Brasó-Maristany, F., Kuderer, N.M., and Prat, A. (2022). A perspective on the development and lack of interchangeability of the breast cancer intrinsic subtypes. npj Breast Cancer *81*, 1–4. https://doi.org/10.1038/s41523-022-00451-9.

30. Sørlie, T., Perou, C.M., Tibshirani, R., Aas, T., Geisler, S., Johnsen, H., Hastie, T., Eisen, M.B., Van De Rijn, M., Jeffrey, S.S., et al. (2001). Gene expression patterns of breast carcinomas distinguish tumor subclasses with clinical implications. Proc. Natl. Acad. Sci. USA *98*, 10869–10874. https://doi.org/10.1073/pnas.191367098.

31. Gasco, M., Shami, S., and Crook, T. (2002). The p53 pathway in breast cancer. Breast Cancer Res. *4*, 70–76. https://doi.org/10.1186/BCR426.

32. Győrffy, B., Lanczky, A., Eklund, A.C., Denkert, C., Budczies, J., Li, Q., and Szallasi, Z. (2010). An online survival analysis tool to rapidly assess the effect of 22,277 genes on breast cancer prognosis using microarray data of 1,809 patients. Breast Cancer Res. Treat. *123*, 725–731. https://doi.org/10.1007/S10549-009-0674-9.

33. Lankelma, J., Dekker, H., Luque, F.R., Luykx, S., Hoekman, K., van der Valk, P., van Diest, P.J., and Pinedo, H.M. (1999). Doxorubicin gradients in human breast cancer. Clin. Cancer Res. *5*, 1703–1707.

34. Perez, E.A. (2001). Doxorubicin and paclitaxel in the treatment of advanced breast cancer: Efficacy and cardiac considerations. Cancer Invest. *19*, 155–164. https://doi.org/10.1081/CNV-100000150.

35. Nitiss, J.L. (2009). DNA topoisomerase II and its growing repertoire of biological functions. Nat. Rev. Cancer *9*, 327–337. https://doi.org/10.1038/NRC2608.

36. Wang, S., Konorev, E.A., Kotamraju, S., Joseph, J., Kalivendi, S., and Kalyanaraman, B. (2004). Doxorubicin Induces Apoptosis in Normal and Tumor Cells via Distinctly Different Mechanisms: INTERMEDIACY OF H2O2- AND p53-DEPENDENT PATHWAYS. J. Biol. Chem. *279*, 25535–25543. https://doi.org/10.1074/JBC.M400944200.

37. Schrader, C., Janssen, D., Klapper, W., Siebmann, J.U., Meusers, P., Brittinger, G., Kneba, M., Tiemann, M., and Parwaresch, R. (2005). Minichromosome maintenance protein 6, a proliferation marker superior to Ki67 and independent predictor of survival in patients with mantle cell lymphoma. Br. J. Cancer *93*, 939–945. https://doi.org/10.1038/SJ.BJC.6602795.

38. Klec, C., Knutsen, E., Schwarzenbacher, D., Jonas, K., Pasculli, B., Heitzer, E., Rinner, B., Krajina, K., Prinz, F., Gottschalk, B., et al. (2022). ALYREF, a novel factor involved in breast carcinogenesis, acts through transcriptional and post-transcriptional mechanisms selectively regulating the short NEAT1 isoform. Cell. Mol. Life Sci. *79*, 391. https://doi.org/10.1007/s00018-022-04402-2.

39. Burma, S., Chen, B.P., Murphy, M., Kurimasa, A., and Chen, D.J. (2001). ATM phosphorylates histone H2AX in response to DNA double-strand breaks. J. Biol. Chem. *276*, 42462–42467. https://doi.org/10.1074/JBC.C100466200.

40. Uyhazi, K.E., Yang, Y., Liu, N., Qi, H., Huang, X.A., Mak, W., Weatherbee, S.D., de Prisco, N., Gennarino, V.A., Song, X., et al. (2020). Pumilio proteins utilize distinct regulatory mechanisms to achieve complementary functions required for pluripotency and embryogenesis. Proc. Natl. Acad. Sci. USA *117*, 7851–7862. https://doi.org/10.1073/PNAS.1916471117/SUPPL_FILE/PNAS.1916471117.SD03.XLSX.

41. Bowden, R.D., Buckwalter, M.R., McBride, J.F., Johnson, D.A., Murray, B.K., and O'Neill, K.L. (2003). Tail profile: a more accurate system for analyzing DNA damage using the Comet assay. Mutat. Res. *537*, 1–9. https://doi.org/10.1016/S1383-5718(03)00056-1.

42. Lu, Y., Liu, Y., and Yang, C. (2017). Evaluating In Vitro DNA Damage Using Comet Assay. J. Vis. Exp. https://doi.org/10.3791/56450.

43. Schiewer, M.J., and Knudsen, K.E. (2014). Transcriptional Roles of PARP1 in Cancer. Mol. Cancer Res. *12*, 1069–1080. https://doi.org/10.1158/1541-7786.MCR-13-0672.

44. Zaremba, T., Thomas, H., Cole, M., Plummer, E.R., and Curtin, N.J. (2010). Doxorubicin-induced suppression of poly(ADP-ribose) polymerase-1 (PARP-1) activity and expression and its implication for PARP inhibitors in clinical trials. Cancer Chemother. Pharmacologist *66*, 807–812. https://doi.org/10.1007/s00280-010-1359-0.

45. Spiegel, J.O., Van Houten, B., and Durrant, J.D. (2021). PARP1: Structural insights and pharmacological targets for inhibition. DNA Repair *103*, 103125. https://doi.org/10.1016/j.dnarep.2021.103125.

46. Jabbour-Leung, N.A., Chen, X., Bui, T., Jiang, Y., Yang, D., Vijayaraghavan, S., McArthur, M.J., Hunt, K.K., and Keyomarsi, K. (2016). Sequential Combination Therapy of CDK Inhibition and Doxorubicin Is Synthetically Lethal in p53-Mutant Triple-Negative Breast Cancer. Mol. Cancer Therapeut. *15*, 593–607. https://doi.org/10.1158/1535-7163.MCT-15-0519.

47. Sofi, S., Mehraj, U., Qayoom, H., Aisha, S., Almilaibary, A., Alkhanani, M., and Mir, M.A. (2022). Targeting cyclin-dependent kinase 1 (CDK1) in cancer: molecular docking and dynamic simulations of potential CDK1 inhibitors. Med. Oncol. *39*, 133. https://doi.org/10.1007/s12032-022-01748-2.

48. Zhang, Y., and Li, Y. (2020). Long non-coding RNA NORAD contributes to the proliferation, invasion and EMT progression of prostate cancer via the miR-30a-5p/RAB11A/WNT/β-catenin pathway. Cancer Cell Int. *20*, 571. https://doi.org/10.1186/S12935-020-01665-2.

49. Kawasaki, N., Miwa, T., Hokari, S., Sakurai, T., Ohmori, K., Miyauchi, K., Miyazono, K., and Koinuma, D. (2018). Long noncoding RNA NORAD regulates transforming growth factor-β signaling and epithelial-to-mesenchymal transition-like phenotype. Cancer Sci. *109*, 2211–2220. https://doi.org/10.1111/CAS.13626.

50. Zhang, J., Li, X.Y., Hu, P., and Ding, Y.S. (2018). LncRNA NORAD contributes to colorectal cancer progression by inhibition of miR-202-5p. Oncol. Res. *26*, 1411–1418. https://doi.org/10.3727/096504018X15190844870055.

51. Yang, X., Cai, J.B., Peng, R., Wei, C.Y., Lu, J.C., Gao, C., Shen, Z.Z., Zhang, P.F., Huang, X.Y., Ke, A.W., et al. (2019). The long noncoding RNA NORAD enhances the TGF-β pathway to promote hepatocellular carcinoma progression by targeting miR-202-5p. J. Cell. Physiol. *234*, 12051–12060. https://doi.org/10.1002/JCP.27869.

52. Miles, W.O., Tschöp, K., Herr, A., Ji, J.Y., and Dyson, N.J. (2012). Pumilio facilitates miRNA regulation of the E2F3 oncogene. Genes Dev. *26*, 356–368. https://doi.org/10.1101/GAD.182568.111.

53. Frisone, P., Pradella, D., Di Matteo, A., Belloni, E., Ghigna, C., and Paronetto, M.P. (2015). SAM68: Signal Transduction and RNA Metabolism in Human Cancer. BioMed Res. Int. *2015*, 528954. https://doi.org/10.1155/2015/528954.

54. Chorostecki, U., Saus, E., and Gabaldón, T. (2021). Structural characterization of NORAD reveals a stabilizing role of spacers and two new repeat units. Comput. Struct. Biotechnol. J. *19*, 3245–3254. https://doi.org/10.1016/j.csbj.2021.05.045.

55. Zhong, L., Li, Y., Xiong, L., Wang, W., Wu, M., Yuan, T., Yang, W., Tian, C., Miao, Z., Wang, T., and Yang, S. (2021). Small molecules in targeted cancer therapy: advances, challenges, and future perspectives. Signal Transduct. Targeted Ther. *61*, 201–248. https://doi.org/10.1038/s41392-021-00572-w.

56. Dias, M.H., and Bernards, R. (2021). Playing cancer at its own game: activating mitogenic signaling as a paradoxical intervention. Mol. Oncol. *15*, 1975–1985. https://doi.org/10.1002/1878-0261.12979.

57. Ricci, M.S., and Zong, W.-X. (2006). Chemotherapeutic Approaches for Targeting Cell Death Pathways. Oncol. *11*, 342–357. https://doi.org/10.1634/THEONCOLOGIST.11-4-342.

58. Li, P., Zhang, X., Wang, L., Du, L., Yang, Y., Liu, T., Li, C., and Wang, C. (2017). lncRNA HOTAIR contributes to 5FU resistance through suppressing miR-218 and activating NF-Kb/TS signaling in colorectal cancer, *8*. https://doi.org/10.1016/J.OMTN.2017.07.007.

59. Kallen, A.N., Zhou, X.B., Xu, J., Qiao, C., Ma, J., Yan, L., Lu, L., Liu, C., Yi, J.S., Zhang, H., et al. (2013). The imprinted H19 lncRNA antagonizes let-7 microRNAs. Mol. Cell *52*, 101–112. https://doi.org/10.1016/j.molcel.2013.08.027.

60. Sun, X., Fu, K., Hodgson, A., Wier, E.M., Wen, M.G., Kamenyeva, O., Xia, X., Koo, L.Y., and Wan, F. (2016). Sam68 Is Required for DNA Damage Responses via Regulating Poly(ADP-ribosyl)ation. PLoS Biol. *14*, 1002543. https://doi.org/10.1371/JOURNAL.PBIO.1002543.

61. Wang, Z., Wang, F., Tang, T., and Guo, C. (2012). The role of PARP1 in the DNA damage response and its application in tumor therapy. Front. Med. *6*, 156–164. https://doi.org/10.1007/S11684-012-0197-3.

62. Tutt, A.N.J., Garber, J.E., Kaufman, B., Viale, G., Fumagalli, D., Rastogi, P., Gelber, R.D., de Azambuja, E., Fielding, A., Balmaña, J., et al. (2021). Adjuvant Olaparib for Patients with BRCA1 - or BRCA2 -Mutated Breast Cancer. N. Engl. J. Med. *384*, 2394–2405. https://doi.org/10.1056/NEJMOA2105215/SUPPL_FILE/NEJMOA2105215_DATA-SHARING.PDF.

63. Kauppinen, S., Vester, B., and Wengel, J. (2006). Locked nucleic acid: High-affinity targeting of complementary RNA for RNomics. Handb. Exp. Pharmacol. *173*, 405–422. https://doi.org/10.1007/3-540-27262-3_21.

64. Kauppinen, S., Vester, B., and Wengel, J. (2005). Locked nucleic acid (LNA): High affinity targeting of RNA for diagnostics and therapeutics. Drug Discov. Today Technol. *2*, 287–290. https://doi.org/10.1016/J.DDTEC.2005.08.012.

65. Lánczky, A., and Győrffy, B. (2021). Web-Based Survival Analysis Tool Tailored for Medical Research (KMplot): Development and Implementation. J. Med. Internet Res. *23*, e27633. https://doi.org/10.2196/27633.

66. Chiva, C., Olivella, R., Borràs, E., Espadas, G., Pastor, O., Solé, A., and Sabidó, E. (2018). QCloud: A cloud-based quality control system for mass spectrometry-based proteomics laboratories. PLoS One *13*, e0189209. https://doi.org/10.1371/JOURNAL.PONE.0189209.

67. Costanzo, M., Fiocchetti, M., Ascenzi, P., Marino, M., Caterino, M., and Ruoppolo, M. (2021). Proteomic and bioinformatic investigation of altered pathways in neuroglobin-deficient breast cancer cells. Molecules *26*, 2397. https://doi.org/10.3390/MOLECULES26082397.

68. Costanzo, M., Caterino, M., Cevenini, A., Jung, V., Chhuon, C., Lipecka, J., Fedele, R., Guerrera, I.C., and Ruoppolo, M. (2020). Proteomics reveals that methylmalonyl-coa mutase modulates cell architecture and increases susceptibility to stress. Int. J. Mol. Sci. *21*, 4998–5029. https://doi.org/10.3390/IJMS21144998.

69. Perez-Riverol, Y., Bai, J., Bandla, C., García-Seisdedos, D., Hewapathirana, S., Kamatchinathan, S., Kundu, D.J., Prakash, A., Frericks-Zipper, A., Eisenacher, M., et al. (2022). The Pride database resources in 2022: a hub for mass spectrometry-based proteomics evidences. 50. https://doi.org/10.1093/NAR/GKAB1038.